In vivo gene silencing in the liver with siRNA loaded non-biodegradable and biodegradable cationic nanohydrogel particles for antifibrotic therapy

A Thesis for the award of the degree of

DOCTOR OF NATURAL SCIENCES

Submitted at

Faculty of Chemistry, Pharmacy and Geoscience

Johannes Gutenberg-University Mainz

By

Leonard Kaps

Born in Wetzlar, Germany

on 25.11.1984

Mainz, August 2017

Declaration

"I hereby declare that I wrote the dissertation submitted without any unauthorized external assistance and used only sources acknowledged in the work. All textual passages which are appropriated verbatim or paraphrased from published and unpublished texts as well as all information obtained from oral sources are duly indicated and listed in accordance with bibliographical rules. I highlight that parts of this thesis have been already published in L Nuhn, L Kaps, *et. al.* Adv. Healthcare Mat., 2015[1] and N Leber, L Kaps, *et. al.* J. of Controlled Release[2]. In carrying out this research, I complied with the rules of standard scientific practice as formulated in the statutes of Johannes Gutenberg-University Mainz to insure standard scientific practice."

Leonard Kaps

Dean:

1. Reviewer: [redacted]

2. Reviewer: [redacted]

Day of defense:

Acknowledgements

First of all, I would like to thank my supervisor [redacted] for his strong scientific guidance and the countless fruitful discussions during my PhD studies, as well as for providing an international atmosphere in his institute. I am deeply grateful that he gave me the opportunity to combine my PhD studies with my second degree in human medicine. A very special thanks to my second supervisor [redacted] who supervised my thesis from the chemical perspective. He had always a friendly ear for me and my research. Further, I would like to thank [redacted] and especially [redacted] for their tireless efforts, providing us with abundant nanoparticles. His previous work for nanohydrogel particles, his big help conceiving the manuscripts as well as proofreading of my doctoral thesis were inevitable for the success of my PhD. I am also grateful for the strong bonds and support built up in the group over the years. In particular my long-standing laboratory colleagues [redacted] for their continual support. The assistant of [redacted], [redacted] I would like to thank for smooth running the institute. The good soul of the institute [redacted] I would like to thank for her support and kindness, even though giving me a helping hand when experiments did not end in time.

My close friends, I thank for their emotional support and their full understand when I came occasionally too late from laboratory to our appointments.

The greatest acknowledgement I reserve for my family, to whom a dedicate this dissertation, for their tremendous support and for giving me the best start in life, a child could have ever hoped for.

Summary

Cationic nanohydrogel particles are interesting vehicles for systemic siRNA delivery. For the first time, optimized anti-procollagen α1(I) siRNA loaded cationic nanohydrogel particles were tested *in vivo* as an antifibrotic therapy in a mouse model of liver fibrosis, induced by oral gavage of CCl_4.

After thorough validation of siRNA loaded nanohydrogel particles *in vitro* for cell toxicity, cellular uptake and knockdown performance, particles qualified for further biological evaluation *in vivo.*

After systemic administration, siRNA loaded particles almost exclusively accumulated in liver, while lungs, spleen and kidneys were only targeted to a minor extend. On the cellular level, complexes addressed primarily activated myofibroblasts, the major collagen producing cells in liver fibrosis, and to a lesser extend endothelial cells and macrophages.

Anti-procollagen α1(I) siRNA loaded cationic nanohydrogel sequence specifically and significantly suppressed hepatic procollagen α1(I) transcript levels and total collagen accumulation in liver fibrotic mice. Furthermore, a significant reduction of α-SMA, a surrogate marker of myofibroblast activation, supported the potent antifibrotic effect of the anti-procollagen α1(I) siRNA/nanoparticle treatment. Thus, cationic nanohydrogel particles qualified as promising vehicle platform for siRNA delivery to nonparenchymal liver cells.

Since these first generation cationic nanohydrogel particles proved to be an attractive tool for systemic siRNA delivery, we attempted to improve their *in vivo* degradability and thus tolerability. This improvement is desirable, especially to prevent potential long-term side effects by tissue and cellular accumulation. A second generation of novel nanohydrogel particles was generated that contained a cationic biodegradable acid-labile cross-linker, endowing the next generation of nanohydrogel particles with enhanced biodegradability (bioNP).

The first generation (non-bioNP) were compared 1:1 vs. the second generation cationic nanohydrogel particles (bioNP), loaded with anti-procollagen α1(I) siRNA, in another set of liver fibrosis studies. *In vitro,* acid-labile biodegradable complexes loaded with anti-procollagen α1(I) siRNA could compete with non-biodegradable complexes and showed no cytotoxicity (up to 400 nM siRNA), high cellular uptake (~100% after 24h) and an even improved knockdown efficiency for procollagen 1α(I) transcript mRNA (up to 80% for bioNP or 60% for non-bioNP) in murine fibroblasts.

In vivo biodistribution in CCl_4 induced liver fibrotic mice, using near infrared (NIR) imaging of NP that were labeled with two different NIR-dyes (one coupled to the siRNA, one coupled to the NP shell) showed an equally efficient siRNA delivery to liver and liver resident myofibroblasts for both NP species. However, *in vivo* half-lives of NP and their siRNA cargo differed between the first and second generation of cationic nanohydrogel particles. After repetitive *iv* injection BioNP/siRNA-complexes exhibited, compared to their first generation, an enhanced biodegradability with less tendency to (over)-accumulate in fibrotic and healthy livers.

Nevertheless, anti-procollagen α1(I) siRNA loaded bioNP induced a potent procollagen α1(I) mRNA knockdown and prevented fibrosis progression as determined by liver biochemical and morphometrical collagen quantification.

Long-term monitoring of the carriers in the body revealed a significantly enhanced clearance for the acid-degradable carrier, especially after multiple dosing. In healthy mice, both species showed a broad therapeutic index in doses escalation studies up to 10mg siRNA/kg body weight.

Therefore, the novel acid-degradable cationic bio-NP could be validated as a promising novel platform for siRNA delivery *in vivo* to treat fibrotic liver diseases. Since these NP also target other nonparenchymal cells, especially macrophages and endothelial cells, further studies to deliver siRNA to these cells are warranted.

Zusammenfassung

Kationische Nanopartikel (NP) sind interessante Vehikel zur systemischen Applikation von siRNA. Wir testeten *in vivo* zum ersten Mal optimierte anti-procollagen α1(I) siRNA beladene NP zur antifibrotischen Therapie in CCl_4 induzierten leberfibrotischen Mäusen.

Nach gründlicher *in vitro* Untersuchung der anti-procollagen 1α(I) siRNA beladenen Partikel hinsichtlich ihrer Zytotoxizität, Zellaufnahme und ihrer Knockdown-Effizienz (in 3T3-Fibroblasten), konnten sie sich als vielversprechende siRNA Träger für *in vivo* Versuche qualifizieren.

Nach intravenöser Applikation akkumulierten die siRNA beladenen Partikel beinahe ausschließlich in der Leber und nur marginal in Lunge, Milz und Niere. Auf zellulärer Ebene wurden die Komplexe primär von aktivierten Myofibroblasten und nur zu einem kleinen Teil von Endothelzellen, Makrophagen und Hepatozyten aufgenommen.

Anti-procollagen α1(I) siRNA beladene NP reduzierten signifikant und sequenzspezifisch hepatisches prokollagen α1(I) mRNA Transkript, sowie die Gesamtmenge an Kollagen in leberfibrotischen Mäusen. Des Weiteren zeigte die Reduktion von α-SMA, ein Surrogatemarker für aktivierte Myofibroblasten, einen Erfolg der antifibrotischen Therapie. Somit qualifizierten sich NPs als geeignete siRNA Träger zur Adressierung nicht-parenchymale Zellen in der Leber.

Da die erste Generation von NP/anti-procollagen α1(I) siRNA Komplexen bereits überzeugende Therapierfolge in fibrotischen Mäusen zeigte, versuchten wir ihre Bioabbaubarkeit und somit ihre Verträglichkeit zu verbessern. Eine verbesserte Abbaubarkeit der Partikel war wünschenswert, um bei längeren Anwendungen toxische Akkumulationen in Gewebe und Zellen zu verhindern.

Für die zweite Generation von NP wurde ein säurelabiler Ketal-Linker, anstelle des vorherigen inerten Spermin-Linkers, zur Quervernetzung verwendet. Im Rahmen einer *in vivo* Vergleichsstudie wurde die erste Generation (nicht-bioNP) vs der zweiten Generation (bioNP), als Träger für anti-procollagen 1α(I) siRNA, verglichen.

In vitro zeigten anti-procollagen 1α(I) siRNA beladene bioNP gegenüber nicht-bioNP keine Nachteile hinsichtlich Zytotoxizität (bis zu 400nM siRNA) und Zellaufnahme (~100% nach 24h). BioNP/anti-procollagen 1α(I)1 Komplexe wiesen bemerkenswerterweise einen effizienteren Knockdown für procollagen 1α(I) mRNA Transkript (bis zu 80% für bioNP) in 3T3 Fibroblasten auf.

Beide Partikelspezies zeigten, nach intravenöser Injektion in (leber-)fibrotischen Mäusen, hinsichtlich ihrer *in vivo* Biodistribution (IVIS-*imaging*) für den *carrier* (NP) und ihr siRNA *cargo* (NP und siRNA mit verschiedenen nahinfraroten Fluorochromen markiert) eine vergleichbare effiziente Anreicherung in der Leber, als auch auf zellulärer Ebene in aktivierte Myofibroblasten (α-SMA+ Zellen). Die *in vivo* Halbwertszeit der säurelabilen bioNP/siRNA-Komplexe konnte, im Vergleich zu ihren Vorgängern, signifikant reduziert werden. Nach Akkumulation in der Leber wurden die bioNP/siRNA-Komplexe deutlich schneller abgebaut.

Die verbesserte Abbaubarkeit der bioNP ging nicht auf Kosten ihrer therapeutischen Knockdown-Effizienz. Anti-procollagen 1α(I) siRNA beladene bioNP versus non-bioNP/ anti-procollagen 1α(I) siRNA Komplexe erzielten eine vergleichbare effiziente Reduktion des procollagen 1α(I) mRNA Transkripts als auch der Gesamtkollagenlast in fibrotischen Lebern.

Im Rahmen eines Langzeit-*in vivo*-Monitorings (über 13 Tage) wiesen die säurelabilen siRNA Träger der zweiten Generation, nach wiederholter intravenöser Applikation, eine signifikant verbesserte Bioabbaubarkeit im Vergleich zu ihren Vorgängern auf.

Beide siRNA beladene Partikelspezies wurden bei Dosis-Eskalationen bis zu 10mg/kg siRNA Körpergewicht von gesunden Mäusen sehr gut vertragen und lassen daher eine große therapeutische Breite vermuten.

Die NP der zweiten Generation behielten alle positiven Eigenschaften ihrer Vorgänger bei und zeigten zusätzlich eine deutlich verbesserte *in vivo* Bioabbaubarkeit. Somit stellen bioNP, als eine vielversprechende Weiterentwicklung ihrer ersten Generation, eine neue Plattform für siRNA Träger dar.

Da die NP, neben aktivierten Myofibroblasten, zusätzlich andere nicht-parenchymale Zellen insbesondere Makrophagen und Endothelzellen erreichen, können weitere therapeutische Ansätze mit ihnen als *in vivo* siRNA Träger ausgelotet werden.

Designed cover page

Introductive figure: Cover page designed for the manuscript L Kaps, L Nuhn, *Adv. Healthcare Mat.*, 2015[1]. (The figure has been designed by Cristina Sala, Valencia, Spain, 2015)

List of abbreviations

A absorbance

α alpha

mAb (monoclonal) antibody

bp base pair

β beta

cDNA complementary DNA

Col1a1 procollagen α1(I) gene or transcript

Cy5 Cyanine 5

ddH_2O double distilled water (Millipore)

DMEM Dulbecco's Modification of Eagle's medium

DNA deoxyribonucleic acid

dsRNA double-stranded RNA

ECM excess extracellular matrix

FACS fluorescence activated cell sorting

FCS fetal calf serum

FITC fluroescein isothiocyanate

g gram

h hour(s)

iv intravenous

kb kilo base

kJ kilo Joule

kV kilo volts

l liter

µ micro

µg micro gram

µl micro liter

List of abbrevations

min minute(s)

mA milli amps

mM milli molar

miRNA micro RNA

mRNA messenger RNA

nm nano meter

OD optical density

PBS phosphate buffer salt solution

PCR polymerase chain reaction

pH (the negative of the logarithm to base 10 of the activity of the hydrogen ion)

PI principal investigator

RNA ribonucleic acid

RNAi interference

rpm rotation per minute

RT room temperature

RT PCR reverse transcription PCR

s second

shRNA short hairpin RNA

siRNA short interfering RNA

TAM tumor associated macrophages

U units

vs versus

W watts

w/w weight-to-weight

List of figures and tables

Table of contents

1. Introduction

1.1 Liver fibrosis

1.1.2 General aspects

Fibrosis is characterized by an excessive wound healing response that occurs in most forms of chronic liver disease and results in the deposition of scar tissue, i.e., excess extracellular matrix (ECM)[3]. With continuous liver damage, fibrosis can advance to cirrhosis, which is characterized by a severe distortion of the liver vasculature and architecture[3]. Cirrhosis, as the end stage of most liver disease, is the major determinant of morbidity and mortality in patients with liver disease, predisposing to liver failure and primary liver cancer[3].

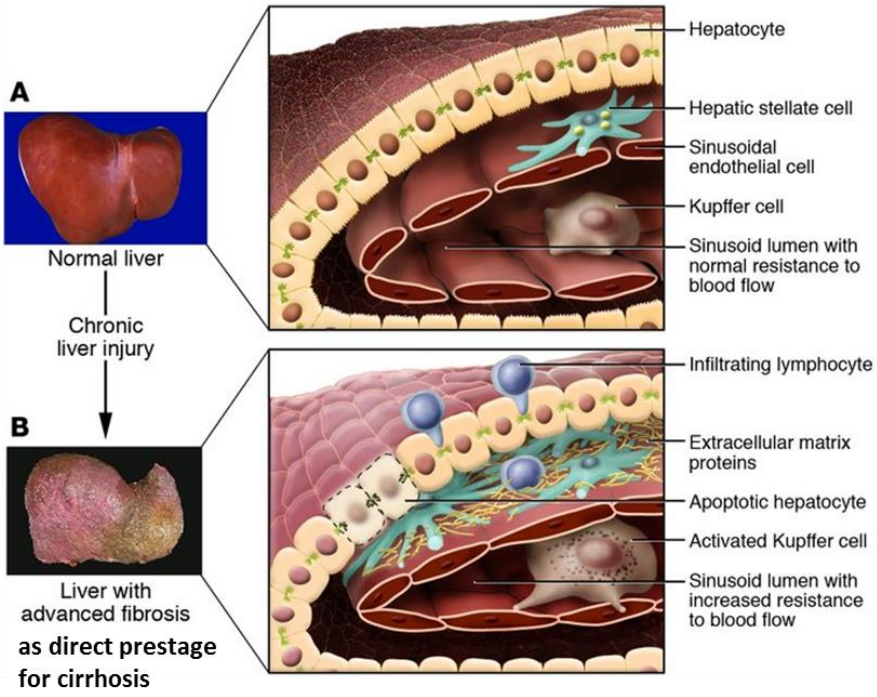

Figure 1. Macroscopic changes in the normal hepatic architecture (A) associated with advanced hepatic fibrosis (B) as a prestage to cirrhosis. Following chronic liver injury inflammatory immune cells (e.g monocytes-macrophages followed by lymphocytes) infiltrate the hepatic parenchyma. Some hepatocytes undergo apoptosis and hepatic stellate cells (fat-storing cells, Ito cells) are activated, releasing fibrogenic mediators. Hepatic stellate cells as well as (portal) fibroblasts proliferate and transform into activated myofibroblasts, the major ECM producing cells. Sinusoidal endothelial cells lose their fenestrations, and the tonic contraction of the myofibroblasts leads to increased resistance to blood flow in the hepatic sinusoid (modified from figure 1 in Brenner *et al*, J. *Clin Invest* 2005)[4].

1.1.3 Clinical appearance

In the clinic, fibrosis is mainly caused by chronic viral hepatitis B or C, autoimmune and biliary diseases, alcoholic steatohepatitis (ASH) and, increasingly, nonalcoholic steatohepatitis (NASH)[5][6][7][8][9]. Patients with *compensated* cirrhosis, i.e., when the liver still fulfills its vital functions, run a yearly risk of 2-7% for decompensation and of 1-7% to develop hepatocellular carcinoma (HCC)[5]. Thus compensated liver cirrhosis usually progresses towards a decompensated stage, which is characterized by a series of life-threatening clinical manifestations, including ascites, variceal hemorrhage, sepsis and hepatic encephalopathy[10].

As a relevant complication of cirrhosis, HCC is a difficult to treat tumor entity, with many patients presenting in a stage of unresectable HCC, of whom only a minority is eligible for liver transplantation when meeting the strict (Milan) criteria for donor liver allocation[11]. Therefore, potent antifibrotic therapies are urgently needed to prevent or even reverse fibrosis, and to stop the progression towards cirrhosis and HCC[5].

1.1.4 Pathogenesis and novel therapeutic perspectives for liver fibrosis

Several promising targets for therapeutic treatment of liver fibrosis are currently under investigation. Here, the pathogenesis of liver fibrosis in respect to therapeutic antifibrotic options is briefly discussed.

Following liver injury and/or in the presence of profibrotic stimuli, hepatic stellate cells transform to a phenotyp with myofibroblast-like features, including increased collagen production and enhanced cell contractility[3][12]. Thus, activated hepatic stellate cells and myofibroblasts (here collectively termed activated MF), represent the major producers of excessive ECM during liver fibrogenesis and have been intensively investigated as target cell for antifibrotic target[13][14]. Activated MF over-express alpha smooth muscle actin (α-SMA), a highly conserved protein that is involved in cell and especially myofibroblast contractility and motility[15]. α-SMA, as activation marker of myofibroblasts, closely correlates to a certain degree with ECM production in fibrotic liver and other tissues, and therefore serves as surrogate marker of fibrogenesis[16].

Targets for antifibrotic therapies are cells, signaling pathways, and molecules (e.g. cytokines) critical for fibrosis progression or reversal. Thus, antifibrotic therapy addresses HSC activation/recruitment, cells located upstream of HSC activation, profibrogenic growth factors, cytokines and other mediators, intracellular profibrogenic signaling pathways in HSC and also the stimulation of fibrolytic processes to reverse existing fibrosis[3]. Under profibrotic conditions, activated MF can derive from several origins like from liver periportal, perivascular fibroblasts, bone marrow-derived circulating fibrocytes, and possibly liver epithelia[3][17][18][19][20]. Furthermore, activated cholangiocytes exhibit a profibrotic phenotyp in a cross-talk with MF by secreting fibrogenic growth factors such as transforming growth factor beta (TGFβ1, TGFβ2), connective tissue growth factor (CTGF), and platelet-derived growth factor (PDGF)[3][21].

Although the role of macrophages in liver fibrosis is manifold and not yet fully understood, macrophages and their polarizations play an important role in both fibrosis progression and regression (Figure 2)[22][5]. Ramachandran P. *et. al.* reported that selective depletion of pro-fibrolytic (pro-resolution) or profibrogenic macrophages (here defined as CD11b^{hi} F4/80^{int} Ly-6C^{lo} (for M1) or - Ly-6C^{hi} (for M2)) had a significant impact on fibrosis progression or resolution in CCl_4 induced liver fibrotic mice[23]. M1/M2 phenotypes can be in part discriminated by their metabolic intermediates and by (over)-expression of cell surface markers [24][25]. CD206 mannose receptors are predominantly present on M2 polarized macrophages and dendritic cells, where they play an important role for innate and adaptive immune responses[26]. It was shown that CD206 expressing M2 macrophages can be specifically targeted by drug loaded mannosylated chitosan decorated nanoparticles[26].

Thus, reeducating of liver macrophages from a putatively fibrogenic M2-type to a putatively fibrolytic M1-type macrophages may promote fibrolysis. However, the *in vitro* generated M1 and M2-type macrophages represent only the extremes of polarization and it is likely that intermediate phenotypes, such as fibrolytic M2-type macrophages exist. Allover, the beneficial switching of macrophage phenotype represents an interesting immune-modulatory approach not only restricted to liver fibrosis therapy[22][23].

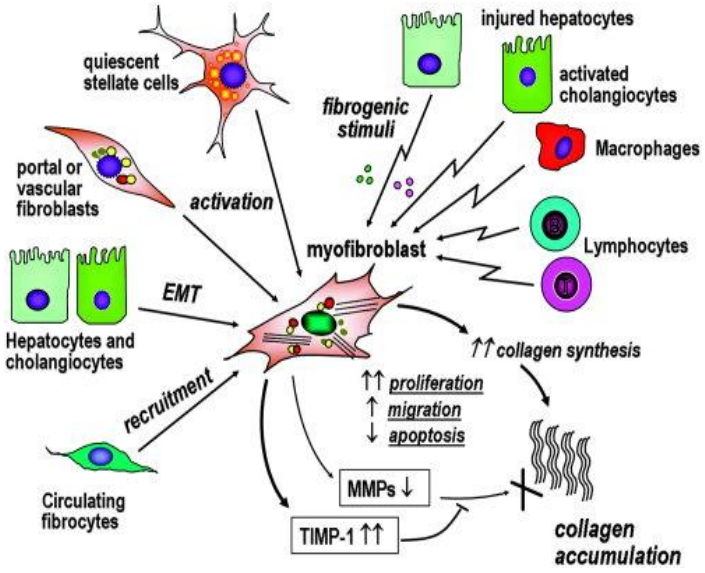

Figure 2. The manifold activation pathways of myofibroblasts as major collagen producing cells in liver fibrosis. Activated hepatic stellate cells/myofibroblasts are a heterogeneous cell population arising from transdifferentiation of quiescent HSC, liver fibroblasts, and possibly but to a lesser degree from activated/injured liver epithelia by way of epithelial-to-mesenchymal transition (EMT) or from bone-marrow-derived circulating fibrocytes. This myofibroblast phenotype shows increased proliferation, migration, and contractility, and a relative resistance to apoptosis. Beside up-regulated synthesis and deposition of various ECM components, fibrolysis is further hampered by way of an increased synthesis of tissue inhibitors of metalloproteinases (especially TIMP-1) and a decreased production of fibrolytic metalloproteinases (MMPs). Fibrogenesis is maintained by crosstalk with various other cell types. In contrast, if these stimuli arrest and/or with the help of antifibrotic agents, fibrosis can be resolved by way of proteolytic removal of excess ECM, often by the same cells that play a central role in fibrogenesis, such as HSC and macrophages/Kupffer cells (modified from figure 1 in Schuppan D. *et al.*, Clinics Re. Hepa. Gastro, 2015)[3].

However, the activation/transformation into activated myofibroblasts is downstream of all these complex profibrogenic cascades. The myofibroblasts are, the major ECM (collagen) producing cells, and therefore mainly contribute to deposition of excess ECM in fibrosis. The fibrotic ECM consists out of four major classes of components, namely collagens, non-collagenous glycoproteins, proteoglycans and elastin. Out of these classes, collagen I and III represent the most abundant protein, establishing the fibril network, with which the other components interact, to endow the ECM with stability, elasticity or stiffness, and many other functions, including regulated solute and mediator exchange, and positional and functional information for the cells embedded in it.

In cirrhotic human livers, collagen I is over-expressed vs. III, representing more than ~70% (vs. ~50% in normal liver) of the total collagen. The col1α1, col1α2 gene encode the procollagen-α1(I) and the procollagen-α2(I) protein chains that form the collagen I triple helix already intracellularly [27]. Procollagen I is composed out of two pro-α1(I) and one pro-α2(I) chains,

which is further aggregated laterally in a staggered way to larger collagen fibrils after further extracellular processing by with N- and C terminal procollagen proteinases that remove the large terminal propeptides (Figure 3)[27].

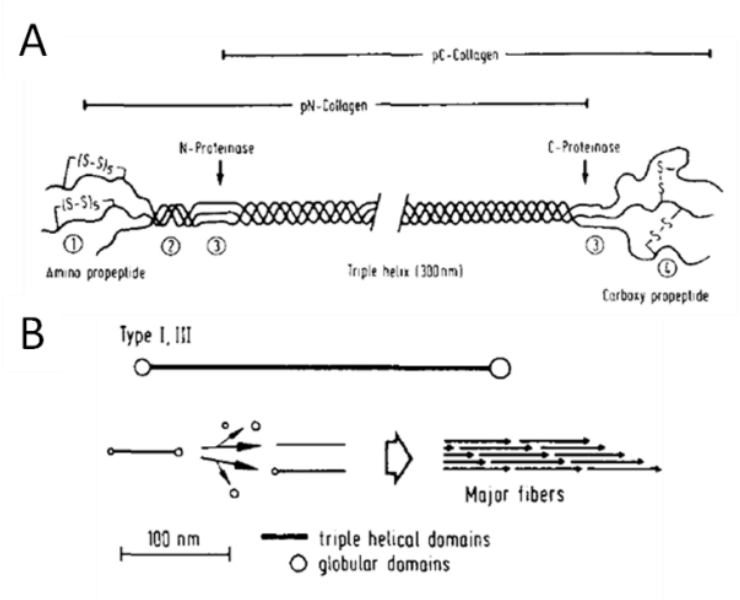

Figure 3. Structural model and processing of fibril forming procollagens I and III, and assembly of major collagen fibers (which consist largely of type I and III collagen). A: Type I and Ill procollagens consist of a 300 nm long triple helix which is covalently linked to aminoterminal and carboxyterminal propeptides. Mature collagen I/III is formed by cleaving their propeptides, by extracellular N- or C-proteinases, respectively. B: Major collagen fibril growth, containing both collagen I and III, is accelerated after removal of propeptides (modified from figure 1 and 2 in Schuppan D., *Sem. liver dis.*, 1990)[27].

In clinical trials, current (antifibrotic) therapies address the cause for the underlying fibrosis because the pathologically overexpressed ECM (collagen) is difficult to target with small molecule drugs which have been difficult to develop and which may have unwanted side effects[5]. However, in a first preclinical study of our group, it could be shown that targeting the colα1(I) mRNA transcript by RNA interference (RNA*i*), using small interfering RNA (siRNA), could be a potent strategy to reduce the collagen amount in liver[28].

1.2 RNAi - gene silencing

Gene silencing with small interfering RNAs has become a powerful research tool during the last 2 decades and has begun to make its way towards first clinical applications. Using siRNA technology, virtually every gene in the human genome contributing to a disease becomes targetable, thus, opening unprecedented opportunities for novel drug development, including current diseases[29].

1.2.1 Historical background

In 1990, Napoli and Jorgensen were the first to report on RNAi phenomenon as they investigated the enzyme chalcone synthase (CHS) in anthocyanin biosynthesis[30][31]. This pathway is responsible for the deep violet coloration in petunias. In order to generate violet petunias, Napoli and Jorgensen over-expressed chalcone synthase in petunias, which unexpectedly resulted in white petunias. This unexpected phenomenon rapidly caught the scientists' attention, as the levels of endogenous as well as induced CHS were 50-fold lower

than in wild-type petunias. They hypothesized that the introduced transgene somehow "suppressed" the endogenous CHS gene. Just two years later in 1992, Romano and Macino observed a similar phenomenon in *Neurospora crassa,* where introduction of a homologous RNA sequences caused suppressing of the endogenous gene[30][32].

In higher organisms, RNAi was first reported by Guo and Kemphues in *Caenorhabditis elegans*[30][33]. They observed that the injection of sense or antisense RNA to par-1 mRNA resulted in degradation of the par-1 mRNA[33][30]. The fact that even sense RNA could induce down-regulation of the target transcript was not easily explainable that time, since sense RNA should not have hybridized with the target sequence of the mRNA. This finding could be finally explained by Fire and Mello in 1998 as they hypothesized that the trigger for gene silencing was not single-stranded RNA (ssRNA) but double-stranded RNA (dsRNA)[30][34]. They reasoned that the observed silencing effect from sense RNA, observed by Guo *et. al.*, actually resulted from contamination of dsRNA (at this time a well-known problem, in ssRNA production by bacterial polymerases)[30][34]. In their control experiments, Fire and Mello *e. al.* ensured that their ssRNAs were thoroughly purified before injection. They discovered that (sense or antisense) were consistently 10- to 100-fold less effective than corresponding dsRNA targeting the same mRNA[30][34]. And indeed, ssRNA was found to be effective only if the sense strand, followed by the antisense strand or *vice versa* was injected into the animals, suggesting that hybridization of ssRNA to form dsRNA occurred *in vivo*[30].

Hamilton and Baulcombe searched for stable intermediates of dsRNA which crucially influence degradation of the target mRNA[30][35]. They hypothesized that antisense RNA could serve as a guide, binding to the mRNA and causing its degradation[30]. When Hamilton and Baulcombe detected highly effective antisense RNA of an estimated length of 25 nucleotides for gene knockdown, they suggested that this length was necessary for RNAi specificity.

Tuschel *et al.* tested chemically synthesized small interfering RNA (siRNA) vs. luciferase mRNA in *Drosophila* cells[30][36]. For the first time, they could prove that these synthetic small RNA fragments (siRNA) could efficiently knockdown target mRNA not only of heterologous but also of endogenous genes in mammalian cells[30][37]. From then on, this new siRNA biotechnology was continuously developed for applications in experimental research and thereby attracted increasing attention also of pharmaceutical companies[38].

Finally in 2006, the discovery of RNA interference was honored with the most prestigious award for scientist, as Andrew Fire and Craig C. Mello received the Nobel Prize in Physiology/Medicine "for their discovery of RNA interference - gene silencing by double-stranded RNA"[39].

1.2.2 RNAi-molecular mechanism

RNAi is a regulatory mechanism operative in most of eukaryotic cells, as they use small double stranded RNA (dsRNA) molecules to direct homology-dependent control of their gene activity[29]. Nowadays, different structural types of siRNA exist which can be applied for post-transcriptional gene silencing[40].

In the following, I focus on therapeutic drugs relevant small interfering RNA (siRNA), for a more comprehensive understanding of the molecular silencing pathway even by short hair-pin siRNA (shRNA/miRNA), which primarily acts through translational inhibition.

Optimized siRNAs, ∼21–22 base pairs long dsRNA molecules have a characteristic 2 nucleotides 3′ overhang that is recognized by the enzymatic machinery of RNAi that eventually leads to homology-dependent degradation of the target mRNA. In mammalian cells siRNAs are produced from cleavage of longer dsRNA precursors by the RNaseIII endonuclease Dicer[41][42]. Dicer endonuclease, together with the RNA binding protein named TAR-RNA, navigates siRNAs to the RNA-induced silencing complex (RISC), which provides the actual "slicing" protein Argonaute 2 that degredades the target mRNA molecules between bases 10 and 11 relative to the 5′ end of the antisense siRNA strand[41]. The crucial catalytic components of RISC are the Argonaute (Ago) family members, among which in humans only Ago-2 possesses an active catalytic domain for cleavage activity[41][43][44]. In the RISC complexe double stranded siRNA becomes activated by Ago-2 mediated cleaving of the "passenger" strand. The now activated RISC complex, only containing the single-stranded "guide" RNA molecule, navigates the "guide" ssRNA to its target mRNA to which it specifically hybridizes by intermolecular base pairing[41][45]. Rules that effect selectivity of strand loading into RISC are based upon differential thermodynamic stabilities at the ends of the siRNAs[41][46][47]. The less thermodynamically stable end is favored for unwinding of the 5′ end of the guide strand which binds to the so called PIWI domain (P-element induced wimpy testis) of Ago-2[41]. mRNA molecules with (near-) perfect complementarity to the guide RNA are recognized and cleaved by Ago-2, leading to a sequence specific knockdown of the targeted mRNA transcript (for an overview of the RNAi mechanism - see Figure 4). An imperfect match of siRNA to target mRNA may in certain cases repress translation or destabilize the transcripts if the binding mimics microRNA (miRNA) interactions with target sites and consequent activities, contributing to unwanted side-effects e.g. off-target effects[41].

MicroRNAs are endogenous substrates for the RNAi silencing machinery and pursue the same downstream pathway like siRNA. At the beginning, they are expressed as long primary transcripts (pri-miRNAs), which are processed within the nucleus into 60-70 bp hairpins by the microprocessor, consisting of Drosha-DGCR8[41][48][49]. By further processing in the cytoplasm, the loop is removed by the RNAse III enzyme Dicer and one of the two strands is loaded into RISC[41]. The mature miRNAs does not exhibit full complementarity with sequences in the 3′UTR of target mRNAs. Here, the primary silencing mechanism of miRNAs is translational repression and putative mRNA degradation[41][50] (Figure 4).

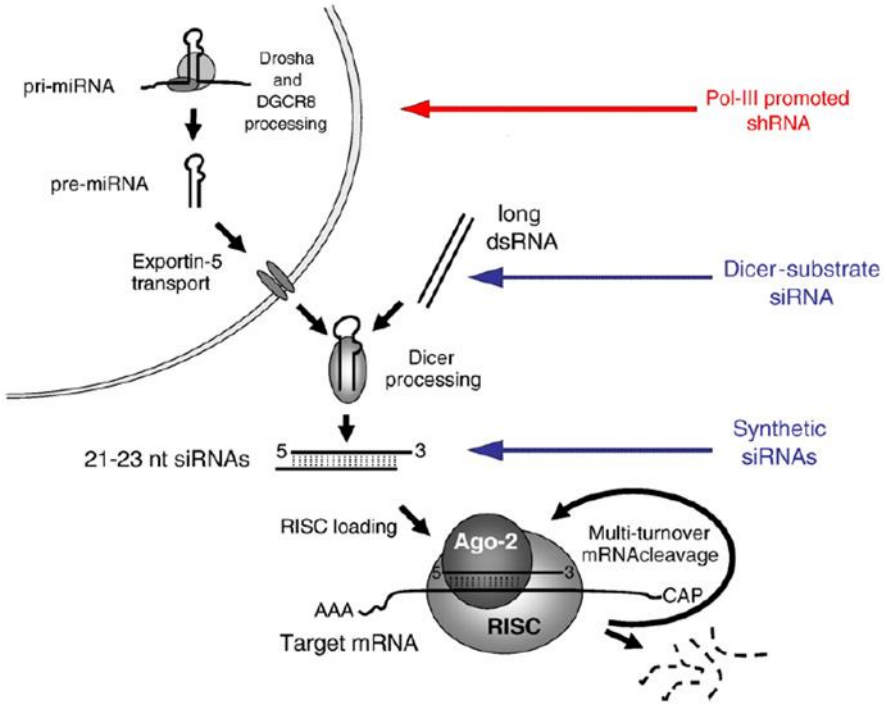

Figure 4: On the left side: Schematic diagram of the mammalian RNAi pathway and formation of small interfering RNAs (siRNA) that mediate homology dependent target mRNA degradation in the cytoplasm through the RNA-induced silencing complex (RISC). On the right side: Different entry point for artificial DNA-derived (marked in red) or RNA-based (marked in blue) siRNA drugs that enter and activate RISC for gene silencing (modified from figure 1 in Rossi J. *et al.*, *Advanced Drug Delivery Reviews*, 2007)[41].

Beside liver fibrosis therapy, basically every human disease caused by activity from one or a few genes should be amenable for RNAi-based intervention[41]. Thus, initial therapeutic results with iRNA were promising and siRNA drugs have already made it to the clinics (e.g. intravitreal injection of anti-VEGF siRNA for the treatment of age-related macular degeneration), the major bottleneck remains *in vivo* delivery after systemic administration of these macromolecules, with targeted cell, tissue or organ specific delivery [41][51][52].

In the upcoming chapter, I will introduce the common applied *in vivo* siRNA delivery strategies and discuss further important aspects which should be considered for systemic siRNA delivery.

1.2.3 Strategies and critical aspects for *in vivo* siRNA application

RNAi can be achieved basically *via* RNA-based strategies where the effector siRNA, ~21 nb duplexes, is delivered into the cytoplasm of the targeted cells or *via* DNA-based approaches by which siRNA effector duplexes are produced by intracellular processing of longer RNA hairpin transcripts (Figure 4).

For (lenti-)viral vectors genome integrated short hairpin RNAs (shRNAs) genes are transcribed by polymerase III/II inside the nucleus. The product mimics so called pri-microRNA (pri-miRNA, Figure 4) and is processed to pre-shRNA by Drosha/DGCR8, a microprocessor complex subunit, before it is exported from the nucleus by Exportin-5. In the cytoplasm pre-shRNA as well as long dsRNA, acting as direct precursor for siRNA, are processed into functional siRNA by the Dicer complex[41].

DNA- vs. RNA-based strategies haver pros and cons for RNAi which should be considered in regard to the intended application. Since siRNA can be loaded directly into the RISC complex, its pathway is less susceptible to be corrupted by transcriptional regulatory elements or incorrect processing/transportation[41]. A further advantage of siRNA is that gene silencing potency can be regulated (although not entirely dose dependent) by its applied quantity. There is also a major drawback for gene silencing with siRNA. siRNA induces only transient down-regulation of the target mRNA reaching e.g. a maximum over 5 days (depending mostly on the stability of siRNA and the proliferation rhythm of cells) that requires it to be applied repetitively to guarantee a stable silencing effect over the whole treatment period[41][53]. In contrast, DNA-based RNAi by shRNA bears the potential of being stably introduced in the genome after a single treatment with shRNA delivering, e.g., (lenti-)viral, vectors. Recently, biotechnology companies have focused on shRNA technology based therapeutics and made big efforts to develop them for clinical application in patients[54]. However, shRNA delivery by viral vectors may pose severe safety concerns as some patients treated with viral vectors for the Wiskott-Aldrich syndrome developed acute T-cell leukaemia[55]. After intensive exploration of this severe off-target effect of the treatment, the acquired T-cell leukaemia was found to be caused by viral vector insertion into the host genome, putatively activating oncogenes or deactivating tumor-suppressor genes[55]. Another problem remains the potential over-saturation of RISC with shRNA. When shRNA is expressed at too high levels the cell might not be able to correctly process the endogenous RNA which could cause significant side-effects such as apoptosis/necrosis[56][57].

All these safety concerns and obstacles significantly hampered the development of shRNA technology for clinical trials, favoring, at the least for the time being, siRNA for therapeutic gene silencing[58].

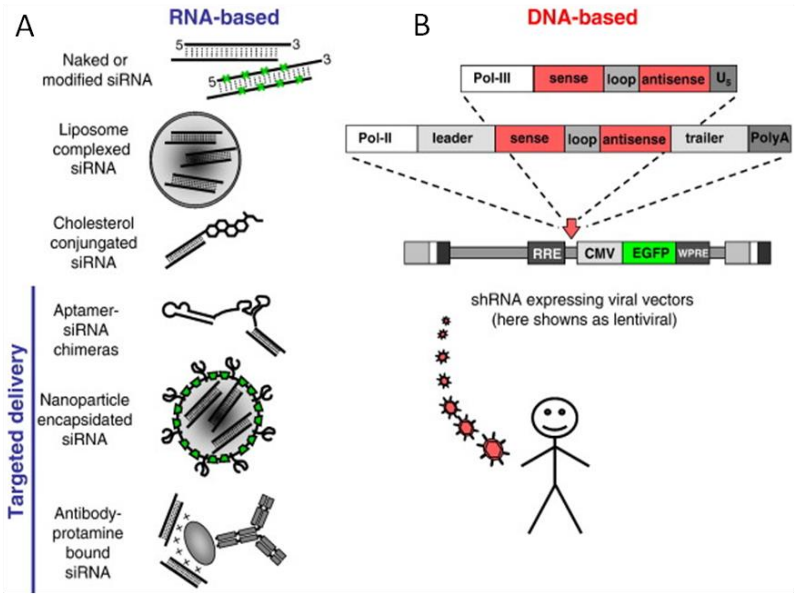

Figure 5: A: Manifold strategies for non-targeted or targeted siRNA delivery *in vivo*. B: Schematic diagram of *in vivo* shRNA delivery using (lenti-)viral vector technology (modified from figure 2 in Rossi J. *et al.*, *Advanced Drug Delivery Reviews*, 2007)[41].

1.2.4 Nanoparticles as siRNA vehicles

Due to their hydrophilic nature and negative charge and size, siRNAs cannot cross the cell membrane. Therefore, cellular delivery of siRNAs is usually achieved by cationic liposome based strategies. The main disadvantage of lipid based delivery systems *in vivo* is 1) the rapid liver clearance and 2) the lack of target tissue specificity[41]. Although cationic polymer and lipid-based siRNA complexes have been tested for systemic delivery in mice, their nanostructure is not covalently stabilized, weakening them in their interactions with serum proteins. Covalently stabilized siRNA carriers showed enhanced robustness in *in vivo* conditions and a prolonged blood circulation time of their siRNA cargo after *i.v.* injection compared to electrostatically stabilized siRNA delivery systems[59].

In 2012, L Nuhn *et al.* reported a new concept of synthesizing polymeric cationic nanohydrogel particles, then only with *in vitro* validation, as novel platform for siRNA delivery[60]. For this purpose, amphiphilic reactive ester block copolymers were synthesized by RAFT (reversible addition–fragmentation chain transfer) polymerization of pentafluorophenyl methacrylate as reactive ester monomer together with tri(ethylene glycol)-methyl ether methacrylate. After polymerization, a self-assembly of these polymers could be observed in aprotic solvent (DMSO), leading to the formation of nanometer-sized polymer aggregates (⌀~40nm). For the first generation of these nanohydrogel particles, the nano-superstructures were covalently cross-linked with stable spermine linkers, and for the second generation, as reported by Leber and Kaps *et al.* 2016, with an acid labile-ketal linker, yielding a well-defined robust nanostructure with a protein-repulsive PEG corona and thus potentially circumventing stability problems of non-covalently stabilized (polymeric) liposomes. After cross-linking, the cationic sponge nature of the nanohydrogel particles in their inner core effectively complexes siRNA and shields its siRNA cargo safely from premature degradation of nucleases or unfavorable (serum) protein interactions (Figure 6).

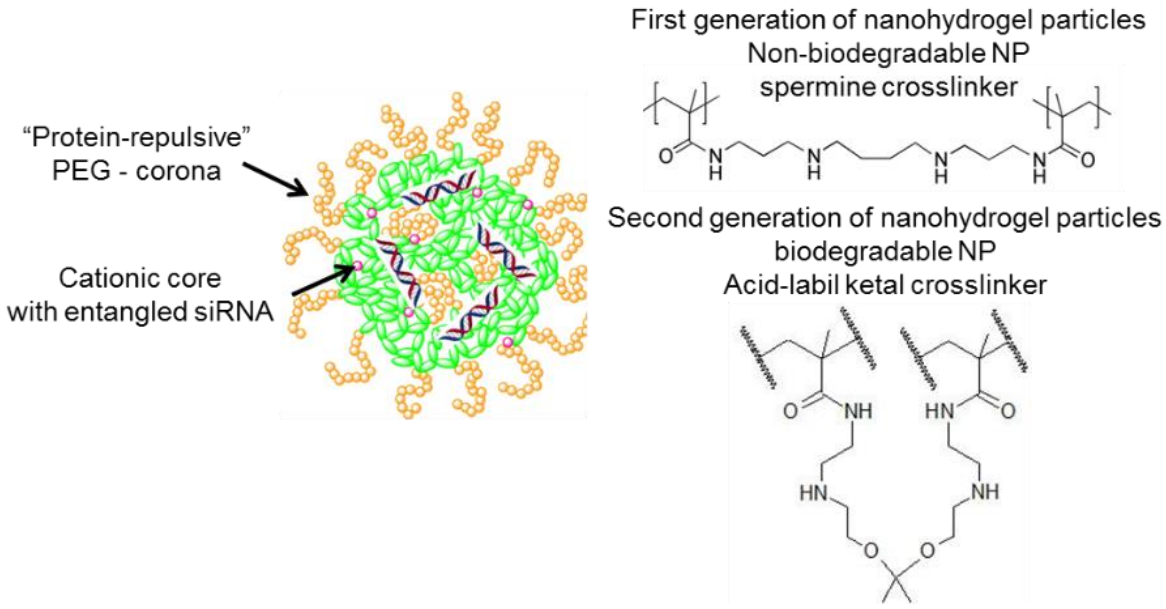

Figure 6: Schematic scheme of siRNA loaded (non)-biodegradable nanohydrogel particles[2]. PEG (polyethylene glycol) corona.

Therefore, these nanohydrogel particles could qualify as siRNA vehicles for *in vivo* therapeutic siRNA delivery to the liver of fibrotic mice and represent an interesting alternative to cationic polymer and lipid-based siRNA complexes[1][2].

1.2.5 Off target effects of siRNA and their vehicles

Off-target effects induced by siRNA or its vehicle are well known pitfalls for gene silencing. They lead to unwanted reductive/inductive activities for the cells' transcriptome, rendering knockdown effects difficult to interpret[61][62]. These off-target effects can originate from siRNA or the carrier itself.

Reductive off-target effects for non-targeted mRNA either via target-specific siRNA or unspecific scrambled siRNA (scsiRNA-negative control siRNA) originate from imperfect pairing of (sc)siRNA strands with sequence motifs that reside primarily in 3′ UTR (untranslated region) regions of cellular mRNAs[61]. Because only short regions of sequence complementarity are required for this type of off-target silencing, many transcripts can be affected and it is inherent to every chemically non-modified (sc)siRNA sequence (Figure 7)[61][63].

The inductive off-target effects, caused by both the carrier or its siRNA cargo, primarily result from an innate immune response, based on the activation of toll-like receptors (TLRs)[61][63]. TLRs, as part of the innate immune system, are responsible for the recognition of pathogen/-associated or other "unknown" exogenous molecular patterns, including RNAs and DNA sequences and other chemical structures, as occur in (non-modified) (sc)siRNA or possibly in the carriers (Figure 7)[61][63]. The siRNA and particle sensing receptors, especially TLR3, TLR7 and TLR8 traffic between the endoplasmic reticulum and intracellular compartments, such as endosomes and lysosomes, and trigger an alarm cascade in the cells, resulting in an (overall) increased transcriptional level mainly of cellular defense relevant genes (e.g. TNFα and IL-6)[61][64][65].

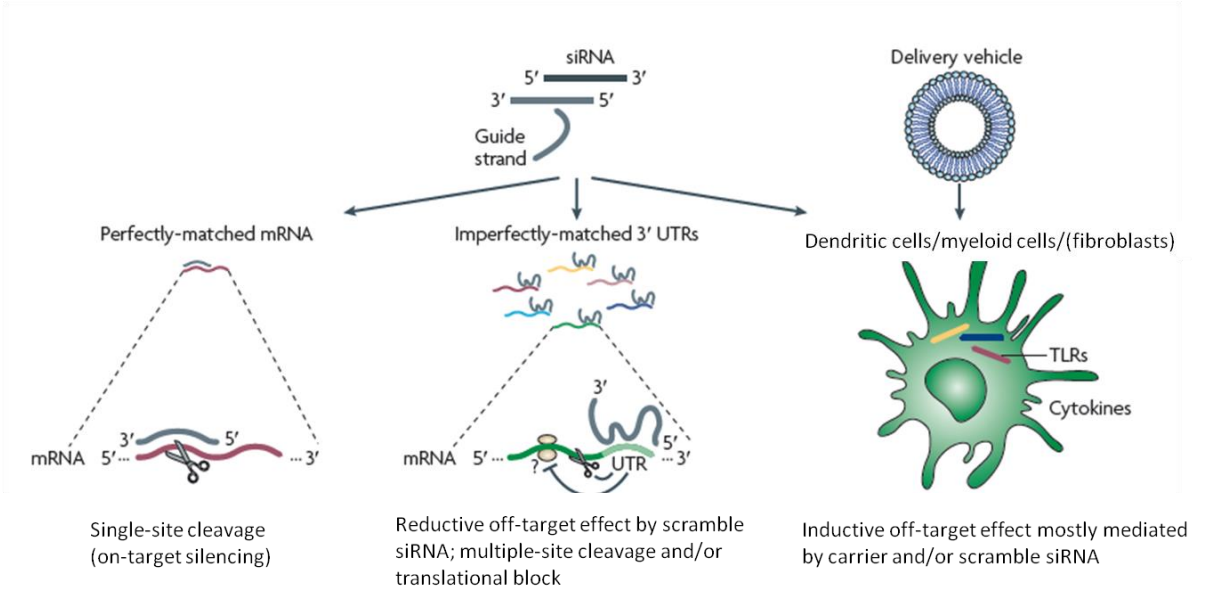

Figure 7. Types of off-target effects observed with siRNA and/or carriers. In addition to the desired on-target silencing, small interfering RNAs (siRNAs) generate several types of off-target effects, inducing/reducing non-targeted genes in the cells' transcriptome (modified from figure 1 in Linsley P. *et al.*, *Nature review, Drug discovery*, 2010)[61].

In order to prevent off-target effects, siRNA can be chemically modified with certain established modification patterns. These modifications must be wisely balanced and selected not to corrupt the siRNAs' sequence specificity for the target transcript[66]. Although the RNA sequences and their specific chemical groups recognized by TLRs are not entirely well defined, there seems to be preferential recognition of uridine (U) and guanosine (G)-rich sequences as well as the 2'-OH group at the ribose backbone of siRNA (Figure 8). It could be shown that siRNA sequences, lacking GU-rich motifs in combination with fluorination or methylation of 2'OH, provided active duplexes with low immunostimulatory activity and high sequence specify[61][67][68]. Until now little is known about the immunostimulatory/modulatory effect of nanoparticles as siRNA vehicles since this mostly depends on the material, size and electrostatic properties of the unique vehicle itself. However, neutral surface charge (zeta potential), adequate biodegradability, diameters <150nm and a protein repulsive corona (e.g. adequate PEG shielding on the surface) seem to be crucial factors to prevent an excessive immune stimulation by the siRNA carriers[69].

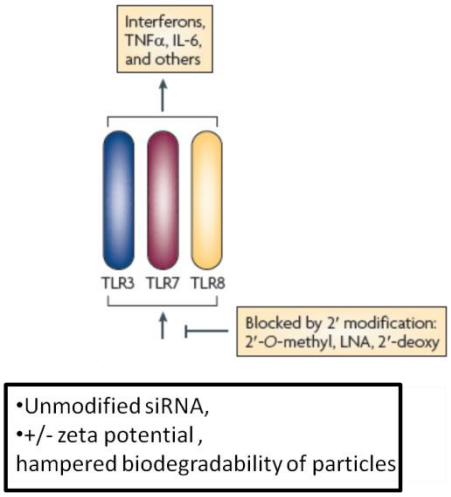

Figure 8: Immune responses to siRNA and carriers. Toll-like receptors (TLRs) protect the host from pathogens by detecting infectious non-self agents including double-stranded RNA (from viruses) and siRNA carriers, especially when they display significant surface charge (zeta potential) and low biodegradability. They are recognized by the immune system as an unwanted invader and trigger an innate immune response. Chemical modifications of siRNA at the 2′ position of ribose block or mitigate recognition by TLR3, TLR7 and TLR8. As a result, appropriate chemical modification of small interfering RNAs (siRNAs) can circumvent the immune response to siRNA delivery (modified from figure 2 in Linsley P. *et al., Nature review, Drug discovery*, 2010)[61].

2. Scope of this thesis

Despite great efforts, liver fibrosis, as an early disease stage towards cirrhosis, remains a hard-to-treat disease. Although remarkable progress in the understanding of the underlying pathologic mechanisms of liver fibrosis has been made, there is no specific and effective treatment available in the clinic. Consequently, patients with advanced fibrosis/cirrhosis have a high risk to develop complications of cirrhosis with live threating and limiting consequences such as severe bleeding from (esophageal or gastric) varices, renal or pulmonary failure due to the hepatorenal or hepatopulmonary syndrome, severe sepsis due to immune compromise, or hepatic encephalopathy coupled with hyperammonemia. Therefore, there is an urgent need for effective antifibrotic drugs in clinics to stop the progression and even induce reversal of liver fibrosis[70].

C Calvente *et al.* reported that lipoplexes loaded with anti-col1*a*1 siRNA can efficiently reduce liver collagen amount in fibrotic mice[28]. Lipoplexes, as non-covalently stabilized siRNA carriers, do not provide unrestricted siRNA/particle complex stability when they are challenged with protein containing media and harsh shear forces, both present in *in vivo* conditions (e.g. in the blood stream after *i.v.* injection). Furthermore, lipoplexes are difficult to decorate with targeting ligands (e.g. sugar moieties, antibodies) for cell specific delivery, since can dramatically affect their aggregation behavior[28].

Covalently cross-linked nanohydrogel particles as siRNA carriers share many positive characteristics with lipoplexes but exhibit increased stability *in vivo* and are well accessible for surface decoration with cell specific linkers. Furthermore, L Nuhn *et al.* have provided *in vitro* evidence that nanohydrogel particles are valuable siRNA carriers for gene knockdown[60].

The aim of this thesis was to study nanohydrogel particles as anti-col1a1 siRNA carriers for *in vivo* antifibrotic therapy of liver fibrosis. After the first generation of nanohydrogel particles (non-bioNP) loaded with anti-col1a1 siRNA were evaluated for liver fibrosis therapy *in vitro*, first (non-bioNP) and second generation of nanohydrogel particles (bio-NP) were to be tested in a head-to-head comparison both *in vitro* and *in vivo*. These (non-)bioNP and bioNP would then be thoroughly validated as siRNA carriers *in vitro* in liver fibrosis relevant cells. Here, *in vitro* cytotoxicity, cellular uptake and col1a1 gene knockdown were to be determined before carriers were assessed *in vivo* for liver fibrosis therapy.

After thorough *in vitro* validation, *in vivo* biodistribution of the siRNA loaded nanohydrogel particles was to be shown for the first time. Beside the biodistribution on the organ level, it might be interesting to test which liver cell types were addressed by non-bioNP and bioNP and their siRNA cargo after *iv* injection in mice. Furthermore, it was of interest to study how far non-bioNP vs bioNP would exhibit a distinct *in vivo* biodistribution pattern.

Non-bioNP and BioNP loaded with anti-col1a1 siRNA would then be evaluated for *in vivo* therapeutic gene knockdown in CCl_4-tretated liver fibrotic mice. Therapeutic collagen reduction as well as reduction of fibrosis surrogate markers were to be comprehensively evaluated on the RNA and protein level, to compare the therapeutic performance of anti-col1a1 siRNA loaded non-bioNP vs bioNP.

Finally, it was also of interest to test if the *in vitro* determined, enhanced biodegradability of bioNP would translate to *in vivo* conditions. Biocompatibility of nanohydrogel particles was to be tested in preliminary dose escalation studies to estimate their therapeutic index.

3. Materials and methods

3.1 Instrumentation

Table 1: Applied instruments

Name	Manufacturer (location, country)
FACS Canto II	BD Biosciences, Heidelberg, Germany
ChemiDoc™ XRS+ system	Bio Rad, Munich, Germany
Wide Mini-Sub Cell GT Cell	Bio Rad, Munich, Germany
PowerPac™ universal power supply	Bio Rad, Munich, Germany
IVIS spectrum imaging system	Caliper LifeSciences, Hopkinton, US
HXP120C kublercodix	Carl Zeiss, Munich, Germany
Zeiss microscope AX10	Carl Zeiss, Munich, Germany
Centrifuge 5804R	Eppendorf, Hamburg, Germany
Eppendorf centrifuge 5804R	Eppendorf, Hamburg, Germany
Eppendorf centrifuge 5415R	Eppendorf, Hamburg, Germany
Rotamax 120	Heidolph Instruments, Schwabach, Germany
Leica EG 1150c	Leica, Wetzlar, Germany
Leica TP1020	Leica, Wetzlar, Germany
Leica CM1950	Leica, Wetzlar, Germany
Microtome Leica RM2255	Leica, Wetzlar, Germany
Microtome Leica HI1210	Leica, Wetzlar, Germany
A&B applied biosystems step one plus real-time PCR system	LifeTechnologies GmbH, Darmstadt, Germany
Gentle MACS dissociator 3013	MACS Milteny-Biotec, Bergisch Gladbach, Germany
Balance Sartorius AX2202	PK Electronic Ettlingen, Germany
Balance Sartorius AX124	PK Electronic Ettlingen, Germany
Ergone Pipette 1000µl	Starlab GmbH, Hamburg, Germany
Ergone Pipette 200µl	Starlab GmbH, Hamburg, Germany
Ergone Pipette 20µl	Starlab GmbH, Hamburg, Germany
Ergone Pipette 10µl	Starlab GmbH, Hamburg, Germany
Ergone Pipette 2,5µl	Starlab GmbH, Hamburg, Germany
TECAN infinite M 200Pro	Tecan, Männedorf, Germany
Centrifuge HeraeusFresco21	Thermoscientific, Schwerte, Germany
HeraeusMultifuge X3R centrifuge	Thermoscientific, Schwerte, Germany
Microtome blade MX 35 premier 34/80mm	Thermoscientific, Schwerte, Germany
Centrifuge VWR mini star	VWR International, Darmstadt, Germany
Rocking platform	VWR International, Darmstadt, Germany
MulticalPH meter pH 538	WTW, Weilheim, Germany
IVIS imaging system	PerKinElmer, Waltham, USA

3.2 Consumables

Table 2: Applied consumables

Name	Manufacturer (location, country)
1000µl Tips	Starlab GmbH, Ahrensburg, Germany
200µl Tips	Starlab GmbH, Ahrensburg, Germany
0,1-20µl GradanteTips	Starlab GmbH, Ahrensburg, Germany
96 well plates flat bottomed	Greiner Bio-One, Frickenhausen, Germany

96-well fast thermal cycling	LifeTechnologies GmbH, Darmstadt, Germany
MicroAmp optical adhesive film	LifeTechnologies GmbH, Darmstadt, Germany
Cellstar tubes (15ml and 50ml)	Greiner Bio-One, Frickenhausen, Germany
Cell strainer (100µm)	BD Bioscience, Heidelberg, Germany
Cryo tubes	Greiner Bio-One, Frickenhausen, Germany
DAKO Pen	Dako Deutschland GmbH, Hamburg ,Germany
Disposal bags	Carl Roth, Karlsruhe, Germany
FACS tubes, polystyrene, 5 ml	BD Biosciences, Heidelberg, Germany
Filter paper	Whatman, Dassel, Germany
Gentle MACS C tubes	Miltenyi Biotec, Bergisch-Gladbach, Germany
Histosette tissue processing/embedding cassettes	Simport, Hague, Netherlands
Inject-F (single use injection) 1ml	B.Braun, Melsungen, Germany
Knittel glass cover slips 24*50mm	Iss, Bradford, United kingdom
Microscope coverslips	LifeTechnologies GmbH, Darmstadt, Germany
PCR tubes 0.2 ml Flat cap	Greiner Bio-One, Frickenhausen, Germany
Polysine slides	Thermoscientific, Braunschweig, Germany
Superfrost ultra plus slides	Thermoscientific, Braunschweig, Germany
Safe-lock tubes 2.0 ml	Eppendorf, Hamburg, Germany
Safe-lock tubes 1.5 ml	Eppendorf, Hamburg, Germany
Serological pipette, sterile (5,10,25 ml)	Greiner Bio-One, Frickenhausen, Germany
Superfrostultraplus slides	Thermoscientific, Braunschweig, Germany

3.3 Reagents and kits

Table 3: Applied reagents and kits

Name	**Manufacturer (location, country)**
β-mercapthoethanol	Sigma Aldrich, Steinheim, Germany
1-Propanol pure	Applichem, Darmstadt, Germany
2-Propanol pure	Applichem, Darmstadt, Germany
4-(Dimethylamino) benzaldehyde	Sigma Aldrich, Steinheim, Germany
70% Ethanol	Carl Roth GmbH, Karlsruhe, Germany
Agarose	Sigma Aldrich, Steinheim, Germany
Ammonium Persulfate	Sigma Aldrich, Steinheim, Germany
Antibody diluent	Dako Deutschland GmbH, Hamburg ,Germany
Bovine serum albumin(BSA)	Sigma Aldrich, Steinheim, Germany
cDNA SuperMix reverse transcription kit	Quanta, Gaithersburg, USA
Chloroform	Applichem, Darmstadt, Germany
Collagenase from Clostridium histolyticum	Sigma Aldrich, Steinheim, Germany
DAB Peroxidase (HRP) Substrate Kit	Vector Laboratories, Inc., Burlingame, USA
DEPC treated water	Life technologies GmbH, Darmstadt, Germany
Direct RED 80	Sigma Aldrich, Steinheim, Germany
DNase I	Sigma Aldrich, Steinheim, Germany
Eosin	Carl Roth GmbH, Karlsruhe, Germany

Ethanol absolute	VWR chemicals, Fontenay-sous-bois, France
Ethylendiamintetraacetatic acid (EDTA)	Sigma Aldrich, Steinheim, Germany
FACS- Flow	BD Bioscience, Heidelberg, Germany
FACS-Clean	BD Bioscience, Heidelberg, Germany
FACS-Rinse	BD Bioscience, Heidelberg, Germany
Fetal calf serum (FCS)	Invitrogen, San Diego, USA
Formaldehyde 4%	Carl Roth GmbH, Karlsruhe, Germany
Glycerol minimum 99%	Sigma Aldrich, Steinheim, Germany
Glycine	Sigma Aldrich, Steinheim, Germany
Hematoxylin	Merck, Darmstadt, Germany
Horse serum	Vector Laboratories, Burlingame, USA
Hydrochloric acid 6N	VWR, Darmstadt, Germany
Hydrogen peroxide 30%	Carl Roth GmbH, Karlsruhe, Germany
Ketamin Hameln 50mg/ml	Hameln pharmaceuticals, Hameln, Germany
L-Hydroxyproline	Merck KGaA, Hessen, Germany
Methanol Technical grade	Applichem, Darmstadt, Germany
OCT compound embedding medium for frozen tissue specimens	Sakura, Torrance, USA
Perchloric acid 70%	Sigma Aldrich, Steinheim, Germany
Phosphatase inhibitor	Roche, Mannheim, Germany
Picric acid	Sigma Aldrich, Steinheim, Germany
Potassium chloride	Carl Roth GmbH, Karlsruhe, Germany
Potassium dihydrogen phosphate	Carl Roth GmbH, Karlsruhe, Germany
Potassium phosphate monobasic	Sigma Aldrich, Steinheim, Germany
Protease inhibitor	Roche, Mannheim, Germany
qScript cDNA SuperMix	VWR(Quantabio) Darmstadt, Germany
Ribozol	Ampresco, Solon , USA
Rompun 2%	Bayer vital GmbH, Leverkusen, Germany
Roti-Histokitt II	Carl Roth, Karlsruhe, Germany
Sodium chloride	Carl Roth GmbH, Karlsruhe, Germany
Sodium citrate Dehydrate	Fisher- scientific New Jersey, USA
Sodium dodecyl sulfate	Sigma Aldrich, Steinheim, Germany
Sodium phosphate dibasic	Carl Roth GmbH, Karlsruhe, Germany
SYBR Green PCR mix	LifeTechnologies GmbH, Darmstadt, Germany
Taqman master mix	LifeTechnologies GmbH, Darmstadt, Germany
Triton^{TM} X-100	Sigma Aldrich, Steinheim, Germany
Trizma base	Sigma Aldrich, Steinheim, Germany
Tween 20	Merck KGaA, Darmstadt, Germany
VECTASTAIN ABC Systems	Vector Laboratories, Inc., Burlingame,USA
Xylene	Applichem, Darmstadt, Germany
GelRed 10,000x	Biotium, Fremont, USA
MTT	Sigma Aldrich, Steinheim, Germany
Lipofectamine®	LifeTechnologies, Darmstadt, Germany
Fixable Viability Dye eFluor® 506	eBioscience, USA, San Diego
Carbon tetrachloride CCl_4	Sigma Aldrich, Steinheim, Germany
Collagenase/Dispase	Roche, Penzberg, Germany
Red blood cell lysis solution	Milteny, Bergisch Gladbach, Germany

Collagenase IV	LifeTechnologies, Darmstadt, Germany
Krebs-Ringer bicarbonate buffer	Sigma Aldrich, Steinheim, Germany
oneComp beads	eBioscience, Frankfurt, Germany

3.4 Antibodies

Table 4: Applied antibodies

Name	**Manufacturer (location, country)**
Anti α-Sma (E148)	Abcam, Cambridge, UK
Pacific-Blue anti CD11b (M1/70)	Biolegend, Fell, Germany
FITC-anti CD45 (30-F11)	Biolegend, Fell, Germany
PE-anti CD31 (390)	Biolegend, Fell, Germany
Anti CD68 (FA-11)	Abcam, Cambridge, UK
PE-anti F4/80 (BM8)	Biolegend, Fell, Germany
Biotinylated goat anti rabbit IgG (H+L) (BA-1000)	Vector Laboratories, Inc., Burlingame,USA
Biotinylated goat anti rat IgG (H+L) (BA-9400)	Vector Laboratories, Inc., Burlingame,USA
Hepatocytes albumin-PE (Clone#188835,)	R&D, Boston, USA
Secondary antibody anti-rabbit-FITC	LifeTechnologies, Darmstadt, Germany
Anti-Mouse CD16/CD32 (2.4G2)	Biolegend, Fell, Germany

3.5 General buffers and solutions

Table 5: Applied solutions and buffers

Acidified water	Glacial acetic acid 5ml ddH_2O 1000ml
Antigen unmasking citrate buffer	2.94g sodium citrate trisodium salt dehydrate to 1l dH_2O Adjust pH to 6.0
Blocking solution	2.5% normal horse serum
Citric acetate buffer	5% citric acid (5g) 7.24% sodium acetate (7.24g) 3.4% natriumhydroxid (NaOH 3.4g) 1.2% glacial acetic acid (1.2ml) dissolve into 100 ml dH_2O, adjust pH to 6.0
Chloramine T	32ml citric acetate buffer pH 6.0 4ml distilled water 4ml n-propanol 564mg chloramine T hydrate shake well to mix , heated around 50°C then RT slightly in water bath to dissolve
Ehrlich's reagent	7.9ml n-propanol 3.31ml 70% perchloric acid 1.91mg 4-Dimethylaminobenyaldehyde recommend to be prepared freshly just before cool down before experiment.
FACS fixation buffer	0.4% Formaldehyde in PBS
Phosphate buffered saline (PBS)	137mM sodium chloride (NaCl 80g) 2.0mM Potassium chloride (KCl 2g)

10X stock solution	10mM Sodium phosphate dibasic (Na_2HPO_4 14.4g) 1.8mM Monopotassium Phosphate (KH_2PO_4 2.4g) to 1l dH_2O adjust pH to 7.4 with hydrochloric acid (HCl)
Tris Buffered Saline (TBS) 10X stock solution	24.2g Trizma Base ($C_4H_{11}NO_3$) 80g Sodium chloride (NaCl) to 1l adjust pH to 7.6 with HCl
PBST 1X	100ml 10X PBS stock solution 900ml d H_2O, 1ml Tween 20
TBST 1X	100ml 10X TBS stock solution 900ml d H_2O, 1ml Tween 20
Loading buffer tris-glycine 10X stock solution	121g Trisma base Glycine 577g dissolve into 4l d H_2O
Running buffer	100ml 10X Tris-Glycine buffer 10ml 10% SDS 890ml dH_2O
Primary Antibody Dilution Buffer	1X TBST with 5% BSA
0.1% Sirius Red solution	Sirius Red 0.5g saturated picric acid 500ml
1% Agarose solution	1g agarose in 100ml 1xTBST
Mild acidic wash solution	0.1M sodium acetate, 0.05M NaCl, pH 5.5

3.6 Real time PCR primer

Table 6: Applied qPCR primers

Target gene	Forward primer (5'-3')	Taqman Probe (if applicable)	Reverse primer (5'-3')
αSMA	ACAGCCCTCGC ACCCA	CAAGATCATTGCC CCTCCAGAACGC	GCCACCGATCCAGA CAGAGT
Procollagen1(a)1	TCCGGCTCCTGC TCCTCTTA	TTCTTGGCCATGC GTCAGGAGGG	GTATGCAGCTGACT TCAGGGATGT
CD68 (SYBR-Green)	CTTCCCACAGG CAGCACAG		AATGATGAGAGGCA GCAAGAG
GAPDH (SYBR-Green)	AGGTCGGTGTG AACGGATTTG		GGGGTCGTTGATGG CAACA
GAPDH	GACGGCCGCAT CTTCTTGT	CAGTGCCAGCCTC GTCCCGTAGA	CACACCGACCTTCA CCATTTT

3.7 Cy5-labeled siRNA and scrambled siRNA

Cy5-labeled anti-col1α1 siRNA (for *in vitro/in vivo* knockdown experiments), based on the sequence

5'-GaG GUa UgC uUG AuC uGu AuU-3'

5'uAc AgA uCa AgC aUa CcU cGg X-3'

and Cy5-labeled anti-Tie2 siRNA (for *in vitro* cellular uptake experiments), based on the sequence

5’-CcA uCa UuU gCc CaG aUa U-3’

5’-uUA UcU gGg CaA aUg AuG G X-3’

and with the 2’-O-methylated bases in lower case letters and the Cy-5 NIR dye attached to the 3’ by a C6 amino spacer (X) was purchased from BioSpring (Germany, Frankfurt). siRNA was purified by HPLC to remove contaminating unbound Cy5 dye.

As scrambled siGENOME Non-Targeting siRNA #2 (Dharmacon, Lafayette (USA)) with the following sequence was used as negative control *in vitro/in vivo*:

5’-UAAGGCUAUGAAGAGAUACUU-3’

5’-GUAUCUCUUCAUAGCCUUAUU-3’

3.8 Preparations of (non)-biodegradable nanohydrogel particles ((non)-bioNP))

All nanoparticle preparations and complexations (cargo loading) were performed by Nadine Leber in the Institute of Chemistry (Director Prof. Rudolf Zentel), University of Mainz and by Dr. L. Nuhn (now-) Faculty of Pharmaceutical Sciences (Group leader Prof. Bruno G. De Geest), University of Ghent, Belgian.

3.8.1 Complexation procedure of siRNA with (non)-bioNP

siRNA was freshly complexed with (non)-bioNP ((w/w) mass ratio siRNA to NP for non-bioNP 1:10 and for bioNP 1:30) in 10mM HEPES solution at pH 7.2 for 1h and 24h at 37ºC. siRNA/(non)-bioNP complex formation was routinely checked by gel electrophoresis before each experiment (Appendix Figure S1). Therefore, a 1% agarose gel was prepared with TBE buffer and substituted with 1xGelRed for nucleic acid staining. After addition of loading buffer, all samples were transferred onto the gel and analyzed at 120 V for 30 min. Visualization occurred in a BioRAD ChemiDoc imaging system.

3.8.2 Synthesis of (non)-bioNP

The synthesis of nanohydrogel particles, first reported by L Nuhn *et. al.* 2012[60], has been conducted *ex domo* by Dr. Lutz Nuhn and Nadine Leber in the group of Prof. Zentel at the University of Mainz (Germany). Parts of the following chapters concerning the synthesis of (non-)bioNP have been published L Kaps, L Nuhn *et. al.*, *Adv. Healthcare Mat.* 2015[1] and L Kaps, N Leber *et.al., J. Control. Release* 2017[2].

Accordingly, for a comprehensive description of the synthesis and the detailed compound analysis as well as for the applied instrumentations, please refer to our above-mentioned publications.

3.8.2.1 Synthesis of the amphiphilic block copolymers poly(oligo(ethylene glycol) methyl ether metacrylate)-block-poly(pentafluorophenyl methacrylate) P(MEOxMA)-b-P(PFPMA)

The syntheses of poly(oligo(ethyleneglycol)methyl-ether-metacrylate)-block-poly(pentafluorophenyl methacrylate) P(MEO_xMA)-b-P(PFPMA) **P1** (M_n = 12300 g/mol, Đ =

1.30), **P2** (M_n = 9600g/mol, Đ = 1.31), **P3** (M_n = 13,900g/mol, Đ = 1.30) and **P4** (M_n = 12000g/mol, Đ = 1.39) were performed as recently described[60]. Here in brief, a reaction mixture consisting of MEO_3MA (4g, 17.24mmol), 4-cyano-4-(phenylcarbonothioylthio)pentanoic acid (CTA) (213.8mg, 0.766mmol) and azobisisobutyronitrile (AIBN) (12.6mg, 0.0766mmol) dissolved in 4ml absolute dioxane was degassed by three freeze-pump-thaw cycles and polymerized under vacuum at 65°C for 18h. After determining monomer conversion by ^{1}H-NMR, precipitation of the homo polymer in *n*-hexane was realized. Threefold precipitation ensured removal of unreacted monomer and after evaporation of remaining solvent under vacuum the final polymer was obtained as a pink viscous oil. For the $MEO_{4/5}MA$ homo polymer the synthesis was done similarly using the corresponding monomer. The final degree of polymerization was calculated by ^{1}H-NMR (for ^{1}H-NMR analysis in detail[2]).

For block copolymer synthesis the homo polymers could be used as macro chain transfer agents. Therefore, PFPMA (7.45g, 29.55mmol), macro-CTA (3.0g, 0.513mmol) and AIBN (8.4mg, 0.0513mmol) were dissolved in 8mL anhydrous dioxane and again degassed by three freeze-pump-thaw cycles. Polymerization was performed for 66h at 65°C under vacuum. Conversion was determined by ^{1}H-NMR analysis of the reaction mixture. Threefold precipitation in *n*-hexane yielded the corresponding block copolymer **P3** as a pink solid. The final repeating units were again calculated by ^{1}H-NMR (for ^{1}H-NMR analysis in detail[2]).

Removal of the dithiobenzoate endgroups was done by reaction of the corresponding polymer **P3**' (5.5g, 0.375mmol) with 30-fold excess of AIBN (1.84g, 11.25mmol) in 10mL dioxane for 16h at 65°C yielding the final polymer **P3** as a colorless powder after three times precipitation in n-hexane and drying (4.5g, 0.324mmol) (for ^{1}H-NMR and ^{13}C-NMR analysis in detail[2]).

3.8.2.2 Synthesis of the ketal-based cross-linker (2,2-Di-[5-amino-3-azapent-1-oxy]-propane) for bioNP

The synthesis of 2,2-Di-[N,N'-bis(benzyloxycarbonyl)-5-amino-3-azapent-1-oxy]-propane **P6** and its precursors for the ketal-based cross-linker have already been reported earlier in literature[71][72] and[2].

Under constant shaking and hydrogen atmosphere **P6** (1.62g, 2.06mmol) was dissolved in methanol pH 7 and catalytic amounts palladium hydroxide on charcoal (83mg, 0.29mmol) were added according to literature[73]. After 9h complete conversion was confirmed by thin-layer chromatography (TLC). The catalyst was removed by filtration followed by removal of the solvent under reduced pressure yielding 2,2-di-[5-amino-3-azapent-1-oxy]-propane **P7** as a yellow oil (0.5g, 2.01mmol) (for ^{1}H-NMR and ^{13}C-NMR analysis in detail[2]).

3.8.2.3 Cross-linking of near infrared/FITC labeled (non-)bioNP

In brief, in a round-bottom flask equipped with a magnetic stirrer and argon atmosphere the polymer **P3** (40 mg, 2.9µmol or 92.8µmol PFPMA units) was dissolved in anhydrous DMSO at a final concentration of 10mg/ml. To enhance polymer dispersion and self-assembly into micelles the mixture was sonicated for 1-2h until a clear solution was obtained.

For fluorescent labeling, (non-)bioNP were stirred with Oregon Green®488 cadaverine or CS800® (both obtained from LifeTechnologies, Darmstadt, Germany), (184µl of a 2.5mg/ml stock solution in DMSO, 0.928µmol) and ~10% (7.2µl) of the total triethylamine amount for 18h at room temperature.

For cross-linking, spermine, an endogenous produced oligoamine[74], for non-bioNP or ketal cross-linker **P7** (11.5mg, 46.4µmol) for bioNP and triethylamine (77.2µL, 556.8µmol) were added and the reaction mixture was stirred for 18h at 50°C. Complete conversion of PFPMA was confirmed by ^{19}F-NMR. Yet, for removal of remaining PFPMA below the NMR detection limit, methoxy triethylene glycol amine (15.1mg, 92.8µmol) was added. The reaction was continued for 18h and then dialyzed for one week against water containing 0.1% ammonium hydroxide. The remaining aqueous solution was lyophilized yielding the nanohydrogel particles as dry powder.

Determination of critical aggregation concentration (CAC) by pyrene fluorescence spectroscopy was done as earlier reported[60].

The size of Cy5-siRNA/(non-)bioNP complexes were determined by fluorescence correlation spectroscopy measurements (FCS) and performed with a commercial FCS setup consisting of an Olympus IX70/ FluoView300 confocal microscope with a PicoQuant FCS extension (for a detailed description of FCS analysis, please refer to N Leber N, L Kaps *et. al. J. Contr. Release* 2016[2])

3.9 *In vitro* validation of (non-)bioNP

3.9.1 Cell culture[1][2]

Murine 3T3 fibroblasts, murine macrophages RAW 264.7, human hepatocytes HepG2 macrophages, murine hepatocytes AML-12 and small vascular endothelial cells SVEC were cultured in Dulbecco's modified Eagle's medium (Sigma-Aldrich, Taufkirchen, Germany) supplemented with 10% FBS, 1% penicillin, 1% L-glutamine, and 1% streptomycin in 5% CO_2 at 37°C. The medium was routinely changed every 2 days and the cells were separated by cell scraping (only for RAW macrophages) or trypsinization with trypsin-EDTA (0.05%) plus phenol red from LifeTechnologies (Darmstadt, Germany) before reaching confluency.

3.9.2 *In vitro* cytotoxicity of scramble siRNA loaded (non-)bioNP[1][2]

The MTT (3-(4,5-dimethylthiazol-2-yl)-2,5-diphenyltetrazoliumbromide) assay was used to assess the cytotoxic effects of siRNA-loaded bioNP and non-bioNP on RAW, 3T3, and SVEC. In brief, cells were seeded into 96-well plates at a density of approximately 7,000 cells per well. After a 24h of incubation, the supplement containing medium with increasing concentrations of siRNA/NP (10:1 weight-to-weight ratio of NP:siRNA for non-bioNP and 30:1 for bioNP) corresponding to 5, 10, 20, 50, 100, 200 and 400nM siRNA was added to displace the old cell culture medium. After 48h of incubation, 20µL of MTT PBS (4 mg/mL) was added to the culture medium and incubation was carried out for another 4h, followed by removal of the medium and addition of 15µL of DMSO and placement on an orbital shaker for 1h under exclusion of light. Finally, the 96-well plates were measured on an Infinite M200Pro

spectrofluorometer (TECAN, Männerdorf, Switzerland) at 570 nm. As reference the OD570 of nanoparticles treated cells was normalized with the OD570 of cells exposed to PBS alone.

3.9.3 *In vitro* gene knockdown mediated by anti-col1α1-siRNA loaded (non-) bioNP[1][2]

To assess knockdown efficiency, collagen producing 3T3 cells were seeded in 12-well culture plates at a density of 250,000 cells per well and allowed to adhere overnight. 24h before the knockdown cells were preincubated with supplemented DMEM medium containing 5ng/ml TGFβ1 (R&D SYSTEMS, Minneapolis, USA). After the plates were washed three times with PBS, the cells were incubated with final anti-col1α1 or scrambled siRNA (complexed by bio/NP at 30:1 weight-to-weight ratio of NP:siRNA or by non-bio/NP at 10:1) concentration at 25, 50nM and 100nM for 48h at 37°C. Further controls were an equivalent volume of PBS buffer or naked siRNA at a final concentration of 100nM. Anti-col1α1 siRNA mixed with Lipofectamine® was used according to the manufacture's protocol and served as positive control. All experiments were performed in triplicates (n=3).

3.9.4 *In vitro* cellular uptake of Cy5-siRNA loaded (non-)bioNP by FACS[1][2]

Murine RAW macrophages and 3T3 cells fibroblasts were seeded in 6-well culture plates at a density of 700,000 cells per well and allowed to adhere overnight. Afterwards the plates were washed with PBS and incubated with a final concentration of 25, 50 and 100nM Cy5-labeled off-target anti-Tie2 (endothelial cell marker) siRNA (to prevent interference with endogenous mRNA transcripts of RAW macrophages or 3T3 fibroblast cells) complexed with non-bioNP or bioNP (10:1 weight-to-weight ratio of non-bioNP:siRNA and corresponding 30:1 ratio for bioNP:siRNA, respectively) for 1h and 24h at 37ºC.

To rule out auto-fluorescence of siRNA-particle, cells were incubated with a final concentration of 100nM unlabeled scrambled siRNA complexed with unlabeled non-bioNP or bioNP (10:1 weight-to-weight ratio of non-bio NP:siRNA and corresponding 30:1 ratio for bio NP:siRNA, respectively) for 24 h in the cell incubator before harvest for flow cytometry. In addition, control cells were incubated with similar particle and siRNA concentrations for 24h at 4°C. At the preselected time intervals (1h and 24h), culture medium was removed and the cells were washed with cold PBS followed by a mild acidic wash (0.1M sodium acetate, 0.05M NaCl, pH 5.5) for 5min at 4°C to remove unspecific bound siRNA/NP aggregates from the cell surfaces. After washing with ice-cold PBS cells were detached as described above and stained with a viability dye (Fixable Viability Dye eFluor® 506, eBioscience, USA, San Diego) according to the manufacture's protocol. Cells were then fixed with 4% formaldehyde for 15 min at 37°C and subjected to flow cytometry (BD FACSCantoII, BD Bioscience, Canada, Mississauga) the next day. Compensation was performed by BD FACSDiva software version 7.0 with oneComp eBeads (eBioscience, Frankfurt, Germany). 10,000-50,000 cells were measured per staining. Further data analysis was carried out using open source Flowing Software 2.5.0 (Perttu Terho, Turku Centre for Biotechnology, Finland).

3.9.5 Quantitative RT-PCR[1][2]

After indicated incubation times of the 3T3 fibroblasts with anti-col1α1 siRNA loaded in non-bioNP or bioNP (described above) or after isolation of cells from homogenized harvested livers

by Tissue LyserII (Qiagen, Venlo, Netherlands) (described below) RNA was extracted with GeneMATRIX Universal RNA Purification Kit (EURX, Germany, Berlin) according to the manufacturer's protocol. 1µg of total RNA was reverse transcribed into cDNA using the qScript cDNA SuperMix (Quantas, Beverly, USA). The TaqMan/CyberGreen primers and (TaqMan probes) for Col1α1, αSMA were synthesized by Eurofins (Mannheim, Germany). TaqMan and CyberGreen reaction mixtures were purchased by Applied Biosystems (Darmstadt, Germany). Transcript levels of glyceraldehyde phosphate dehydrogenase (GAPDH) were used to normalize data and to control for RNA integrity. Samples were amplified by the TaqMan/CyberGreen technology and analyzed using a Step One Plus sequence amplification system from LifeTechnologies (Darmstadt, Germany). Results were expressed as the ratio of the copy number of the target gene divided by the number of copies of the housekeeping gene (GAPDH) within individual PCR runs.

3.9.6 Laser scattering confocal microscopy for *in vitro* cellular uptake[1][2]

RAW macrophages/3T3 fibroblasts were cultured overnight on chamber slides (Nunc-Lab-Tek, ThermoFisher Scientific, USA) in protein rich media until their complete adherence on the slide. After incubation with NP, cells were fixed with 4% PFA and nuclei counter stained with DAPI. After fixation, slides were embedded with Fluoroshield (DAKO, Glostrup, Denmark) and imaged on a Zeiss LSM 710 NLO (Germany, Jena) laser scanning microscope.

3.10 Biodistribution of Cy5-siRNA loaded (non-)bioNP by IVIS imaging

3.10.1 *In vivo* imaging of Cy5-siRNA loaded near infrared (NIR) labeled (non-)bioNP[1][2]

In vivo NIR fluorescence imaging of NIR labeled non-bioNP or bioNP loaded with Cy5-dye labeled anti-col1α1 siRNA was performed with the IVIS Spectrum Imaging system (Caliper LifeSciences, Hopkinton, US). After injection at predetermined time points, mice were transferred into the machine's image chamber and anesthetized temporarily with isoflurane. A picture integration time of 4s was set for the fluorescence source. Filters were adjusted with excitation at 745nm and emission at 800nm to visualize IRDye 800RS (CS800®) labeled nanohydrogel particles (non-bioNP or bioNP), and for Cy5-dye labeled anti-col1α1 siRNA it was set to excitation at 640nm and emission at 700nm.

3.10.2 *Ex vivo* imaging of Cy5-siRNA loaded near infrared (NIR) labeled (non-)bioNP[1][2]

48h after the second injection of siRNA loaded non-bioNP or bioNP mice were sacrificed and liver, spleen, lungs, heart and kidneys immediately transferred into the imaging chamber of the IVIS Spectrum Imaging system (PerKinElmer, Waltham, USA). Image acquisition was performed with the same settings as described above for IRDye 800RS labeled non-bioNP or bioNP and for Cy5-dye labeled anti-col1α1 siRNA. *Ex vivo* fluorescence's (IVIS imaging) quantification was quantified with the provided IVIS software (Living Image® *software*) by drawing nicely fitting regions of interests (ROI) around the analyzed organs. This procedure allowed accurate and reproducible fluorescence's quantification in the organs[28].

3.10.3 Biodistribution on cellular level of Cy5-siRNA loaded (non-)bioNP

3.10.3.1 Preparation of lung single cell suspensions[1][2]

Directly after the *ex vivo* imaging lungs were digested according to the manufactures protocol (Collagenase/Dispase, Roche, Penzberg, Germany). Briefly, lungs were washed by intrapulmonary injection with ice cold PBS, minced in ice cold PBS into small pieces and collagenase/dispase solution (Roche, Penzberg, Germany) was added to a final concentration of 2mg/mL. Lungs were incubated under smooth rotation for 45 min at 37°C. The digest was cleared through a 70µm filter (Milteny, Germany, Bergisch Gladbach) and centrifuged at 500g for 6 min. After removal of the supernatant the remaining cell pellet was resuspended in 10mL 1× Red Blood Cell Lysis Solution (Milteny, Bergisch Gladbach, Germany).

3.10.3.2 Preparation of liver single cell suspensions[1][2]

After the *ex vivo* imaging livers were rinsed with PBS and after removal of the gall bladder digested with 5,000U/mL of collagenaseIV in Krebs-Ringer buffer pH 7.4. The livers were then carefully homogenized with a gentleMACS™ dissociator (Milteny, Germany, Bergisch Gladbach) and incubated for 30 min at 37°C. The homogenization step was repeated and the cell suspension filtered over a 100µm cell strainer to remove non-digested material. The filtered cell suspension was centrifuged at 17–21g for 4 min at 4°C to remove hepatocytes, the supernatant transferred into new tubes and centrifuged at 300g for 10 min at 4°C to collect all non-parenchymal cells. The resulting supernatant was removed completely and the remaining cell pellet was resuspended in 10mL 1× Red Blood Cell Lysis Solution (Milteny, Bergisch Gladbach, Germany) for 5 min at RT, followed by three washes with PBS.

3.10.3.3 *In vivo* cellular uptake of Cy5-siRNA loaded (non-)bioNP by FACS[1][2]

The liver and lung cells obtained from mice injected with siRNA loaded (non)-bio NP were blocked with anti-Mouse CD16/CD32 (clone 2.4G2) and subsequently stained with fluorochrome conjugated cell specific antibodies to quantify colocalization of Cy5-labeled anti-col1α1 siRNA complexed with near infrared-labeled NP by FACS analysis. The following antibodies were used: macrophages CD45-FITC (clone 30-F11) combined with F4/80-PE (clone BM8) or CD11b-PacificBlue (clone M1/70, all eBiolegend, San Diego, USA), hepatocytes Albumin-PE (Clone #188835, R&D, Boston, USA), myofibroblasts αSMA (E184, Abcam, Cambridge, UK) combined with secondary antibody anti-rabbit-FITC (LifeTechnologies, Darmstadt, Germany). eFluor506 (eBioscience, San Diego, USA) was used to exclude dead cells. After staining cells were fixed with 4% formaldehyde for 15 min at 37°C and measured using a BD FACSCantoII (BD Bioscience, Canada, Mississauga) flow cytometer on the following day. Compensation was performed automatically by BD FACSDiva software version 7.0 with oneComp eBeads (eBioscience, Frankfurt, Germany). 10,000-50,000 cells were measured per staining. Further analysis of flow cytometry data was performed using open source Flowing Software 2.5.0 (Perttu Terho, Turku Centre for Biotechnology, Finland).

3.11 *In vivo* collagen knockdown on RNA and protein level mediated by anti-col1α1 siRNA loaded (non-)bioNP

3.11.1 Liver fibrosis model[1][2]

All animal studies were approved by the local ethics committee on animal care (number 23177-07/612-1-007, Government of Rhineland Palatinate, Germany). 8 weeks old female Balb/c mice (body weight ~20g) were purchased from Charles River (Sulzfeld, Germany) and kept under 12h light-dark cycles at 25°C and 40-60% humidity with humane care. Mice had access to regular chow and water *ad libitum*. At predetermined time points mice were sacrificed by cervical dislocation. Carbon tetrachloride CCl_4 (Sigma-Aldrich, St.Louis, USA) diluted in mineral oil (Sigma-Aldrich, St.Louis, USA) was given by oral gavage 3 times a week in an escalating dose protocol (first dose 0.875ml/kg; 1.75ml/kg week 1; 2.5ml/kg week 2) as reported[14][28]. Mice gavaged with mineral oil alone served as non-fibrotic/CCl_4 vehicle controls.

3.11.2 *In vivo* therapeutic gene knockdown[1][2]

During the second week of fibrosis induction, mice (n=5 per group) were anaesthetized with isoflurane gas and injected retroorbitally with 1mg/kg, 2mg/kg Cy5-labeled anti-col1α1 siRNA loaded non-bioNP or bioNP (siRNA:(non-)NP weight-to-weight ratio as mentioned before). Nanohydrogel particles loaded with scrambled siRNA (applying the corresponding mass ratio siRNA:(non-)NP like mentioned before) mice group (n=5 per group) injected into mice (n=5 per group) served as control. Another control group received 250µL PBS per mouse. NP-IR:siRNA or PBS were injected twice with 48h apart, followed by organ harvest 48h after the last injection. *In vivo* gene knockdown was analyzed by quantitative RT-PCR of harvested liver tissues as described in 2.9.5.

3.11.3 *In vivo* collagen quantification on protein level

3.11.3.1 Hydroxyproline quantification[1][2]

Liver collagen content was determined colorimetrically as total hydroxyproline as described recently[1]. Briefly, snap frozen liver specimens from the left, right and middle lobes, each weighing between 50 and 100mg, were combined and homogenized in 3 mL of 6N HCl, followed by overnight hydrolysis at 110°C. Triplicates of 5µL were placed in a transparent 96 well-plate (Greiner bio-one, Kremsmünster, Austria) and mixed with 50µL of 0.1M citrate buffer, pH 6.0, and 100µL of 150mg chloramine T dissolved in citrate buffer (0.1M, pH 6.0). After 30 min incubation at RT 100µL of cooled Ehrlich´s reagent (1.25g of dimethyl-benzaldehyde dissolved in 100ml distilled water) was added and incubated at 65°C for 30 min. Absorbance was measured at 550nm in an Infinite M200Pro spectrophotometer (TECAN, Austria). Total hydroxyproline (µg/liver weight) was calculated on the basis of individual liver weights and the corresponding relative hydroxyproline content (µg/100 mg liver tissue). The assay data represent the average of two independent experiments.

3.11.3.2 Morphometrical readout of Sirius Red stained liver sections[1][2]

Formalin fixed liver sections were stained with H&E for 5 min, followed by 5% Picro-Sirius Red (Sigma-Aldrich) at RT for 30 min and washed in distilled water and 0.5% acetic acid. 5

randomly selected fields (x100) were photographed using a Zeiss Scope A.1 microscope and an AxioCam MRC Zeiss camera (Jena, Germany) and the percentage of the Sirius Red stained area was measured by Image J software (open source, National Institutes of Health, Maryland, USA) with an adjusted threshold setting. For an accurate morphometrical quantification of collagen portal areas were excluded and only parenchymal collagen deposition was quantified, representing the pathophysiologically relevant collagen deposition[1]. Percentages of Sirius Red stained area in 5 randomly selected fields from each specimen, as assessed by computerized image analysis, are expressed as means ± SD (n=5 per group; and n=3 per sample).

3.11.3.3 ABC immunohistology and quantification[1][2]

4µm thick formalin fixed liver sections were steam boiled (Tefal VS 4003, Rumilly, France) in citrate buffer, pH 6.0, for 10 min, after preincubation with 3% hydrogen peroxide for 10 min and blocking with 10% normal goat serum (Invitrogen, Darmstadt, Germany) or Vector Lab Blocking Reagent at RT for 60 min at RT. Mouse monoclonal antibody to αSMA (1:2,000 dilution) or CD68 (1µg/mL working concentration, both Abcam, Cambridge, UK) was diluted in 10% normal goat serum (1:2500, Invitrogen, Darmstadt, Germany) and incubated with blocked sections at 4°C overnight, followed by biotinylated horse anti-mouse IgG (1:500, Vector Labs, Peterborough, UK) for 30 min, and Avidin-Biotin-enzyme Complex (ABC) mixture at RT for 30 min and the DAB (3, 3'-diaminobenzidine) solution (all from Vector Labs) for 10 s. Nuclei were counterstained with hematoxylin (Sigma-Aldrich) for 3 min, followed by dehydration and embedding in Mounting Media (Sigma-Aldrich). αSMA positive cells were quantified from 5 randomly selected fields (x200) using a Zeiss Scope A.1 microscope and an AxioCam MRC Zeiss camera (Jena, Germany). The area occupied by αSMA positive cells was analyzed by Image J software (freeware, Maryland, USA) in 5 randomly selected fields from each specimen, as assessed by computerized image analysis (means ± SD; n = 5 per group; n = 3 per sample).

3.12 Serum chemistry for acute *in vivo* toxicity[1][2]

Alanine transaminase (ALT), aspartate transaminase (AST), total bilirubin (Bili), alkaline phosphatase (ALP), gamma-glutamyl transferase (GGT) and creatinine (Crea) levels were determined in mouse sera using standardized kits (Abbott, Green Oaks, USA) and an automated analyzer ARCHITECT (Abbott, Green Oaks, USA)

3.13 Statistics[1][2]

Statistical analysis was performed using Microsoft Excel software (Redmond, USA). Data are expressed as means ± SD. The statistical significances of differences were evaluated by the independent variables t-test or one-way ANOVA (if indicated) using GraphPad Prism version 5.0 (San Diego, USA).

4. Results

4.1 Synthesis of non-biodegradable (non-bioNP) and biodegradable nanohydrogel particles (bioNP) as siRNA vehicle in liver fibrosis therapy

(Non-)bioNP were synthesized by reversible addition fragmentation transfer (RAFT) block-copolymerization of tri(ethylene glycol) methylether methacrylate (MEO_3MA) and pentafluorophenyl methacrylate (PFPMA). The narrowly distributed amphiphilic reactive ester block copolymers spontaneously self-assembled in polar-aprotic solvents (e.g., dimethylsulfoxide) into nano-sized micellar aggregates (Ø~40 nm, compare Table 7). These nano-sized superstructures were cross-linked with spermine for non-bioNP and acid-labil ketal-linker for bioNP by full conversion of the fuorophenyl reactive ester moieties with the functional amine groups of the spermine/ketal linker (Figure 9). The resulting covalently crosslinked nanoparticles were transferred from DMSO into aqueous medium *via* dialysis against water (for bioNP supplemented with 0.1% ammonium hydroxide solution to avoid ketal degradation) and then isolated by lyophilization. The complexation ratio (w/w) (non)-bioNP vs. siRNA was determined for non-bioNP 10:1 and for bioNP 30:1, using this ratio most of the siRNA remained safely entangled in the NP after agarose gel-electrophoresis run (Appendix Figure S1 and Appendix Figure S2). Their physicochemical properties are summarized in Table 7. No significant difference in size was found for both particles in comparison to the self-assembled precursor block copolymer micelles. Only the cationic zeta potential was partially reduced for bioNP due to the chemical variation of the more hydrophobic ketal cross-linker. Compared to the spermine cross-linker, the ketal cross-linker bears additional oxygens which alter the degree of protonation for the secondary amines inside the core, resulting in a reduced siRNA complexation efficiency. The acid-liability (biodegradability) of bioNP was assessed by dynamic light scattering DLS, indicating disintegration at pH 4.5 over 12 h (Appendix Figure S4). For *in vitro* cellular uptake assays and *in vivo* biodistribution studies, non-bioNP were labeled with FITC-(Oregon Green 488®) or near infrared-dye IR (CS800®), respectively (Figure 9).

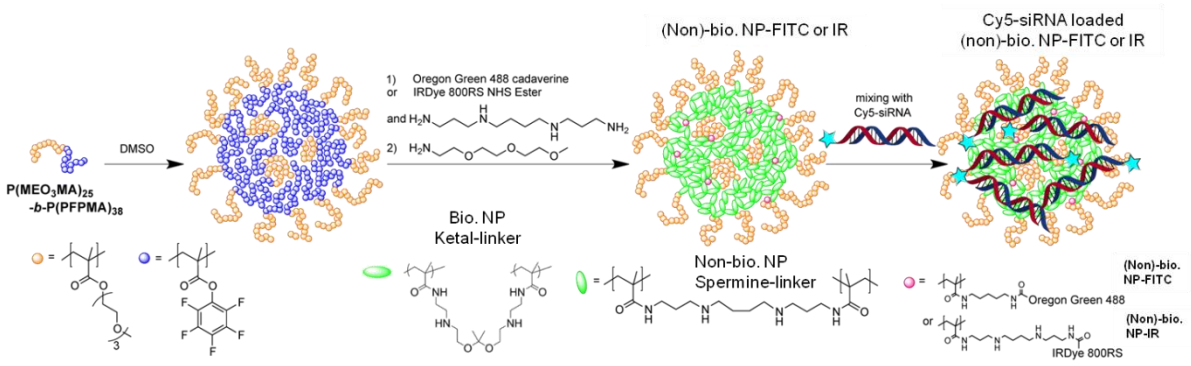

Figure 9:(Non)-bioNP for siRNA delivery. a) Synthetic scheme for the synthesis and siRNA complexation of cationic nanohydrogel particles NP (non-labeled), non-bioNP-FITC (labeled with Oregon Green 488) and non-bioNP-IR (labeled with IRDye CS800).

Table 7. Overview of (non-)bioNP showing the corresponding cross-linker, hydrodynamic radius, ζ zeta-potential and complexation ratio NP:siRNA

Name	Cross-linker	Hydrodynamic radius[a]/nm	ζ[c] (NP only)/mV	Complexation ratio[b] NP:siRNA
bioNP	ketal cross-linker	11.9 ± 0.7	8.7 ± 2.5	30:1
non-bioNP	spermine	13.5 ± 0.6	20.7 ± 2.5	10:1

[a] determined by DLS; [b] determined by agarose gel electrophoresis; [c] determined by Zeta-Sizer.

4.2 Validation of first generation non-bioNP for liver fibrosis therapy

4.2.1 *In vitro* validation of first generation non-bioNP loaded with anti-col1α1/(sc)siRNA loaded for liver fibrosis therapy

In vitro cytotoxicity of scrambled siRNA (scsiRNA) loaded non-bioNP (scsiRNA/non-bioNP) was assessed by MTT assay[75]. Scrambled siRNA was chosen as cargo for non-bioNP in order to avoid the toxicity of the highly positively charged uncomplexed carrier systems which could obscure eventual cytotoxic effects in the tested cell lines (relevant cells for liver fibrosis[28][17]). ScsiRNA/non-bioNP were thoroughly well tolerated and did not show significant cytotoxic effects up to 400nM siRNA (far above reasonable siRNA concentrations for *in vitro* or corresponding *in vivo* experiments).

As determined by FACS analysis, Cy5-siRNA loaded FITC labeled non-bioNP (Cy5-siRNA/non-bioNP-FITC) were efficiently taken up to 100% (double positive cells siRNA and non-bioNP), in a dosage dependent manner, after 1h incubation in 3T3 fibroblasts and RAW macrophages. Noteworthy, cells incubated with Cy5-siRNA/non-bioNP-FITC at 4°C overnight did not show a significant cellular uptake, indicating an energy dependent uptake mechanism for the nanohydrogels (Figure 10). Non-single positive cells neither for siRNA or non-bioNP-FITC alone could be observed, indicating throughout a good stability in protein containing media, as demonstrated already earlier by dynamic light scattering studies in serum or intravital confocal videography in the bloodstream of mice[76].

In analogy to earlier *in vitro* knockdown studies that revealed a size-dependent knockdown efficiency of the nanohydrogel particles, size-optimized nanohydrogel particles (diameters < 50 nm) were selected for the following studies[77]:

In vitro knockdown performance of anti-procollagen 1α(I) siRNA (anti-col1a1 siRNA) loaded non-bioNP (anti-col1a1 siRNA/non-bioNP) was assessed in 3T3 fibroblasts, mimicking *in vitro* myofibroblasts cultures, the main effector cells in liver fibrosis[78]. Anti-col1a1 siRNA/non-bioNP achieved a significant and sequence specific knockdown at reasonably low siRNA concentrations ranging from 25 to 100 nM. The knockdown performance of non-bioNP as

siRNA vehicle was comparably effective as the positive transfection controls with Lipofectamine® (a commercially available transfection agent which can only be used *in vitro*). Moreover, controls (scrambled siRNA loaded non-bioNP) did not show significant off target effects, supporting the sequence specific knockdown for anti-col1a1 siRNA/non-bioNP vs procollagen 1α(I) mRNA transcript.

Since (sc)siRNA loaded non-bioNP exhibited good biocompatibility *in vitro*, showed a high cellular uptake (up to 100% after 1h) in fibrosis relevant cell lines (macrophages, fibroblasts and hepatocytes) and induced a significant and sequence specific col1α1 mRNA knockdown up to 70% in 3T3 fibroblasts, the nanohydrogels particles qualified for further biological *in vivo* evaluation.

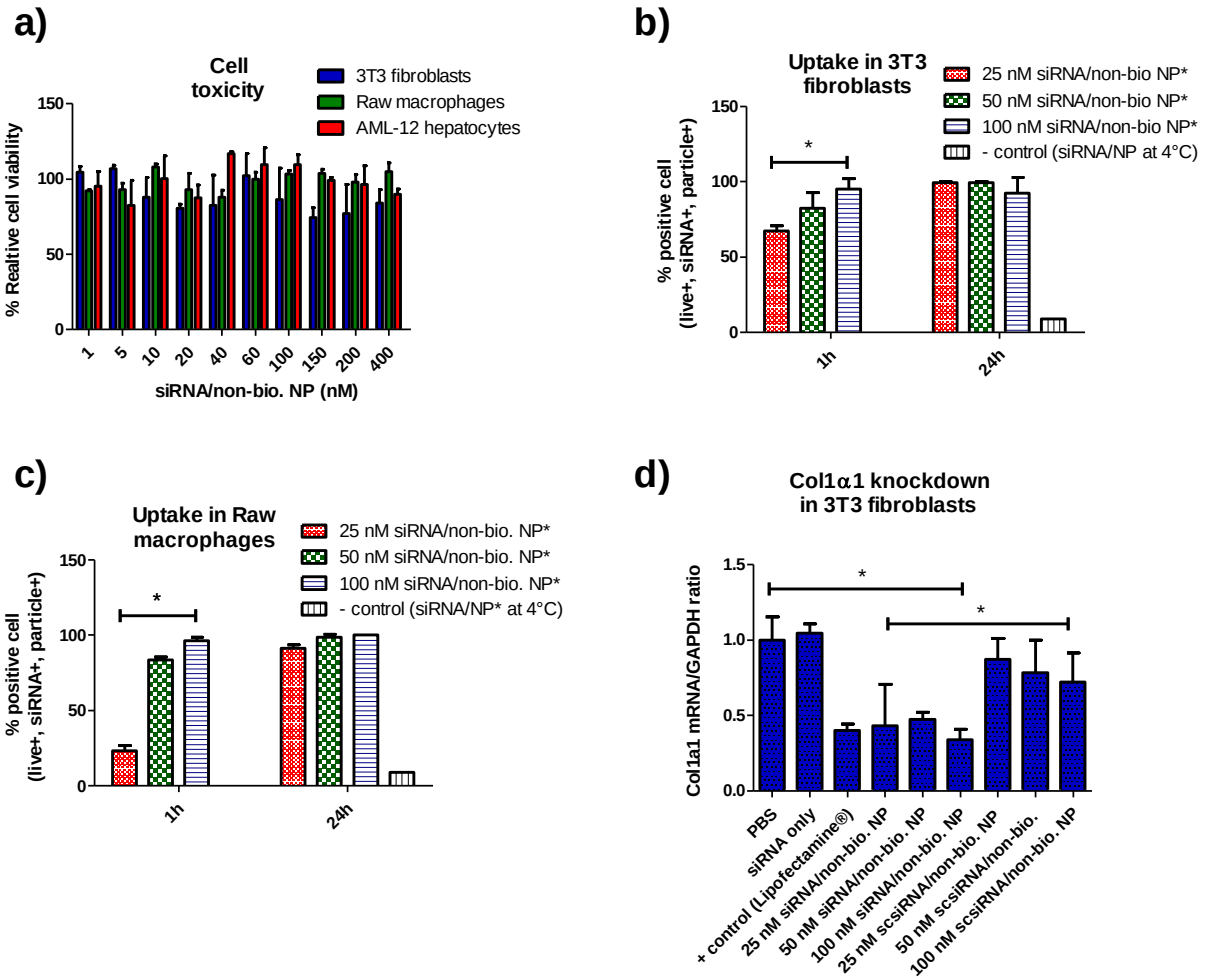

Figure 10. *In vitro* performance of siRNA loaded non-bioNP. a) Cell viability as determined by the MTT assay after exposure to sc(scrambled) siRNA loaded non-bioNP (10:1 weight-to-weight ratio of non-bio NP: siRNA) at different (sc)siRNA concentrations. The studied murine fibroblasts (3T3), macrophages (RAW) and hepatocytes (AML-12) cell lines represent liver cell types relevant for fibrosis. b) and c) By FACS determined, cellular uptake of Cy5-siRNA loaded non-bioNP-FITC in 3T3 fibroblasts and RAW macrophages (10:1 weight-to-weight ratio non-bioNP-FITC:siRNA) at different (sc)siRNA concentrations and time points. Cellular uptake after 24h was minimal at 4°C, indicating an energy-dependent uptake mechanism for nanohydrogels (*p < 0.05 vs like indicated in graph, means ± SD, n = 3, for the corresponding dot plots and MFI histograms compare Appendix Figure S5 and Appendix Figure S6). d) *In vitro* gene knockdown of col1*a*1 in 3T3 fibroblasts after 48h incubation by anti-col1a1 siRNA loaded non-bioNP (10:1 weight-to-weight ratio of NP:siRNA). Col1a1 mRNA as determined by quantitative real-time polymerase chain reaction (qPCR) was lowered up to 70% (similar to Lipofectamine®), while control samples with scrambled siRNA (scsiRNA) had no effect (*p < 0.05 as indicated in graph, means ± SD, n = 3).

4.2.2 *In vivo* biodistribution of Cy5-siRNA loaded near infrared labeled non-bioNP

A reliable and reproducible mouse model for liver fibrosis was obtained by treatment with escalating doses of carbon tetrachloride (CCl_4) via oral gavage. Therefore, mice (n=5) were treated with an escalating dosage of CCl_4 over two weeks resulting in a moderate advanced liver fibrosis. For the present study, mice (groups of n=5) were treated with CCl_4 for two weeks resulting in modestly advanced liver fibrosis. During the second week mice received in parallel two intravenous doses of 1 or 2 mg/kg Cy5-anti-col1α1 siRNA loaded non-bioNP-IR with 48h between the injections (Figure 11a)).

After the second injection, biodistribution of Cy5-labeled siRNA and IRDye CS800 labeled (non-)bioNP ((non)-bioNP-IR)) were monitored separately by *in vivo* fluorescent near infraread (NIR) imaging. 24h after the second injection, siRNA and non-bioNP prominently accumulated in the liver (Figure 11b)). Only a minor proportion of siRNA was directly excreted by the kidneys, indicating a fast disassembling process of the nanohydrogel/siRNA complexes. However, after 24h most of siRNA and bioNP were colocalized in the liver, as still intact complexes and, thus potentially enabling functional siRNA delivery into liver cells. 48h after the second injection, mice were sacrificed and organs were harvested for *ex vivo* imaging (Figure 11c)). Equal to *in vivo* imaging, Cy5-siRNA and non-bioNP-IR were colocalized in the liver, where only a minor part of Cy5-siRNA could be detected in the kidneys as correlate for a premature disassembling process after injection. However, the best colocalization between siRNA and nanohydrogels was in the liver (Figure 11c)).

As determined by FACS, siRNA and nanoparticle localization were studied on cellular level of cells isolated from the liver and lungs ((Figure 11e)). Interestingly, nanoparticle and siRNA showed a high *in vivo* uptake up to 50% in αSMA+ myofibroblast and in liver macrophages (up to 20%). Furthermore, cellular uptake of siRNA and nanoparticles was observed in ~20% of CD31+ endothelial cells, ~15% of vimentin+ mesenchymal cells and ~20% of lung macrophages but only to a minor extent in albumin+ hepatocytes (albumin+ cells, representing the most abundant cells in the liver).

Macrophages are crucial for the liver inflammatory response and further for the remodeling of the collagenous matrix after liver injury (fibrogenesis and fibrolysis), making them an interesting therapeutic target cell population in liver fibrosis[79][80]. Yet, the high degree of siRNA/nanohydrogel uptake in collagen producing cells (αSMA+) was highly promising to investigate the nanoparticles' antifibrotic effect in our short-term (two weeks) liver fibrosis model (Figure 11a)).

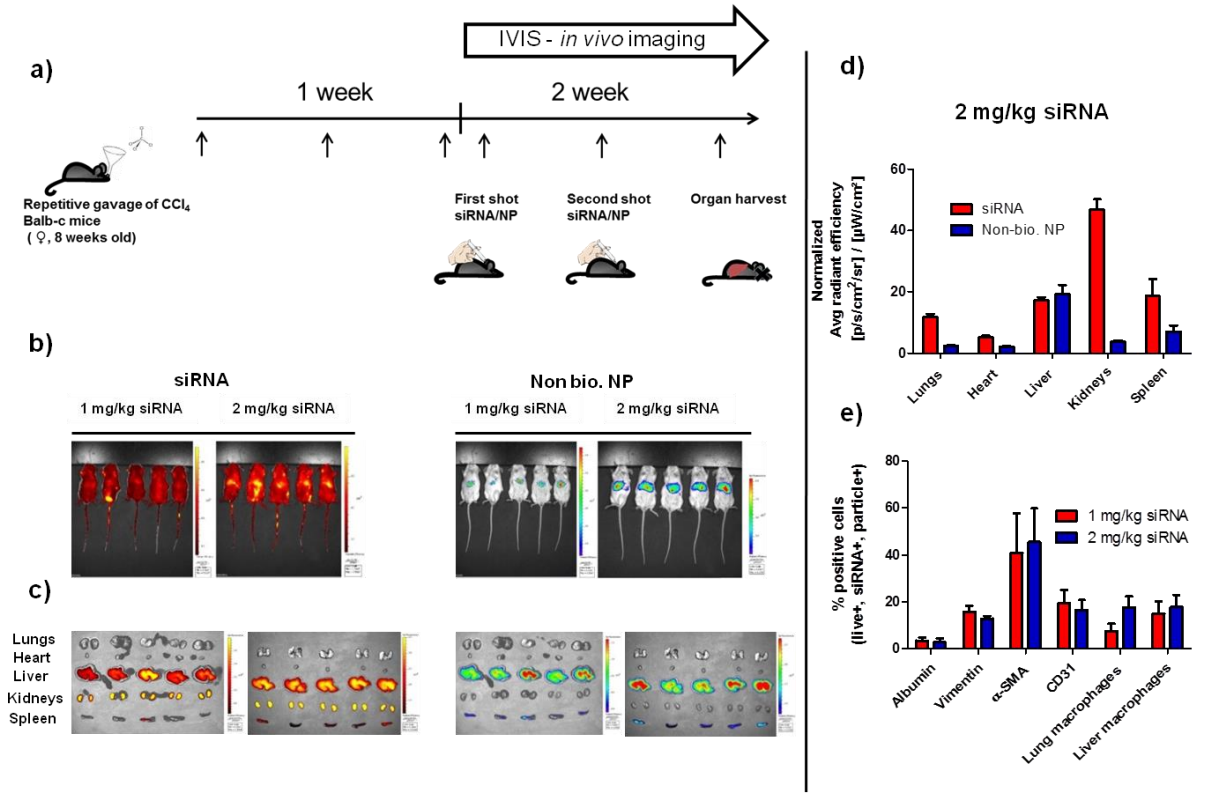

Figure 11. ***In vivo*** **biodistribution of cationic CS800 near infrared labeled non-bioNP (non-bioNP-IR) loaded with Cy5-labeled anti-col1α1 siRNA (10:1 weight-to-weight ratio of non-bio NP:siRNA). a) Scheme of the experimental** ***in vivo*** **setup. To induce liver fibrosis, groups of 5 mice were gavaged with an escalating dose of CCl_4 three times a week for two weeks. During week two, mice received two doses of 1 or 2 mg kg^{-1} Cy5-anti-col1α1 siRNA complexed in non-bioNP-IR with 48h between the injections. After the first dose, the biodistribution of Cy5-siRNA and non-bioNP-IR was monitored over 5 days (as indicated in the scheme), and then organs were harvested and analyzed for uptake. b)** ***In vivo*** **near infrared (NIR) fluorescence imaging of Cy5-siRNA and non-bioNP-IR, respectively, in mice 24h after second injection (for further time points compare Appendix Figure S7). c)** ***Ex vivo*** **fluorescence imaging of Cy5-siRNA and non-bioNP-IR in organs harvested 48h after second injection. d)** ***Ex vivo*** **fluorescence quantification of non-bioNP-IR and Cy5-siRNA in organs as shown in c). e) By FACS determined,** ***in vivo*** **cellular uptake of Cy5-siRNA and non-bioNP-IR in isolated cells, obtained from the harvested livers and lungs, 48h after the second injection of Cy5-siRNA loaded non-bioNP-IR (means ± SD, n=5, for exemplary FACS dot plots compare Appendix Figure S 19).**

4.2.3 *In vivo* collagen knockdown mediated by anti-col1α1 siRNA loaded non-bioNP

48h after the second injection (of 1 or 2 mg/kg anti-col1α1 siRNA loaded non-bioNP), mice were sacrificed and *in vivo* collagen amount of liver were thoroughly quantified on transcriptional mRNA- and protein level (as summarized in (Figure 12)). Liver col1α1 transcript levels were determined by quantitative real-time polymerase chain reaction (qPCR) (Figure 12a). Here, col1α1 mRNA was dose-dependently, significantly and sequence specifically down regulated by up to 50% in fibrotic mice treated with anti-col1α1 siRNA loaded non-bioNP compared to control mice that received PBS. Notably, particles loaded with scrambled siRNA did not show an effect, supporting a sequence specific knockdown by anti-col1α1 siRNA loaded non-bioNP. Furthermore, the therapeutic effect was assessed on the protein level by biochemical determination of hepatic hydroxyproline (HYP) content, a collagen specific amino acid, serving as standard collagen quantification method in fibrosis[14]. Here, both NP doses of anti-col1α1 siRNA/non-bioNP (1 and 2 mg/kg) significantly decreased

HYP to levels of healthy mice (Figure 12c), while PBS or scrambled siRNA loaded nanohydrogel particles were ineffective and did not change the amount of liver collagen. Additionally, liver tissue sections were analyzed for morphometric collagen deposition after Sirius Red staining in liver sections from left and middle liver lobes (Figure 12c). For collagen assessment only pathological and functionally relevant parenchymal collagen was determined by omitting functionally irrelevant major vessel/portal areas that naturally show high collagen levels (Figure 12e)[81]. Here, αSMA protein, as surrogate marker for activated myofibroblasts, was also sequence specifically and significantly reduced in the fibrotic livers at 2 mg/kg siRNA, supporting the antifibrotic therapeutic effect of anti-col1α1 siRNA/non-bioNP[28]. Overall, morphometric quantifications of collagen and αSMA protein were in excellent agreement with the therapeutic reduction of col1α1 transcript levels and hepatic collagen content. In addition, standard serum parameters were monitored and lacked any acute *in vivo* toxicity after application of nanohydrogels (Appendix Figure S8). Conclusively, non-bioNP loaded with anti-col1α1 siRNA exhibited a convincing therapeutic effect by a significant and sequence specific collagen reduction which was combined with a lack of acute *in vivo* liver toxicity (after repetitive *iv* injection) in liver fibrotic mice. Therefore, nanohydrogels qualified, as siRNA carrier platform, for further development in regards to an improved biodegradability.

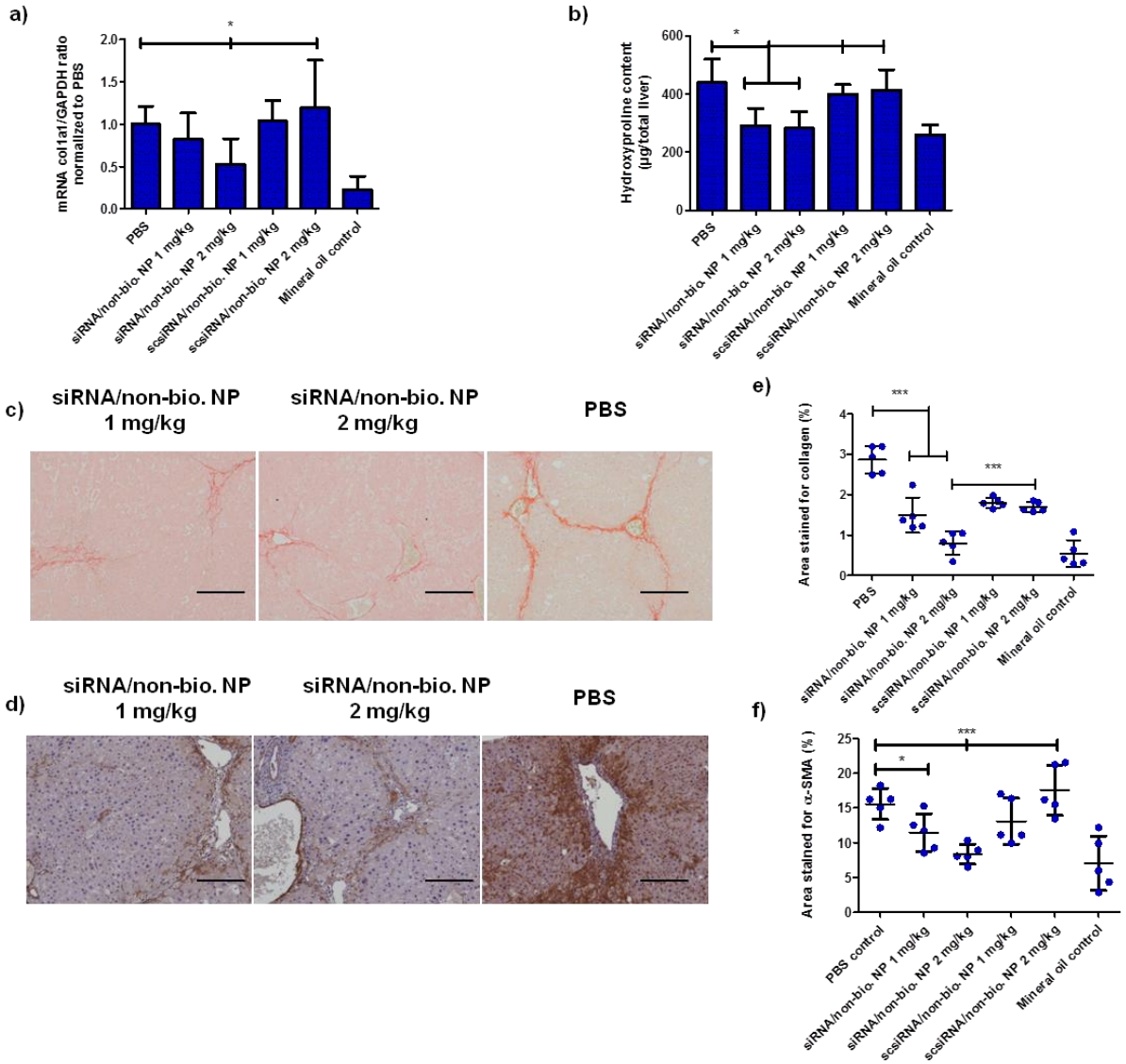

Figure 12. ***In vivo*** **knockdown performance of non-bioNP-IR loaded with anti-col1α1 siRNA (10:1 weight-to-weight ratio (w/w) of non-bio. NP:siRNA) for liver fibrosis therapy. a)** ***In vivo*** **gene knockdown of col1α1 mRNA in fibrotic livers by anti-col1α1 siRNA loaded non-bioNP-IR. Col1α1 transcript levels were determined by quantitative real-time polymerase chain reaction (qPCR) (*p < 0.05 vs. PBS/scsiRNA loaded non-bioNP-IR, determined by one-way ANOVA analysis, means ± SD, n = 5). b) Suppressed collagen synthesis and deposition was further verified by quantification of liver hydroxyproline content (*p < 0.05 PBS/scsiRNA loaded non-bioNP-IR, means ± SD, n = 5). c) Morphometric assessment of collagen deposition in representative liver sections (omitting large vascular structures) after Sirius Red staining (five randomly selected fields of each specimen were taken for collagen quantification; means ± SD, n = 5) confirm the antifibrotic effect: Anti-col1α1 siRNA loaded nanohydrogels lowered excess fibrotic collagen deposition to collagen levels of healthy mice (mineral oil control) (***p < 0.0005 as indicated, means ± SD, bars = 200 µm). d) Morphometric quantification of αSMA expression, a marker for activated myofibroblasts, in liver sections (five randomly selected fields per specimen; means ± SD, n = 5) support the antifibrotic effect of anti-col1α1 siRNA loaded non-bioNP (*p < 0.05, ***p < 0.0005 as indicated, means ± SD, bars = 200 µm).**

4.3 Comparative study of first generation non-bioNP vs second generation bioNP for liver fibrosis therapy

Accumulation and gradual toxic effects of nanohydrogel particles might be a limiting factor for their long-term administration as siRNA carriers especially for chronic diseases where repetitive applications are compulsory. Additionally, improved siRNA releasing properties, once the siRNA/NP complexes were taken up into the cytoplasma of the target cells, could enhance the knockdown efficiency of the carrier system. Therefore, non-bioNP were advanced to bioNP by changing their chemical stable spermine-crosslinker to an acid-labil ketal cross-linker, endowing the second generation of nanohydrogel particles with new putatively valuable characteristics.

4.3.1 *In vitro* validation of anti-col1α1 (sc)siRNA loaded (non-)bioNP

According to our before applied *in vitro* validation for the first generation of nanohydrogels, (non)-bioNP were thoroughly tested in a head-to-head study to reveal whether also nanohydrogel's second generation could compete with the previous non-bioNP, concerning the main features like cytotoxcity, cellular uptake, knockdown performance etc..

By MTT assay, scsiRNA loaded (non-)bioNP (complexation ratio (w/w) NP:siRNA for bioNP 30:1, for non-bioNP 10:1 – see Table 7) were tested for *in vitro* toxicity in three different cells lines relevant for liver fibrosis studies[28]: No significantly reduced cellular viability was detectable in fibroblasts, macrophages or endothelial cells up to corresponding siRNA concentrations of 400 nM (Appendix Figure S9). When *in vitro* cellular uptake was assessed by FACS, Cy5-siRNA loaded (non-)bioNP-FITC were efficiently taken up by 3T3 fibroblasts and RAW-macrophages, in a dosage and time dependent manner, and up to 100% after a 1h incubation, (Figure 13c and d), with macrophages represent another promising cellular target for immunotherapeutic approaches in liver fibrosis[22]. Interestingly, no single positive cells either for particle or siRNA alone were detected, suggesting a robust complexation of siRNA for both nanohydrogels in protein rich media (Figure 13c/d, Appendix Figure S12). By confocal microscopy, (non)-bioNP and siRNA could be found co-localized inside the cell, indicating that both siRNA loaded NPs are actively internalized by the cells and not unspecifically bound to the cell membrane surface (a well-known pitfall in cellular uptake studies, leading to false positive results, Appendix Figure S10 and Appendix Figure S11). As further control, cells were incubated with Cy5-siRNA/(non-)bioNP-FITC at 4°C for 24h, whereby no significant amount of cells had taken up the complexes, implying a predominantly energy-dependent uptake mechanism for particle internalization (Figure 13c/d, Appendix Figure S10 and Appendix Figure S11). Anti-col1α1 siRNA loaded (non)-bioNP were tested for knockdown performance in 3T3 fibroblasts. For stable collagen expression levels, fibroblasts were stimulated with TGFβ1, a potent pro-fibrotic cytokine (Appendix Figure S16). Interestingly, bioNP showed a significant (***$p < 0.0001$ vs PBS/scsiRNA loaded (non)-bioNP) and sequence specific knockdown effect up to 80%, after 48h, even at 50nM siRNA, while non-bioNP lowered the expression levels to ~50% (similar to the previous studies, compare Figure 10d)[1]. Remarkably, bioNP achieved an *in vitro* knockdown as efficient as Lipofectamine® (a potent commercial available transfection agent only applicable *in vitro*). Based on the promising *in vitro*

performances of anti-col1a1 siRNA loaded bioNP, second generation nanohydrogels were also tested for *in vivo* liver fibrosis therapy.

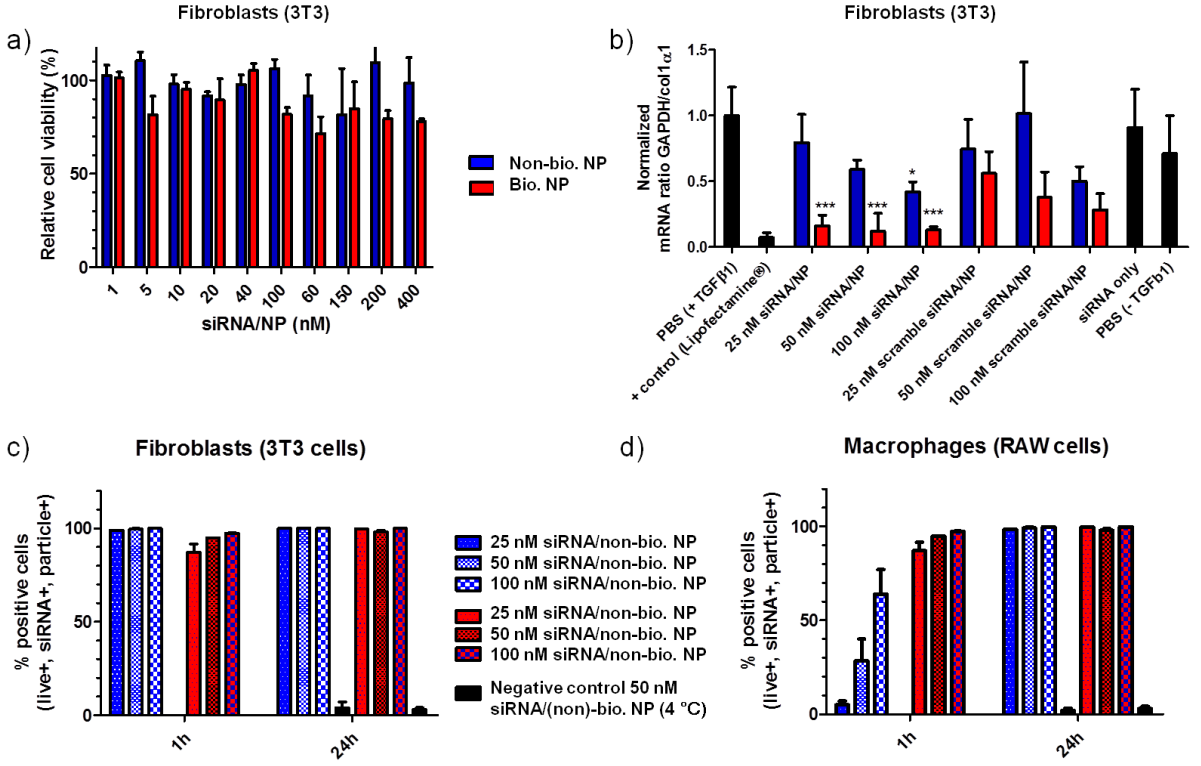

Figure 13. ***In vitro*** **performance of Cy5 labeled siRNA loaded cationic (non-)bioNP. a) By MTT, cell viability of fibroblasts exposed to siRNA loaded non-bioNP and bioNP (10:1 weight-to-weight ratio (w/w) of non-bioNP:siRNA, 30:1 (w/w) of bioNP:siRNA) at different siRNA concentrations (72h, n=3). b)** ***In vitro*** **gene knockdown of procollagenα1(I) (col1α1) mRNA transcript in fibroblasts mediated by non-bioNP and bioNP loaded with anti-col1α1 siRNA after 48h. Col1α1 mRNA was determined by quantitative real-time polymerase chain reaction (qPCR). The expression levels were lowered by up to 80% (similar to Lipofectamine®) for bioNP and up to 50% for non-bioNP, while control samples with scrambled siRNA had only minor off-target effects, indicating sequence specific** ***in vitro*** **gene knockdown (*p < 0.05, ***p< 0.0001 vs PBS/scsiRNA loaded (non-)bio. NP, means ± SD, n=3). c) Uptake of Cy5 labeled siRNA loaded (non-)bioNP in fibroblasts and in d) macrophages at different siRNA concentrations and time points analyzed by FACS. Cellular uptake after 24h was minimal at 4°C indicating energy-dependent uptake mechanisms (means ± SD, n=3).**

4.3.2 *In vivo* biodistribution of Cy5-siRNA loaded near infrared labeled non-bioNP vs bioNP

Based on the promising *in vitro* performance of the novel bioNP, their *in vivo* therapeutic effect in comparison to the already validated, non-bioNP were tested. Therefore, both nanohydrogel particles ((non-)bioNP) loaded with anti-col1α1 siRNA were tested in the established mouse model of short-term liver fibrosis induction with CCl_4 (as described above Figure 11a)[1]. Here in brief, mice were gavaged with escalating doses of carbon tetrachloride (CCl_4), three times a week, over the period of two weeks, while they developed a reproducible and moderately advanced homogenous parenchymal liver fibrosis in livers. After the first week of CCl_4 fibrosis induction, mice received two intravenous injections of 1 or 2 mg/kg anti-col1α1 siRNA loaded in bioNP or non-bioNP, respectively, 48h apart, in parallel to ongoing CCl_4 gavage (Figure 11a).

After the second injection, biodistribution of Cy5 labeled siRNA and IRDye CS800 labeled (non-)bioNP ((non)-bioNP-IR)) were monitored separately by using *in vivo* fluorescence near infrared (NIR) imaging (Appendix Figure S7). Here, 24h after the second injection both nanohydrogels predominantly colocalized with their siRNA cargo in the liver (Figure 14a) I/II). Noteworthy, for bioNP a slightly enhanced Cy5-siRNA signal could be observed in the mice's bladder indicating first signs of *in vivo* degradation and release of its siRNA cargo. 48h after the second siRNA injection mice were sacrificed and their organs were taken out for precise signal quantification of Cy5-siRNA and (non)-bioNP-IR. *Ex vivo* imaging confirmed also a prominent co-localization of Cy5-siRNA and (non)-bioNP-IR mostly in liver (Figure 14b) I/II). Furthermore, for non-bioNP considerable amounts of Cy5-siRNA signal could be detected in spleen and kidneys, suggesting a less pronounced liver targeting (Figure 14c) II). In contrast, Cy5-siRNA encapsulated in bioNP primarily addressed the liver by avoiding almost completely accumulation in lungs and less pronounced accumulation in kidneys and spleen (Figure 14c) II).

To assess, how both nanohydrogels and their cargo were distributed *in vivo* on the cellular level, single cell suspensions were obtained from harvested liver and lung tissues and characterized by FACS. Both particles (bioNP and non-bioNP) and their siRNA were efficiently taken up by activated myofibroblasts (around 20%), as the major collagen producing cell type in liver fibrosis, and by liver macrophages (that are involved in inflammation and liver parenchymal remodeling after injury (Figure 14d)). However, hepatocytes, as the most abundant cells in liver, incorporated both siRNA and nanohydrogel NPs only to a minor extent. Of note, bioNP showed a significant (***$p<0.0001$ vs. (non)-bioNP) uptake also in endothelial cells (up to 30%), making them interesting to treat vascular diseases[82]) Finally, bioNP and non-bioNP were not taken up by lung macrophages which could have imposed a risk of aggregation-induced accumulation in tiny lung capillaries leading to pulmonary embolism[83].

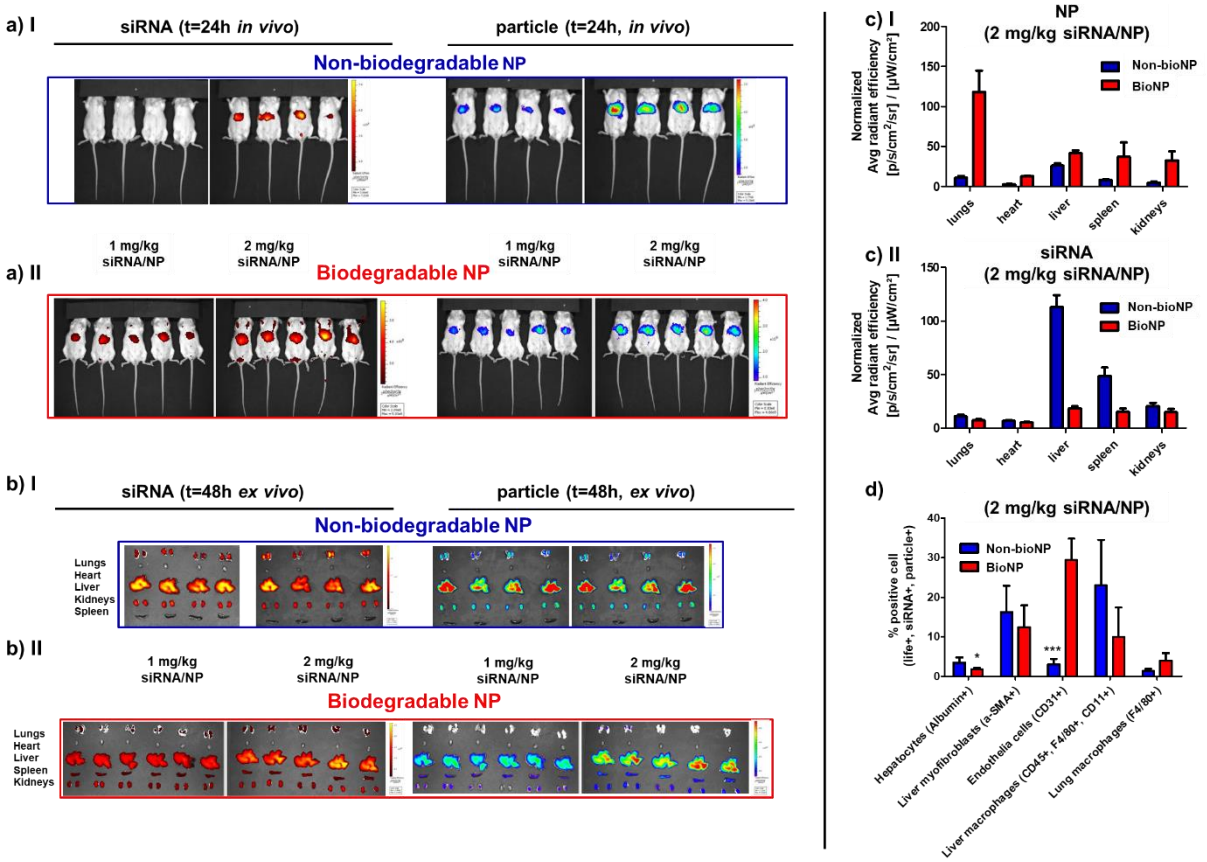

Figure 14. ***In vivo*** **biodistribution of Cy5-labeled anti-col1α1 siRNA loaded cationic CS800 near infrared labeled (non)-bioNP ((non)-bioNP-IR) in murine CCl_4 induce liver fibrosis. Mice were gavaged with escalating doses of CCl_4 three times a week for two weeks. During the second week, mice received two doses of 1 or 2 mg/kg Cy5-anti-col1α1 siRNA encapsulated in non-bioNP-IR or bioNP-IR, respectively, with 48h apart (compare Figure 11). a) I/II:** ***In vivo*** **near infrared (NIR) fluorescence imaging of Cy5-siRNA and (non)-bioNP-IR at 24h after the second injection. b) I/II:** ***Ex vivo*** **biodistribution by near infrared (NIR) fluorescence imaging of Cy5-siRNA and (non)-bioNP-IR in organs harvested at 48h after second injection. c)** ***Ex vivo*** **fluorescence's quantification of (non)-bioNP-IR (c) I) and Cy5-siRNA c) II) in organs (as shown in b)). d) FACS analysis of single cells suspensions obtained from harvested livers and lungs at 48h after second injection of Cy5-siRNA and (non)-bioNP-IR (2 mg/kg siRNA/NP dosage, means ± SD, n = 4-5, *, ***p < 0.05, 0.0001, means ± SD, for exemplary FACS dot plots compare Appendix Figure S 18).**

4.3.3 *In vivo* collagen knockdown of anticol1α1-siRNA loaded (non)-bioNP

In analogy to the previously observed anti-fibrotic effect mediated by anti-col1α1/non-bioNP (Figure 12), collagen was thoroughly quantified on the mRNA- and protein level in fibrotic livers of mice treated with anti-col1α1/(non)-bioNP (Figure 15). Col1α1 transcript levels were determined by quantitative real-time polymerase chain reaction (qPCR). Here, despite first signs of *in vivo* degradation and siRNA release, the bioNP loaded with anti-col1α1 siRNA performed equally well in comparison to non-bioNP/col1α1. Col1α1 mRNA was suppressed significantly up to 60% by anti-col1α1/non-bioNP (*p < 0.05 as indicated in the graph, means ± SD) and up to 80% by bioNP (here at ** p < 0.001, Figure 15a)). Corresponding controls like PBS or (non)-bioNP loaded with scrambled siRNA did not reduce col1α1 mRNA levels significantly. The collagen reduction was further evaluated by hepatic hydroxyproline (HYP) quantification (a post-translationally modified amino acid almost exclusively present in collagen proteins). In accordance to transcript levels, both NP loaded with anti-col1α1 siRNA significantly (*p < 0.05 vs. PBS and scsiRNA/(non)-bioNP) reduced the HYP load of the

fibrotic livers down to levels of healthy mice (treated with mineral oil - as vehicle control for CCl_4), and NPs loaded with scrambled siRNA did not prevent HYP accumulation in the livers (Figure 15b). As additional fibrosis assessment on the protein level, liver tissue sections from left and middle lobes were quantified for morphometric collagen deposition after Sirius Red staining (as demonstrated in Figure 15c). Only pathological relevant collagen was determined by omitting larger vessel areas that are naturally enriched in collagen. Here, both nanohydrogel particles loaded with anti-col1α1 siRNA significantly reduced histological collagen deposition in parenchymal liver tissue in a sequence specific way (*p < 0.05 and ***p < 0.0001 vs PBS/(sc)siRNA loaded (non-)bioNP) down to level of healthy mice (Figure 15d)).

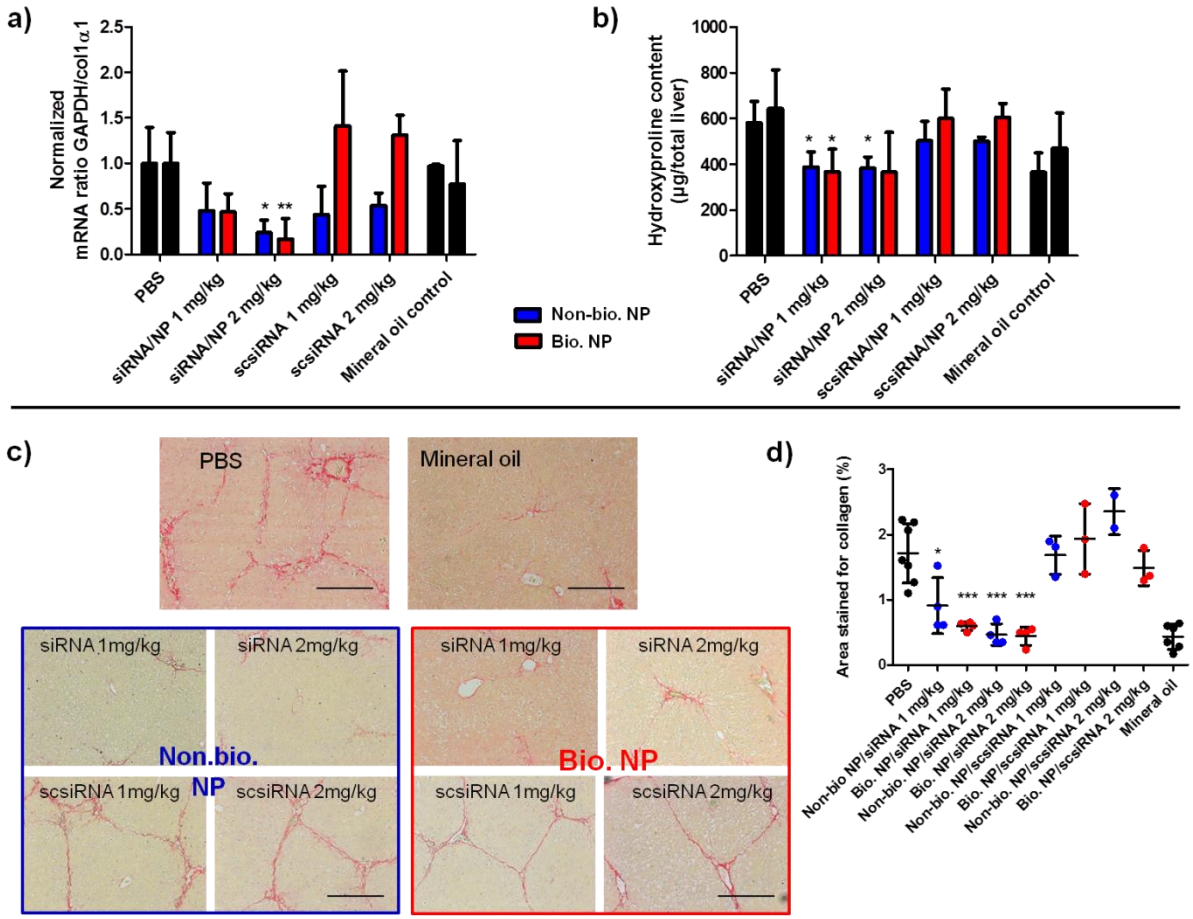

Figure 15. *In vivo* collagen knockdown of Cy5 labeled anti-col1α1 siRNA-loaded (non)bioNP in a murine liver fibrosis model. Mice were gavaged with escalating doses of CCl_4 three times a week for two weeks. During week two, mice received two doses of 1 or 2 mg/kg Cy5-anti-col1α1 siRNA encapsulated in (non)-bioNP with 48h apart. a) *In vivo* gene knockdown of col1α1 mRNA in fibrotic livers by anti-col1α1 siRNA loaded (non)bioNP. Col1α1 transcription levels were determined by qPCR (*,p < 0.05, 0.001 vs PBS and scsiRNA/(non)-bioNP, determined by one-way ANOVA, means ± SD, n = 4-5 per group). b) Suppressed collagen synthesis and deposition was further verified by quantification of liver hydroxyproline content (*p < 0.05 vs PBS and scsiRNA/(non)-bioNP, means ± SD, n=4-5). c) Histologic characterization of collagen after Sirius Red staining in randomly selected liver tissue sections of mice treated with anti-col1α1 siRNA loaded (non)-bioNP. d) Morphometric assessment of collagen deposition in representative liver tissue sections (five randomly selected fields of each specimen omitting large vascular structures; means ± SD, n=5) confirm an antifibrotic effect: Both anti-col1α1 siRNA loaded NPs lowered excess collagen deposition down to nonfibrotic control levels (mineral oil control) (***p<0.0005 vs PBS and scsiRNA/(non)-bioNP, means ± SD, bars = 200 µm).**

Furthermore, the antifibrotic effect of the (non)-bioNP/siRNA treatment was determined by quantification of α-SMA, representing a surrogate marker for activated myofibroblasts during liver fibrogenesis[17]. Here, αSMA was significantly and sequence specifically down-regulated on the transcript level (determined by qPCR) and further on the protein level (after specific αSMA staining of liver sections and consecutive morphometric quantification) (Figure 16a), b), c)). When testing if the anti-col1α1 siRNA/(non)-bioNP antifibrotic treatment affects the inflammatory status in liver, the pan-macrophages marker CD68 was significantly down regulated on the mRNA-(qPCR) as well as on the protein level (morphometric quantification) (Figure 16d), e), f)), suggesting a favorable anti-inflammatory effect of the pharmacological collagen suppression.

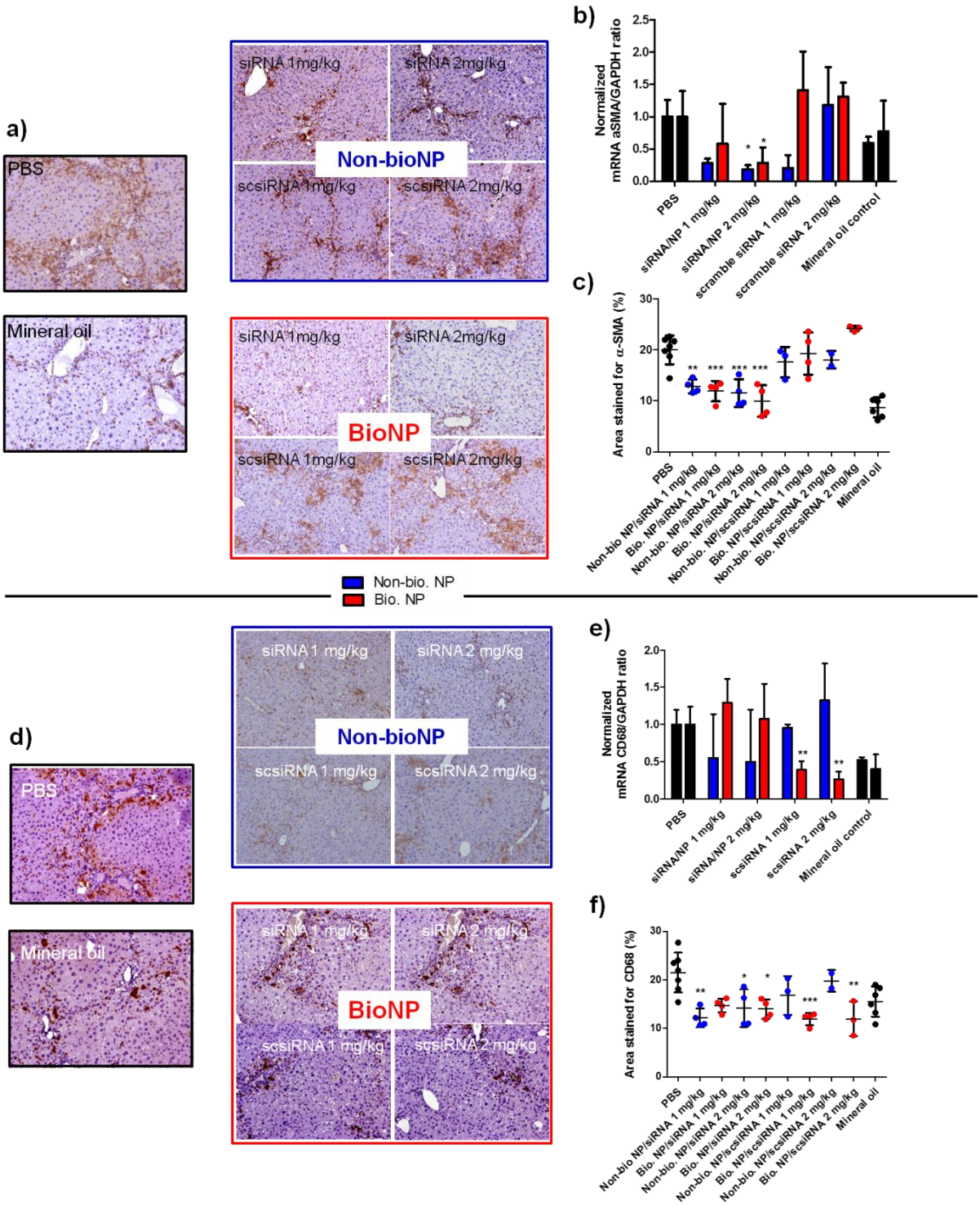

Figure 16. ***In vivo*** **antifibrotic and anti-inflammatory effect of Cy5 labeled anti-col1α1 siRNA-loaded cationic (non)-bioNP in liver fibrotic mice. a) Histologic characterization of αSMA after IHC staining in randomly selected liver tissue sections of mice treated with anti-col1α1 siRNA/scsiRNA loaded (non)-bioNP. b)** ***In vivo*** **knockdown of αSMA mRNA, a surrogate marker for activated myofibroblasts, in fibrotic livers mediated by anti-col1α1 siRNA loaded (non)-bioNP supported an antifibrotic effect of the siRNA/(non)bioNP treatment. αSMA transcript levels were determined by quantitative real-time polymerase chain reaction (qPCR) (*p < 0.001 vs. PBS and scsiRNA/(non)-bioNP, determined by one-way ANOVA, means ± SD, n = 4-5 per group). c) Morphometric assessment of αSMA in representative liver tissue sections (five randomly selected fields of each specimen) supported an antifibrotic effect: Both anti-col1α1 siRNA loaded NPs lowered the fibrosis surrogate marker αSMA almost down to non-fibrotic levels (mice treated with mineral oil control) (means ± SD, **,***p < 0.001, 0.0001 vs PBS and scsiRNA/(non)bioNP, n=5, bars=200 µm). d) Histologic characterization of CD68 after IHC staining in**

randomly selected liver tissue sections of mice treated with anti-col1α1 siRNA/scsiRNA loaded (non)-bioNP. e) *In vivo* reduction of CD68 mRNA, a pan-macrophages marker (acting as a surrogate marker for the inflammatory status in the liver), in fibrotic livers mediated by anti-col1α1 siRNA/scsiRNA loaded (non)-bioNP (*p < 0.0001 vs. PBS and scsiRNA/(non)-bioNP, determined by one-way ANOVA, means ± SD, n =4-5 per group). f) Morphometric assessment of CD68 in representative liver tissue sections (five randomly selected fields of each specimen) suggested an anti-inflammatory effect: Both (sc)siRNA loaded NPs lowered the pan-macrophages marker CD68 down to non-fibrotic levels (mineral oil control) (*, **, ***p < 0.05, 0.001, 0.0001 vs PBS and scsiRNA/(non)-bioNP, means ± SD, n=4-5, bars=200µm).**

4.3.4 *In vivo* kinetics and biocompatibility of (sc)siRNA loaded (non-)bioNP

To investigate the acid-induced biodegradability *in vivo*, one short-term (5 days with two consecutive injections) and one long-term (13 days with one single injection) monitoring experiment were performed. For short-term monitoring, healthy mice received two consecutive injections (48h apart) of scsiRNA loaded near infrared labeled (non-)bioNP, following the before described therapeutic treatment. After each injection body NIR fluorescence over the liver regions was monitored over 48h. As shown in Figure 17b), fluorescence of the bioNPs decreased significantly (*p<0.05 vs scsiRNA/(non-)bioNPs) about 50% after 48h, while the fluorescence of the non-bioNP signal remained nearly constant. After the second injection these trends continued, i.e., non-bioNP accumulated further, while the fluorescence signal of bioNP highly significantly (***p<0.0001) continued to decrease. For long-term monitoring, *in vivo* kinetic of scsiRNA loaded nanohydrogels was also investigated over a 13 days period after a single injection of scsiRNA loaded particles. Here, the before observed tendency of an accelerated fading of the fluorescence signal of bioNPs vs non-bioNPs could be confirmed, falling under the fluorescence signal of non-bioNPs 48h after a single injection of scsiRNA loaded particles (Figure 17a)). A good biocompatibility of vehicles for siRNA delivery is compulsory especially for long-term treatment. To further explore the NPs' biocompatibility, healthy mice were challenged with escalating doses of scrambled siRNA loaded in (non-)bioNPs ranging from 1 mg/kg - up to 10 mg/kg siRNA concentrations. Here, both particles were all over well-tolerated up to an overdose of 10 mg/kg scsiRNA/(non-)bioNP, whereby one mouse died in the non-bioNP group after the 8 mg/kg siRNA injection.

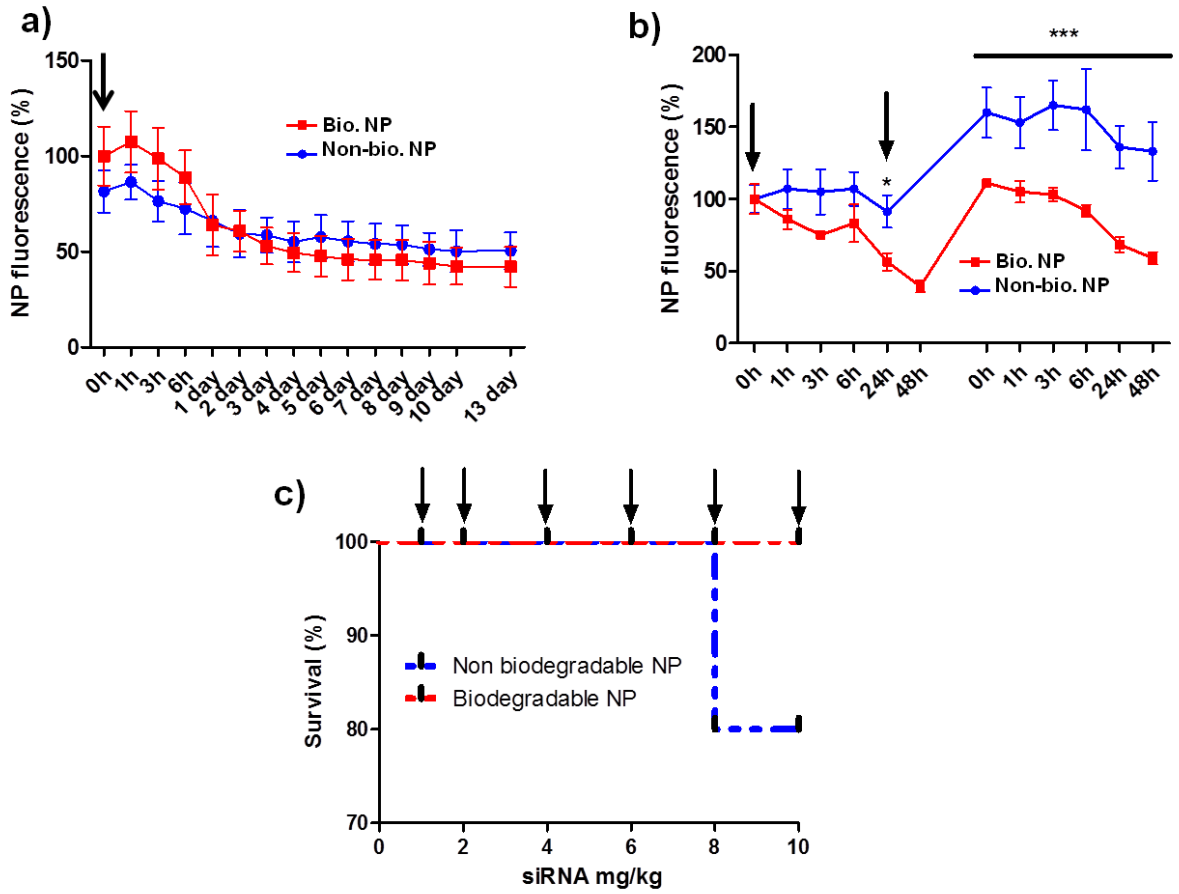

Figure 17. ***In vivo*** **kinetics and biocompatibility of scrambled siRNA loaded cationic (non)-bioNP in liver fibrotic mice. a)** ***In vivo*** **kinetic of near infrared (CS800) labeled non-bioNP (ratio NP:siRNA (w/w) 10:1) and bioNP (ratio NP:siRNA (w/w) 30:1) complexed with (non-labeled) scrambled siRNA. The NPs' body fluorescence signal was monitored by IVIS after one** ***iv*** **injection (dose 2 mg/kg scsiRNA/(non-)bioNP) over 13 days (n=4 per group): The initially higher bioNP signal (due to the adapted ratio for bioNP:siRNA (w/w) 30:1) declined more prominently vs the non-bioNP signal, suggesting an accelerated biodegradation for bioNPs vs non-bioNPs. b)** ***In vivo*** **kinetics of near infrared (CS800) labeled non-bioNP and bioNP complexed with (non-labeled) scrambled siRNA monitored by IVIS after two consecutive injections 48h apart: After two consecutive injections, the decay of the bioNP signal was more prominent vs the non-bioNP signal, confirming the improved biodegradability of bioNP (*, *** $p<0.05$, 0.001 vs the corresponding time of scsiRNA/(non)-bioNP, n=3-5 per group, arrows indicate scsiRNA/NP injections). c)** ***In vivo*** **Kaplan Meier survival curve of healthy mice challenged with escalating doses of (non-)bioNP loaded with scrambled siRNA (2, 4, 6, 8, 10, 12 mg/kg siRNA) by, 48 apart,** ***iv*** **injections: In this dose escalation experiment, both NPs were overall well tolerated up to high doses of scsiRNA/(non)-bioNP, indicating a broad therapeutic index especially for the (biodegradable) nanohydrogels (n=5 per group, arrows indicate the scsiRNA/NP injections).**

5. Discussion

siRNA interference is a powerful tool to potentially address difficult-to-treat diseases and has already proven its potential in clinical trials[84]. Although remarkable progress for the stabilization of naked siRNA *in vivo* has been made, nanoparticles as siRNA vehicles are still the gold standard for functional siRNA delivery *in vivo* [85]. Not all organs are equally targetable for siRNA delivery systems. Here, liver, spleen, lungs and kidneys are well accessible organs for siRNA therapy, due to their high perfusion and since nanoparticular systems can be trimmed by shape, size and electrostatic properties to accumulate and release their siRNA cargo in high concentrations in these organs[85]. Nevertheless, the hurdle of a functional vehicle for siRNA remains challenging and is not yet satisfactorily solved for liver fibrosis therapy[86][28]. For effective anti-fibrotic therapy in liver, siRNA delivery systems must prevent siRNA from degradation in serum by nucleases, rapid clearance by kidneys and liver, and the reticuloendothelial system, to permit high accumulation of siRNA in liver. Therefore, on the one hand siRNA should be sufficiently entangled in the nanoparticles to prevent its premature degradation and body clearance, and on the other hand taken up specifically by liver cells, via facilitated release of siRNA cargo into the cytoplasm. This balance between protective complexation and sufficient cargo release after delivery is essential for successful liver specific therapy[28].

After the promising results of lipoplex-particles loaded with anti-col1α1 siRNA for liver fibrosis therapy reported by C Calvente *et. al.*[28], siRNA delivery systems that could provide further beneficial qualities in terms of therapeutic performance, biocompatibility and targeting, appeared feasible. Although lipoplex formulations could already be validated as suitable siRNA carriers for liver fibrosis therapy, they exhibited also difficult to abolish drawbacks. Thus, the only structure-building counterpart during the nanoparticle self-assembling process represented the siRNA cargo itself. As siRNA is rather short, this limits the stability of the formed complexes. In addition different siRNA cargos or modifications of siRNA will lead to different lipoplexes[87][88]. Despite big efforts to enhance *in vivo* (protein containing environment) stability of lipo- or polyplexes by covalently cross-linking them after aggregation, to date no convincing strategy has been devised to overcome this problem.

Alternatively, nanohydrogel particles as nano-sized siRNA delivery systems that were predefined in size and shape but independent of their siRNA cargo could serve as ideal carriers with improved stability for *in vivo* applications[87][88]. Once nanohydrogels were complexed with siRNA, their cationic character was neutralized, endowing the complexes with remarkable protein repulsive effects in human blood sera[77]. In *in vivo* experiments using intravital confocal videography, unloaded nanohydrogel particles alone assembled to larger aggregates in the bloodstream, bearing a high risk for thrombosis, whereas siRNA loaded particles continued circulating without formation of larger aggregates[89]. The *in vitro* knockdown performance of nanohydrogel particles as a function of their size their was studied by L Nuhn *et. al.* [77]. Only the 40 nm sized cationic nanohydrogels induced a robust knockdown for up to 3 days. The authors could show that these small (in contrast to bigger 100 nm) sized nanohydrogel particles were able to evade lysosomal compartments and thus early degradation after cellular uptake and assumed that this contributed to their enhanced knockdown performance[77]. After cellular uptake nanohydrogels are supposed to release their siRNA cargo into the cytoplasm for

functional siRNA delivery. Thereafter, they should be degraded, to prevent cellular accumulation. First attempts to improve biodegradability of nanohydrogels were made by equipping them with a disulfide-modified spermine cross-linker[90]. It could be shown that in reductive environment (as present in the cytoplasm) the particles were more easily degraded by reductive cleavage of the crosslinking units, releasing their siRNA into the cytoplasma. However, due to the incorporated hydrophobic disulfide linkers the cationic character of the particles was reduced, compromising their siRNA loading efficiency[90]. In the following generation of stimuli-responsive nanohydrogels, this drawback could be overcome by substituting the disulfide linkers with acid-labile ketal linkers. Particles cross-linked with these novel ketal-linkers showed no significant reduction of their siRNA loading capacity[2]. They were easily degraded in acidic conditions (pH ~4-5), which prevail in (late) endosomes, the first cell compartment where ~40 nm sized nanohydrogel particles accumulated after cellular uptake[77][90][91]. Besides the first generation of nanohydrogel (non-bioNP), I have also tested their next generation which contains an acid-labile linker in the inner core, endowing them with enhanced biodegradability, for therapeutic knockdown in our liver fibrosis mouse model.

Furthermore, nanohydrogels can be trimmed for cell specific delivery by surface decoration with appropriate linkers. Nanohydrogel particles were equipped with MUC1-glycopeptide, expressed on epithelial tumor cells, and P2, a T-cell epitope, for antitumor vaccination[92]. Thus, nanohydrogel particles showed to be accessible for cell surface decoration with glycopeptides/proteins as potential targeting units for cell specific delivery in future[92].

Considering all these positive characteristics of nanohydrogel particles and after an intensive *in domo in vitro* screening (in terms of cytotoxicity, cellular uptake and knockdown performance), nanohydrogels were selected as alternative to (lipo-)polyplexes siRNA vehicles that were previously tested in our group tested.

5.1 Synthesis of (non-)biodegradable nanohydrogel particles

As part of the collaborative research initiative 1066 (*Sonderforschungsbereich 1066*), both particles (non-)bioNP were synthesized and physicochemically characterized by our cooperating group (Director Prof. Zentel at the Department of chemistry, University of Mainz). Here, L Nuhn *et. al.* have designed a novel synthetic route to access well-defined cationic nanohydrogel particles with adjustable size for cellular siRNA delivery[60][1]. By reversible addition-fragmentation-transfer (RAFT) block-copolymerization of tri(ethylene glycol) methylether methacrylate (MEO_3MA) and pentafluorophenyl methacrylate (PFPMA) narrowly distributed amphiphilic reactive ester block copolymers were generated that self-assemble into nano-sized micellar aggregates in polar-aprotic solvents (e.g., dimethylsulfoxide) due to the solvophobic nature of the fluorinated reactive ester blocks. These superstructures can be permanently stabilized by cross-linking with spermine (for non-bioNP) or with the acid-labile ketal linker (for bioNP), while the pentafluorophenyl reactive ester moieties inside the core are fully converted into a hydrophilic cationic network for siRNA complexation. Such carriers provide a safe and protective environment for sensitive oligonucleotides shielding them from nucleases present in the blood stream[93]. During siRNA complexation, the carriers do not change their size of around diameters 30 – 40 nm (indicating an entanglement of siRNA in the core of the carries). Only their surface charge is neutralized, thereby preventing aggregation in

the blood circulation of mice[89]. The biodegradability of bioNP was analyzed by DLS, showing disintegration at pH 4.5 (present in late-endosmes/lysosomes) over a 12h timeframe but stability at pH 7.4 (physiological pH) (see Appendix Figure S4). (Non)-bioNP were labeled with two different dyes depending on our analysis. For *in vitro*/*in vivo* cellular uptake or *in vivo* biodistribution, particles were labeled with Oregon Green® (FITC like dye) or with CS800® (near infrared dye with good tissue penetration for *in vivo* biodistribution monitoring). Therefore, amine-functionalized dyes were attached to the reactive ester precursor polymers via covalent amide bonds, while different linkers (ketal-linker for bioNP and spermine for bioNP) were used for cross-linking of the particles as described above.

The labeled particles were freshly complexed with Cy5 labeled siRNA before each experiment, guarantying the best possible functional integrity for the siRNA. Our double labeling approach allowed distinct monitoring for the particle and the siRNA regarding cellular uptake and biodistribution studies.

The optimal mass ratio (minimal applied nanohydrogel mass for efficient siRNA complexation) between siRNA and nanohydrogels was determined by agarose gel electrophoresis. Here, for non-bioNP the best (w/w) ratio was determined to be 1:10 for siRNA:non-bioNP and 1:30 for bioNP:siRNA, without leakage of siRNA out of the carries, as assessed by gel electrophoresis (Appendix Figure S1, Appendix Figure S2 and Appendix Figure S3). The lower siRNA loading (w/w) for bioNP (1:30) compared to non-bioNP (1:10) is due to a reduced cationic potential generated by the ketal cross-linkers (compare zeta potential values in Table 7).

5.2 First generation of non-biodegradable nanohydrogel particles for liver fibrosis therapy

5.2.1 *In vitro* validation of anticol1α1 (sc)siRNA loaded non-bioNP

Prior to nanohydrogels being applied *in vivo*, they were thoroughly characterized *in vitro* to test their cell compatibility, knockdown efficacy and target specificity (to rule out significant cytotoxic effects, poor cell uptake and insufficient knockdown performance) prior to further therapeutic studies in mice. To qualify as suitable siRNA carrier for antifibrotic therapy, siRNA vehicles had to meet three primary needs:

1. Carriers need to exhibit a low cytotoxicity in the major liver cell types. Therefore, the potential cytotoxicity of NP loaded with scrambled siRNA was tested in murine fibroblast, macrophages and hepatocytes. Scrambled siRNA was chosen as cargo to neutralize the NP's cationic charge (the zeta-potential of uncomplexed NP is around 10 mV – compare Table 7) and to avoid possible off-target effects within the transcriptome of the tested cells. Off-target effects could also induce or obscure cytotoxic effects of the carriers. Therefore, uncomplexed NP were not assessed, because they do not reflect the physiochemical character of NP when complexed with siRNA. Fortunately, nanohydrogels loaded with scrambled siRNA did not show any signs of cytotoxicity up to siRNA concentrations corresponding to 400nM (far above applicable concentrations for *in vitro* or *in vivo* experiments) in the tested cell lines when using the MTT assay (Figure 13a). Although the MTT assay does not fully reflect the potential multifactorial cytotoxicity of the nanohydrogels *in vivo*, it is a reasonably good predictor

for biocompatibility, especially when no cytotoxicity is observed up to high concentrations of 400nM siRNA)[75].

2. Nanohydrogel particles had to show a robust cellular uptake in the tested cells, which is crucial for efficient siRNA delivery into the cytoplasm (the place of action where mRNA knockdown occurs)[94]. Therefore, Cy5 labeled anti-Tie2 (Cy5-anti-Tie2) siRNA loaded nanohydrogel particles labeled with Oregon Green® were tested for cellular uptake in murine RAW-macrophages and 3T3-fibroblasts (both being cell lines relevant for fibrosis studies). Cy5-anti-Tie2 siRNA was selected as siRNA cargo, since the marker Tie2 represents a specific gene that is prominently expressed in endothelial cells, ensuring only minimal off-target effects in the tested (non-endothelial) cells. By FACS, the double labeling approach allowed a distinct monitoring for NP-FITC and Cy5-siRNA. Here, the siRNA/NP were quantitatively taken up in a dosage and time dependent manner, achieving 100% double positive cells (NP-FITC+ and Cy5-siRNA+) at 100nM siRNA 1h after addition both in macrophages and fibroblasts (Figure 10c/d). There were no cells detected that took up either particle or siRNA alone, indicating a robust stability of siRNA/NP complexes in protein rich media. Notably, cells incubated with siRNA/NP (100nM) at 4°C overnight did not show significant uptake, ruling out unspecific binding on the cell's surface (a well-known pitfall in cellular uptake studies, showing also false positive cells by FACS) and additionally indicating an energy-driven uptake mechanism[1].

3. Anti-col1α1 siRNA/NP had to perform a functional siRNA delivery, which was proven by col1α1 mRNA knockdown in fibroblasts. As determined by qPCR, the complexes achieved a robust knockdown up to 60% for the targeted collagen transcript in the tested cells after 48h of incubation when applied at reasonable siRNA concentrations (25-100nM) (Figure 10b). Noteworthy, NP loaded with scrambled siRNA did not show any off-targets effects, proving a sequence specific knockdown with anti-col1α1 siRNA/NP. Off-target effects of the carrier or (sc)siRNA can lead to unwanted reductive/inductive effects for the cells' transcriptome, relativating the knockdown effect of the siRNA/nanohydrogel complexes[61][62]. They originate from the complexed scrambled siRNA and/or the carrier system itself. Unwanted reductive effects that were mediated by the scsiRNA, can be due to imperfect pairing of the scrambled siRNA strands with sequence motifs that reside primarily in 3′ UTR regions of cellular mRNAs[61]. Because only short regions of sequence complementarity are required for this type of off-target silencing, many transcripts can be affected and the effect is inherent to any (scrambled) siRNA sequence (Figure 7)[61][63]. The inductive off-target effect, here caused by the carrier or its siRNA cargo, could result from an innate immune response, based on the activation of toll-like receptors (TLRs)[61][63]. TLRs are responsible for the recognition of pathogen/exogenous agent-associated molecular patterns (Figure 7)[61][63]. Once TLRs are activated, they initiate an alarm cascade in the (innate immune) cells, resulting in an increased transcriptional level for cellular defense relevant genes, which can render results of knockdown experiments difficult to interpret[64][65]. However, no off-target effects were observed, neither for our applied scrambled siRNA or carriers, suggesting no unwanted activation of innate immunity.

Since after these pretestings all criteria were fulfilled by the siRNA loaded nanohydrogels, they were selected for further *in vivo* evaluations in mice.

5.2.2 *In vivo* biodistribution of Cy5-siRNA loaded near-infrared labeled non-bioNP

A reproducible liver fibrosis mouse model was established in our lab by treating mice (Balb/c) with escalating doses of carbon tetrachloride (CCl_4) via oral gavage which results in modestly advanced liver fibrosis already after 2 weeks[95]. Prior to performing studies in fibrotic mice, the biodistribution of (non-)bioNP/siRNA complexes was tested in healthy mice (Appendix Figure S 17). A detailed comparison of the siRNA/(non-)bioNP complexes' biodistribution in healthy vs fibrotic mice would then be relevant to study the therapeutic application in liver fibrosis, but also the potential to use siRNA targets different from col1*a*1, but was beyond the scope of the current thesis.

Fibrotic mice received two intravenous doses of 1 or 2 mg/kg Cy5-siRNA encapsulated in NP-IR, 48h apart (Figure 11a). After the second *iv* injection, biodistribution of siRNA and nanoparticles was monitored at multiple consecutive time points (0, 1, 3, 6, and 24h), revealing the kinetics of the biodistribution. Here, directly after injection a minor amount of Cy5-siRNA accumulated in the mice's urinary bladders, indicating a premature liberation in the blood stream (Appendix Figure S7). After *iv* injection, free siRNA is rapidly cleared by the kidneys and afterwards quickly excreted via the urine (compare Appendix Figure S 17)[96]. However, siRNA and NP prominently remained co-localized in the liver even 48h after injection, confirming a preferential accumulation of stable siRNA/NP complexes in the liver (Figure 11b).

Since the Cy5 dye (of the siRNA) and CS800-IR dye (of the particle) are significantly absorbed by tissues and fur (although both dyes emit in the near infrared region, featuring a moderate-to-good tissue penetration compared to shorter wavelength emitting dyes), organs were taken out at different time points for a more quantitative *ex vivo* imaging. In *ex vivo* imaging, the best co-localization of siRNA and NP could again be detected in liver, enabling a functional siRNA delivery in fibrotic livers (Figure 11c/d). Furthermore, elevated signals of siRNA, detected in kidneys and spleen, most probably resulted from a premature disintegration of the complexes in the blood stream (Figure 11d). Since siRNA, as hydrophilic molecule, must be encapsulated (except for some highly specialized applications – e.g. compare reference[97]) in a carrier to efficiently cross the lipophilic cell membrane as well as be transported to the liver after *iv* injection, a colocalization of siRNA and carrier on the macroscopic and cellular level is compulsory for knockdown in the addressed organs/targeted cells[57].

Since (*in vivo/ex vivo*) macroscopic biodistribution of siRNA/NP does not unveil the uptake on the cellular level, FACS analysis of single cell suspensions from the livers was performed. Besides activated myofibroblasts (α-SMA+ liver cells, cellular uptake ~50%,), the major collagen producing cells in liver fibrosis, macrophages (cellular uptake ~20%) were identified as important target cells of the complexes. Macrophages are crucial for remodeling the collagenous matrix during and after liver injury and play a key role in fibrogenesis as well as fibrolysis[1][98][70][99]. Hence, liver macrophages could also become an attractive target for gene-

silencing strategies for liver fibrosis therapy, using our NPs, as also demonstrated by the efficient *in vitro* uptake of the siRNA/NPs in RAW-macrophages[1].

The mechanism, by which activated myofibroblasts, the primary effector cells in fibrosis, take up the NPs so efficiently could not yet be entirely explored and is subject of another current thesis in our group. A plausible mechanism could be that α-SMA+ cells have a relevant phagocytic active after CCl_4 induction which would allow them to efficiently incorporated efficiently siRNA/NPs[100].

In conclusion, after *iv* injection siRNA/NP accumulate primarily in the liver (shown by IVIS *in* and *ex vivo* imaging) and are efficiently taken up by activated myofibroblasts (shown by FACS). As activated myofibroblasts represent the major collagen producing cells in liver fibrosis (and other fibrotic conditions), they represent a central target cell population for anti-fibrotic therapy. In view of the promising *in vitro* knockdown results with col1α1-siRNA/NP in fibroblasts and the favorable *in vivo* targeting of activated liver myofibroblasts, these carriers were tested for their antifibrotic potential in liver fibrotic mice.

5.2.3 *In vivo* collagen knockdown mediated by anticol1α1 siRNA loaded non-bioNP in liver fibrotic mice

Liver fibrosis in mice (Balb/c) was induced in mice according to our established CCl_4 gavage scheme (compare Figure 11a). After two intravenous doses of anti-col1α1siRNA loaded NP (1 or 2 mg/kg) procollagen type I expression was significantly reduced on the transcriptional level (as determined by qPCR) whereby scrambled siRNA did not show an effect, indicating a sequence specific knockdown (Figure 12a). Quantification of col1α1 mRNA by qPCR does not fully correlate with the translated protein or collagen deposited in the tissue[101]. Therefore, quantification of total collagen deposition (of which type I is the most prominent subtype) is compulsory to study a reliable anti-fibrotic effect of the treatment *in vivo*. Total hydroxyproline (HYP), as the gold standard collagen for quantification, was significantly down-regulated (Figure 12b). In addition, morphometric quantification of collagen deposition after Sirius Red staining (a specific stain for fibrillar collagen) in paraffin sections supported the antifibrotic effect of the siRNA/NP treatment. Here, collagen was even highly significant reduced (for 1 mg/kg siRNA ~60% and for 2 mg/kg siRNA ~75% reduction of collagen, ***p <0.0001 vs PBS/scsiRNA loaded NP). Sirius Red provides an accurate quantification of collagen in liver, since we established quantification of only functional relevant collagen by omitting large portal vascular areas which have a high collagen, with little effect on liver function[81].

The collagen reducing effect mediated by anti-col1α1 siRNA/NP at 1 or 2 mg/kg siRNA concentration could compete with the antifibrotic effect triggered by optimized anti-col1α1 siRNA loaded lipoplexes (~80% reduction of collagen for 200 µg/kg of an anti-col1α1 siRNA loaded in lipoplexes (LNP) – compare Figure 18b/e)) reported by our group (C Calvente *et. al.*, Hepatology 2015[28]). In this study mice were gavaged with escalating doses of CCl_4, according to the protocol in this thesis, for 5 (for the progression model) or 8 weeks (for the regression model). Mice received 4 *iv* injections of 200 µg/kg anti-col1α1 siRNA loaded lipoplexes in the last two weeks of the CCl_4 treatment (2 injections per week, progression model), or in the four weeks after termination of the CCl_4 treatment (1 injection per week, regression model) (Figure 18a/d demonstrates these results for comparison).

Overall, the antifibrotic effect mediated by the anti-col1α1 siRNA/NP was comparable, although a higher siRNA amount had to be applied (1000 or 2000 µg/kg siRNA loaded nanohydrogels vs. 100-400 µg/kg siRNA loaded lipoplexes). Taking into account that the high siRNA transfection efficiency of lipoplexes often correlates with their high cytotoxicity[102], this can be considered a favorable profile. For example, Grandinetti *et al.* reported that direct interactions between polyplexes/lipoplexes with the mitochondria membrane during transfection can cause severely impaired mitochondrial function through membrane depolarization which may be a major reason for high cytotoxicity in non-covalent stabilized siRNA vehicles[103][104]. This kind of cytotoxic effects was not observed with the covalently stabilized siRNA vehicles e.g. nanohydrogels[102].

αSMA is a marker for activated myofibroblasts and therefore acting as a surrogate marker for fibrogenesis. The αSMA reducing effect, induced by the anti-col1α1 siRNA/NP, was similar to the anti-col1α1 siRNA loaded lipoplexes' effect (C Calvente *et. al.*, compare Figure 18c/f).

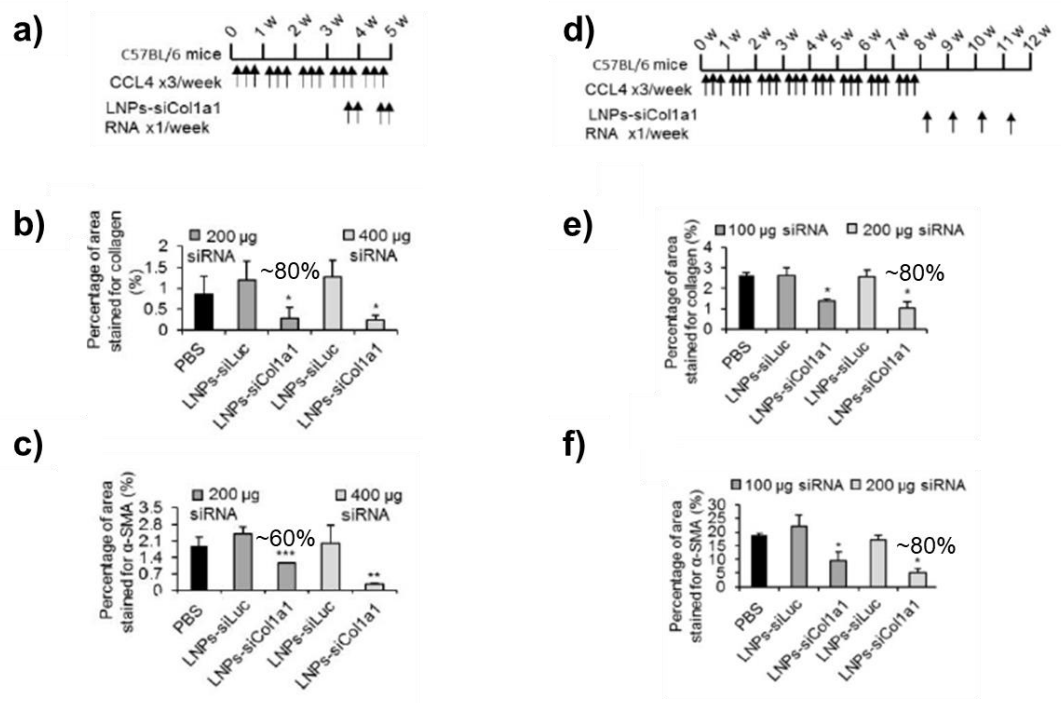

Figure 18. Anti-col1α1 siRNA loaded lipoplexes (LNP-siCol1α1) showed a pronounced antifibrotic effect in CCl_4-induced liver fibrosis (data from C Calvente et al., Hepatology 2015[28]). a) Experimental design of the progression model. C57BL/6 mice were gavaged with escalating doses of CCl_4 3 times a week for 5 weeks. During the last two weeks, mice received once weekly *iv* injections of PBS, LNP-siCol1α1 siRNA or LNP-siLuc at 200 and 400 µg/kg siRNA doses biweekly for 2 weeks. Liver specimens were harvested at 24 h post-injection. b) and c) Quantification of Sirius Red and αSMA-positive areas in 5 randomly selected fields of each specimen (means ± SD, n = 10). *p<0.05 vs. LNP-siLuc. d) Experimental design of the regression model: C57BL/6 mice were gavaged with escalating doses of CCl_4 3 times a week over 8 weeks. 24h after the last CCl_4 gavage mice were *iv* injected with PBS, LNP-siCol1α1, or LNP-siLuc (LNP-siLuc represents scrambled siRNA) at 100 and 200 µg/kg of siRNAs once weekly for 4 weeks. e) and f) Percentage of Sirius Red and αSMA positive area in 5 randomly selected fields from each specimen, as assessed by computerized image analysis (means ± SD; n=5/group, n=3 per sample). *p < 0.05 vs LNP-siLuc.

After consecutive injections of siRNA/NP, there were no significant (sub-) acute toxic effects (e.g. liver/biliary/kidney toxicity since AST/ALT (indicating liver damage), γ-GT, alkaline

phosphatase (cholestasis parameters) or creatinine (indicating kidney damage) remained in the normal range (compare Appendix Figure S8 and Appendix Figure S14).

Conclusively, nanohydrogel particles loaded with anti-col1α1 siRNA showed a significant and sequence specific antifibrotic effect by efficient procollagen type I knockdown (at moderate siRNA concentrations of 1 and 2 mg/kg siRNA) in our short-term CCl_4 mouse model. Additionally, no adverse cytotoxic *in vivo* effects could be observed. Thus, nanohydrogel particles qualified as promising siRNA carrier platform for further developments, including next generation NPs, e.g. with improved biodegradability.

5.3 Comparative study of first generation non-bioNP vs second generation bioNP as anti-col1α1 siRNA vehicle for liver fibrosis therapy

5.3.1 *In vitro* comparison between (sc)siRNA loaded (non-)bioNP with bioNP

Second generation nanohydrogels were chemically modified to improve their biodegradability. To this aim, the inner spermine cross-linker was substituted by an acid-labile ketal cross-linker, endowing second generation nanohydrogels (bioNP) with improved biodegradability in low pH cellular compartments (e.g. lysosomes with pH 4.5, compare Appendix Figure S4 for bioNPs disintegration at pH 4.5 over 12h) [105].

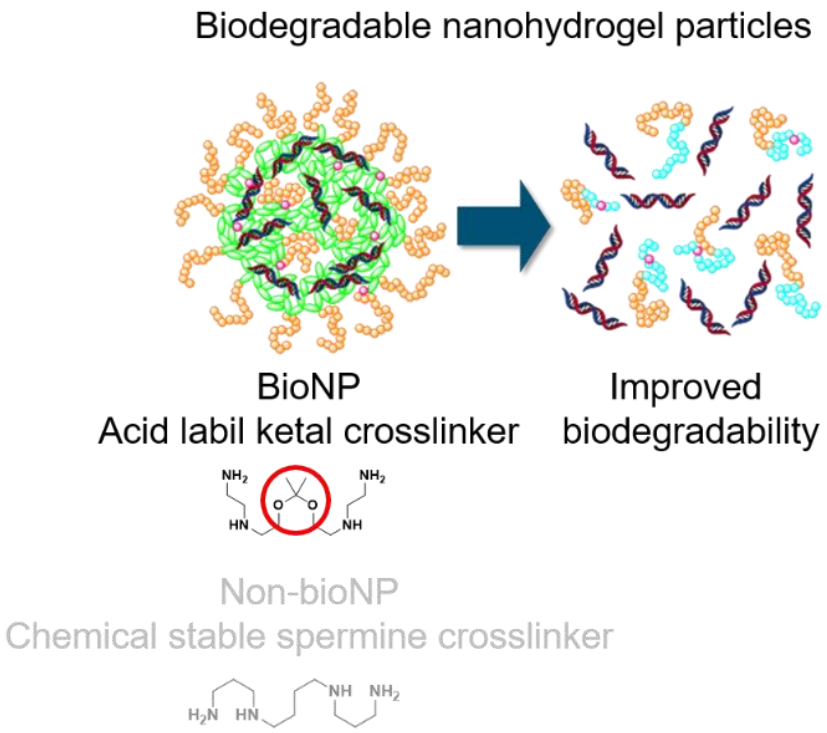

Figure 19. Second generation of nanohydrogel particles - biodegradable nanohydrogel particles: Non-biodegradable nanohydrogel particles were modified by substituting the chemical stable spermine cross-linker with an acid labile ketal crosslinker, endowing bioNP with enhanced biodegradability.

Since bioNP exhibited a reduced siRNA complexation efficiency due to the more hydrophobic ketal linker, the complexation ratio (w/w) siRNA:NP 1:10 for non-bio-NP had to be adapted to 1:30 for bioNP.

In vitro toxicity of both nanohydrogels loaded with scramble siRNA ((non)-bioNP/scsiRNA) did not show any cytotoxic effects up to high siRNA concentrations (up to 400nM (sc)siRNA) (Figure 13a). Even an ultrahigh load of bioNP vs non-bioNP did not affect the viability of the cells.

Cellular uptake of Cy5-siRNA loaded bioNP was equally efficient (~100% after 1h incubation for 50 and 100nM siRNA) compared to Cy5-siRNA/non-bioNP in fibroblasts and macrophages (Figure 13c/d). Distinct labeling of siRNA (Cy5-dye) and (non)-bioNP (Oregon-Green® dye) allowed to assess complex stability of siRNA loaded nanohydrogels in protein rich media. However, cellular uptake analysis of siRNA/NP complexes restricted to either carrier or its cargo (siRNA) alone does not necessarily reflect cellular uptake efficiency. Uptake pathways are very heterogeneous and, besides the classically known pathways (endocytosis, pinocytosis, phagocytosis), cellular uptake pathways like "kiss-and-run" (reported by Mailänder *et. al.* for delivering hydrophilic molecules with lipid-like-droplets to mammalian cells) could also apply to nanohydrogels, whereby the vehicle is not incorporated and only the siRNA cargo is released[106][107]. However, using fluorescence microcopy and FACS for both nanohydrogels loaded with siRNA no single dye-positive cells, either for NP-FITC or Cy5-siRNA alone, could be observed, indicating a comparable robust complex stability for bioNP and non-bioNP in protein rich media (compare Appendix Figure S10, Appendix Figure S11 and Appendix Figure S12).

Anti-col1α1 siRNA/bioNP complexes induced a sequence specific and highly significant col1α1 mRNA *in vitro* knockdown (~80%, ***$p<0.0001$ vs. PBS and bioNP/scrambled siRNA) at reasonable siRNA concentrations (25, 50 and 100nM siRNA) after 48h in fibroblasts (equally efficient compared to the commercially available Lipofectamine® transfection agent that can only be used for *in vitro* transfections (Figure 13b). In parallel, for the anti-col1α1 siRNA loaded non-bioNP once again their knockdown efficiency *in vitro* was confirmed (~50%) after 48h at 100nM siRNA (*$p<0.05$ vs PBS and non-bioNP/scramble siRNA).

Interestingly, anti-col1α1 siRNA loaded bioNP induced a ~4 to 5 times more effective knockdown (for col1α1 mRNA) vs anti-col1α1/non-bioNP at low siRNA concentrations of 25nM siRNA. A hypothesis for the improved *in vitro* knockdown efficiency of anti-col1α1/bioNP in fibroblasts, especially at low siRNA concentrations, is the improved degradation feature of bioNP in the endosomal compartments together with the disassembly into single cationic polymers that may interact with the vesicular membranes and trigger an alleviated siRNA release in the cytoplasm. Still, the complexing affinity of the newly synthesized ketal cross-linker (of bioNP) was as sufficient for siRNA stabilization and nanocarrier-triggered uptake into cells as the cations in the non-bioNP in protein containing media. However, due to the improved degradation under acidic conditions in the late endosomes/lysosomes an altered *in vitro* knockdown efficiency of bioNP as siRNA carrier seemed to be especially prominent at low siRNA concentrations (around 25nM), with a lower amount of siRNA for a significant target knockdown[85]. Based on these optimized *in vitro* results of siRNA loaded bioNP, they qualified for further biological evaluation in a 1:1 comparison to siRNA loaded non-bioNP *in vivo* study.

5.3.2 *In vivo* biodistribution of Cy5 siRNA-loaded near infrared labeled (non)-bioNP

A minor quantity of Cy5-siRNA and non-bio/bioNP were rapidly excreted by the kidneys after *iv* injection), indicating a partial disassembly in the blood stream (macromolecules with hydrodynamic radius <5.5 nm) are usually rapidly cleared by the kidneys[108][109]. However, 6h after injection this clearance process stagnated and no further particle or siRNA enrichment could be detected in the bladder (see Appendix Figure S13). Non-covalently stabilized liposomes/polymersomes for siRNA delivery (in contrast to our covalently cross linked nanohydrogels) bear the risk to be excreted by the kidneys before they arrive in the liver[110]. However, after 6h the majority of non-bio/bioNP and Cy5-siRNA had accumulated almost exclusively in the liver as intact complexes, indicating an early predominantly enrichment and stabilization in the liver (Figure 14a). Macroscopically, no significant difference between the first vs. second generation of nanohydrogels could be found.

Gref *et al.* were the first to report the critical characteristics of NP to prolong blood circulation time after *iv* administration. Here, NPs with <100 nm in size and a neutral or anionic charge combined with PEG (>5 kDa) coating on the surface showed the longest blood circulation time preventing sequestration in the spleen and enabling a decelerated accumulation in the liver[111]. Applying these principles to the nanohydrogels, it can be concluded that these were small enough in size (ø~<40 nm, compare Table 7) and sufficiently shielded by their protein repulsive PEG corona to entirely avoid retention in the spleen. After charge-neutral complexation with siRNA the cationic nanohydrogel particles still seemed to attract a non-aggregating protein corona in the blood stream, which may have promoted their accumulation especially in the fibrotic tissue of the liver[112]. Such a promising macroscopic biodistribution is highly advantageous for antifibrotic therapy by evading premature renal excretion and unfavorable sequestration in other organs/tissue.

IVIS *ex vivo* imaging allowed an accurate quantification of the Cy5-siRNAs and CS800-nanohydrogels (NP-IR), confirming the previous *in vivo* findings that the complexes accumulated predominantly in the liver (Figure 14b).

FACS analysis disclosed which liver cells were targeted preferentially by the nanohydrogels. For most of the studied cells, biodistribution on the cellular level did not change between the two nanohydrogels. Both nanohydrogels and their siRNA cargo were efficiently taken up by αSMA+ activated myofibroblasts (~20%), liver macrophages (~20%), but only to minor extent by albumin+ hepatocytes (~2-5%) (Figure 14d). Noteworthy, Cy5-siRNA/bioNP were taken up highly efficiently (~30%) by endothelial cells. It is possible that a preferential interaction of certain serum components with the bioNP-IR, due to their newly introduced functionality, could have caused this preference for endothelial cells[2]. However, both nanohydrogels efficiently delivered Cy5-siRNA to αSMA+ activated myofibroblast, the major collagen producing cells in liver fibrosis, and to liver macrophages, a suitable cell target for immunomodulatory therapy fibrosis[22][99]. As for non-bioNP-IR/Cy5-siRNA, hepatocytes, as the most abundant cells in liver, showed a minor uptake of bioNP-IR/Cy5-siRNA (~2-5%). Therefore, the preferential uptake in activated myofibroblasts and macrophages cannot be attributed to quantitative effects,

but rather a preferential uptake in these cell types. The specific cellular uptake pathways of siRNA loaded nanohydrogels are currently under investigation[113].

5.3.3 Comparison of *in vivo* therapeutic collagen knockdown efficiency mediated by anti-col1α1 siRNA loaded non-bioNP vs bioNP

Based on the *in vivo* imaging results that the second generation of nanohydrogels robustly delivered siRNA to liver myofibroblasts, the antifibrotic effect (knockdown efficiency) of anti-col1α1 siRNA loaded non-bioNP vs bioNP in the established CCl_4 short-term fibrosis model was compared (see Figure 11a).

Total collagen protein amount in treated livers, when determined biochemically via HYP, was significantly (for both particles *p< 0.05) and specifically suppressed (~35% vs PBS or scsiRNA/(non)-bioNP treated mice, see Figure 15b). Both anti-col1α1 siRNA loaded nanohydrogels also equally and highly significantly reduced the functionally more relevant parenchymal collagen deposition as determined by Sirius Red morphometry (~60-70%, ***p<0.0001 vs the PBS and the corresponding scrambled siRNA/nanohydrogel controls, Figure 15c/d).

Consistent with the collagen reductive effect, both particles loaded with anti-col1α1 siRNA significantly reduced αSMA on the transcriptional and protein level as determined by quantitative IHC (Figure 16a/d).

Both siRNA loaded nanohydrogels did not show any acute liver toxicity in mice as determined by routine serum parameter (see Appendix Figure S8 and Appendix Figure S14)[114].

In conclusion, the antifibrotic effect (reduction of collagen and *α*SMA both on the transcriptional and protein level) mediated by anti-col1α1 siRNA non-bioNP and bioNP in the fibrosis mouse model was comparable to the antifibrotic effect of LNP-siCol1α1 (at 200 µg/kg siRNA) reported by C Calvente *et. al.* (see Figure 18c/f).

The toxicity of siRNA nanocarriers is often a limiting factor in translational studies, being complex and in part unpredictable. The excellent *in vivo* biocompatibility of the nanohydrogels is essential for long-term antifibrotic treatment, since such treatment needs to be long-term (e.g. chronic advanced fibrosis/cirrhosis due to chronic virus hepatitis, even with the recently developed highly effective antiviral therapies, for alcohol and nonalcoholic fibrosis, and congenital as well as autoimmune liver diseases)[79][4]. Here biocompatibility should be closely correlated with biodegradability, since the siRNA carriers must be degraded and excreted to prevent accumulation in the body[115]. Considering, the transient nature of siRNA activity (usually less than 1 week, except for highly sophisticated and extremely stable siRNA variants synthesized by Alnylam®) requires a repeated administration to treat chronic diseases, which bears the risk of cumulative toxicity of nanocarriers[116][117]. Thus, progressive accumulation in the liver would overload compartments such as lysosomes/endosomes, with possible cellular damage and secondary immune activation[118]. Once downsized to nano-scale, many normally ‘inert’ materials can become substantially more reactive, probably owing to the dramatic increase in total surface area. Consequently, this results in more extensive interactions between nanoparticles and the biological systems[116].

In order to test the biodegradability of our nanohydrogels, CCl_4 fibrotic mice were *iv* injected with scrambled siRNA loaded non-bio or bioNP at 2 mg/kg siRNA. Ketal crosslinked bioNP were degraded significantly faster than non-bioNP. 48h after injection, the bioNP-IR signal fell far below that of the non-NP (Figure 17a). This trend continued to essential non-detectability in the following 13 days. The (non)-bioNP-IR fluorescence signal decay after *iv* injections was retrospectively quantified from previous monitoring experiments (two consecutives *iv* injections in one week, with 48h between injections – see Figure 11a/b). Here the better biodegradability of bioNP-IR vs non-bioNP was confirmed (*$p < 0.05$ for the first and ***$p<0.0001$ for the second injection) (Figure 17b). In conclusion, the new acid-labile ketal linker endowed bioNP with enhanced biodegradability compared to the first generation nanohydrogels, confirming the accelerated disintegration of bioNP at low pH (pH 4.5) *in vitro* also in *in vivo* and after repetitive application (compare also - Appendix Figure S4).

To assess the therapeutic index of the NP, CCl_4 fibrotic mice were challenged with escalating doses of (non)-bioNP loaded with scrambled siRNA up to overdosed 10 mg/kg siRNA (Figure 17c). While most mice did not display lethal toxicity, 1 out of 5 animals died in the scsiRNA/non-bioNP group when dosed at 8 mg/kg siRNA, which could be due to chance or an untoward effect of the applied non-degradable species (compare also Appendix Figure S8 and Appendix Figure S14 for serum parameters of mice which were repetitively injected with 1 or 2 mg (sc)siRNA/(non)-bioNP per kg body weight). Overall, both nanohydrogels exhibited a broad therapeutic range without overt toxicity up to 10 mg/kg siRNA, a very high and amount of complexed siRNA for gene silencing therapy *in vivo*[119].

The superior *in vitro* knockdown performance of anticol1α1-siRNA/bioNP was not reflected by an improved collagen knockdown in liver fibrotic mice. It is possible that two injections of anti-col1α1 siRNA/nanohydrogels were not sufficient to demonstrate a difference in the therapeutic effect between the carriers and that longer-term treatment might have revealed a distinction. Moreover, also a slightly increased degradation was recorded for the siRNA/bioNP complexes before they reached the liver – thus a reduced amount of complexed siRNA that actually accumulated in the fibrotic liver tissue might have been compensated by an enhanced knockdown performance on a cellular level, as shown *in vitro*.

Due to the enhanced biodegradability of scsiRNA/bioNP vs. scsiRNA/non-bioNP after a single and repetitive injections, the second generation nanohydrogels should be preferable over the first generation for long-term antifibrotic treatment.

6. Conclusion & Outlook

Although significant progress has been made in understanding the pathophysiological principles underlying the development of liver fibrosis and its advanced state cirrhosis, there is yet no specific and effective treatment yet available in the clinic, to stop the progression or to induce the regression of liver fibrosis[99]. Inspired by the convincing *in vivo* therapeutic potential of anti-col1α1 siRNA loaded lipoplexes reported by C Calvente *et. al*., nanohydrogel particles loaded with anti-col1α1 siRNA were investigated, as a novel family as siRNA carriers, for a highly cell and target specific *in vivo* liver fibrosis therapy[28].

Nanohydrogel particles, as covalently stabilized nanoparticles, offer distinct advantages in comparison to purely electrostatic stabilized poly/lipoplexes. Nanohydrogel particles evidently retain their nano-structural integrity in the blood stream and are amenable to surface modification with cell-specific linkers (e.g. small molecules, carbohydrate residues or hydrophilic proteins) for tissue and cell targeted delivery[120][121].

In line with earlier reports by L Nuhn *et. al.*, anti-col1a1 siRNA loaded nanohydrogels, in the smaller size of Ø<50nm, induced a robust *in vitro* knockdown of col1a1 transcripts in murine fibroblasts, which share characteristics with activated hepatic stellate cells and myofibroblasts *in vivo*[77].

Double labeled Cy5-siRNA/NP-CS800 (IR) complexes revealed a high stability in the blood stream, as observed by *in vivo* near infrared fluorescence imaging (IVIS). In the subsequent *ex vivo* fluorescence imaging of the extracted organs, Cy5-siRNA cargo and the IR-NP accumulated primarily in the liver and to a much lesser extent in the lungs and spleen (organ sites prone to sequestrate insufficiently (PEG)-shielded nanoparticles due to aggregation with serum proteins) (Figure 11)[115]. In conclusion, 1) siRNA/NP complexes were small enough in size (Ø<50nm) to pass effectively through the discontinuous liver endothelium (liver endothelial fenestra - Ø 40-100 nm) and through the small capillaries (Ø<5-10µm)[122][123], and 2) they were sufficiently shielded by their PEG-corona to avoid aggregation with serum proteins and subsequent clearance by the mononuclear phagocyte system (MPS) of the spleen. (Figure 11)[124].

On the cellular level *in vivo*, Cy5-siRNA/NP were effectively taken up by activated myofibroblasts (~40%), the major ECM producing cells in liver fibrosis as well as by liver macrophages (~20%). Interestingly, macrophages of the lungs were moderately targeted (~15-20%), while only a small number of complexes were sequestrated in the lungs (Figure 11). Although the role of macrophages and their polarizations in NP uptake are not sufficiently explored, CD206 (over-)expressing M2 macrophages might be a promising cell target for cell specific delivery with mannose residues decorated nanohydrogels, reeducating them to switch to a putatively fibrolytic phenotype[22][125][126][127].

When liver fibrotic mice were treated with anti-col1α1 siRNA loaded NP corresponding to 1 or 2 mg/kg body weight of siRNA, liver collagen was sequence specifically and significantly reduced to the levels of healthy mice, as determined by liver HYP determination and morphometrical collagen quantification in Sirius Red stained liver sections (Figure 12)[17][28]. Standard serum marker assessment of the treated mice, which were repetitively injected with the siRNA/NP complexes, lacked any signs for acute toxicity (Appendix Figure S8). As such, nanohydrogel particles qualified as promising *in vivo* siRNA carriers for liver fibrosis therapy.

As the *in vivo* biodegradability of NP correlates closely with their biocompatibility, nanohydrogels (bioNP) were equipped with acid-labil elements, a pH sensitive ketal cross linker, endowing them with enhanced biodegradability properties[128].

In line with their first generation (non-bioNP), bioNP/scsiRNA complexes missed any signs of *in vitro* cytotoxicity (up to corresponding 400nM siRNA) and were highly efficient taken up (~100% after 24h incubation) in fibroblasts and macrophages (Figure 13). For *in vitro*

knockdown, anti-col1α1/bioNP complexes significantly surpassed their ancestors, reducing col1α1 mRNA transcript up to 90% (at reasonable siRNA concentrations of 100nM) in TGFβ1 stimulated 3T3 fibroblasts. This was as effective as Lipofectamine®, a commercially available transfection agent for *in vitro* but not *in vivo* siRNA delivery (Figure 13). Therefore, the improved knockdown efficiency of bioNP might be due to an improved siRNA cargo release after cellular uptake. Due to their reduced zeta-potential, bioNP complexed their siRNA cargo less stringently, favoring its release into the cytoplasm once the complexes were taken up.

After *iv* injection, the pH sensitive bioNP-IR/Cy5-siRNA complexes co-accumulated mainly in the liver and only to a small proportion in the lungs, spleen, kidneys and heart.

In accordance with *in vitro* studies, bioNP-IR/Cy5-siRNA complexes were effectively taken up by myofibroblasts, liver macrophages (both up to 20%) and, surprisingly, only to a very small percentage by hepatocytes, the most abundant parenchymal cells in liver. Noteworthy, siRNA/bioNP were efficiently taken up by endothelial cells (up to 30%) (Figure 14). E Serda *et al.* reported that in protein containing media the surface charge of silica particles strongly influenced their *in vitro* cellular uptake in endothelial cells[129]. Even though *in vitro* conditions do not reflect the by far more complex conditions *in vivo*, the reduced zeta potential of bioNP, may have promoted the efficient uptake in liver endothelial cells which is enhanced with cationic charge. It is tempting to suggest that cationic bioNP could putatively serve as potential siRNA carriers to treat metabolic dysfunction in the vascular systems, as was already reported for nanoparticles based on poly dl-lactide-co-glycolide polymers[130][131].

In liver fibrotic mice, anti-col1α1 siRNA loaded bioNP induced, similar to their first generation non-bioNP, a specific and significant reduction of col1α1 mRNA transcript levels and a subsequent reduction of (parenchymal) collagen as quantified by biochemically collagen assessment (liver HYP quantification and morphometrical assessment of Sirius Red stained liver sections, Figure 15)[17]. Of note, siRNA as well as scrambled siRNA loaded (non-)bioNP reduced the pan-macrophages maker CD68 on the RNA and protein level, suggesting a beneficial anti-inflammatory effect, which will be investigated in detail in further studies (Figure 16).

The therapeutic effect of anti-col1α1 siRNA loaded (non)-bioNP was comparable to optimized anti-col1α1 siRNA loaded lipoplexes reported by C Calvente *et. al.*, while in the present work 2-3 fold higher siRNA concentrations had to be applied (200-800 µg/kg siRNA/lipoplexes vs 1-2 mg/kg siRNA/(non)-bioNP)[28]. However, the siRNA used in this other study of our group was highly optimized for stability by the largest siRNA biotech company, Alnylam in Boston, unlike the standard modified siRNA that was used in the present study. Thus, ultimate comparison of the NP with the lipoplexes can only be done using the same siRNA with both carrier formulations.

Progressive accumulation after repetitive injections of nanoparticles in liver or other organs (e.g. kidneys) is a potential problem and can pose a serious concern for their long-term application[132][133][134]. *In vivo*, second generation bioNP-IR were degraded significantly faster and thus pose a lower risk of excessive accumulation in the liver or other organs during long-term treatment. ScsiRNA loaded (non-)bioNP exhibited no lethal *in vivo* toxicity nor any other

toxic effects up to very high siRNA concentrations of 10 mg/kg in mice (Figure 17). Hence (non-)bioNP are suggested to possess a broad therapeutic index, at least for shorter term therapies.

Novel cross-linker concepts will combine biodegradability with a tailor-made loading capacity for whatever cargo (siRNA, small molecule or macromolecule drug). In order to reduce the polymer mass ratio in the complexes, future cross-linkers should contain additional secondary amines, improving their siRNA complexing efficacy and *in vivo* siRNA delivery to the liver. Tetra-functional cross-linkers could further combine robust *in vivo* stability with high complexing efficacy. As acid-labile ketal cross-linkers have already endowed bio-NP with improved biodegradability, chemically active imine groups could be integrated into cross-linkers, extending their flexibility for chemical reactions, e.g. for surface modifications or the attachment of drugs (Figure 20).

As further outlook, bioNP can be decorated with cell specific linkers for tissue/cell specific delivery, as J W Park *et al.* reported for anti-HER2 antibody decorated liposomes to target human breast cancer cells[135]. This approach could be tested also for liver fibrosis therapy, using myofibroblast targeting antibodies i.e. anti-PDGFβ receptor decorated particles (Figure 20)[136]. Nevertheless, decoration of nanoparticles with antibodies remains challenging since antibodies after their covalent attachment on the NP's surface often lose or partly lose their binding capacity to the target antigen[137].

For liver macrophage targeting, carbohydrate fragments/residues are very promising[138][139]. Thus, bioNP decorated with (tri)-mannose to target the mannose receptor CD206 on M2 macrophages is a promising approach to deliver (macrophage (re)polarizing) siRNAs (e.g. anti-CSFR1, YM-1 siRNA), which could switch them from a fibrogenic to a fibrolytic M1 macrophage phenotyp (Figure 20)[140][141]. M2 macrophages represent also an attractive cellular target for cancer immunotherapy, since they share many characteristics with tumor-associated macrophages (TAM)[142]. As selective depletion of M2/TAM macrophages ameliorated glioblastoma metastasis in mice[143]

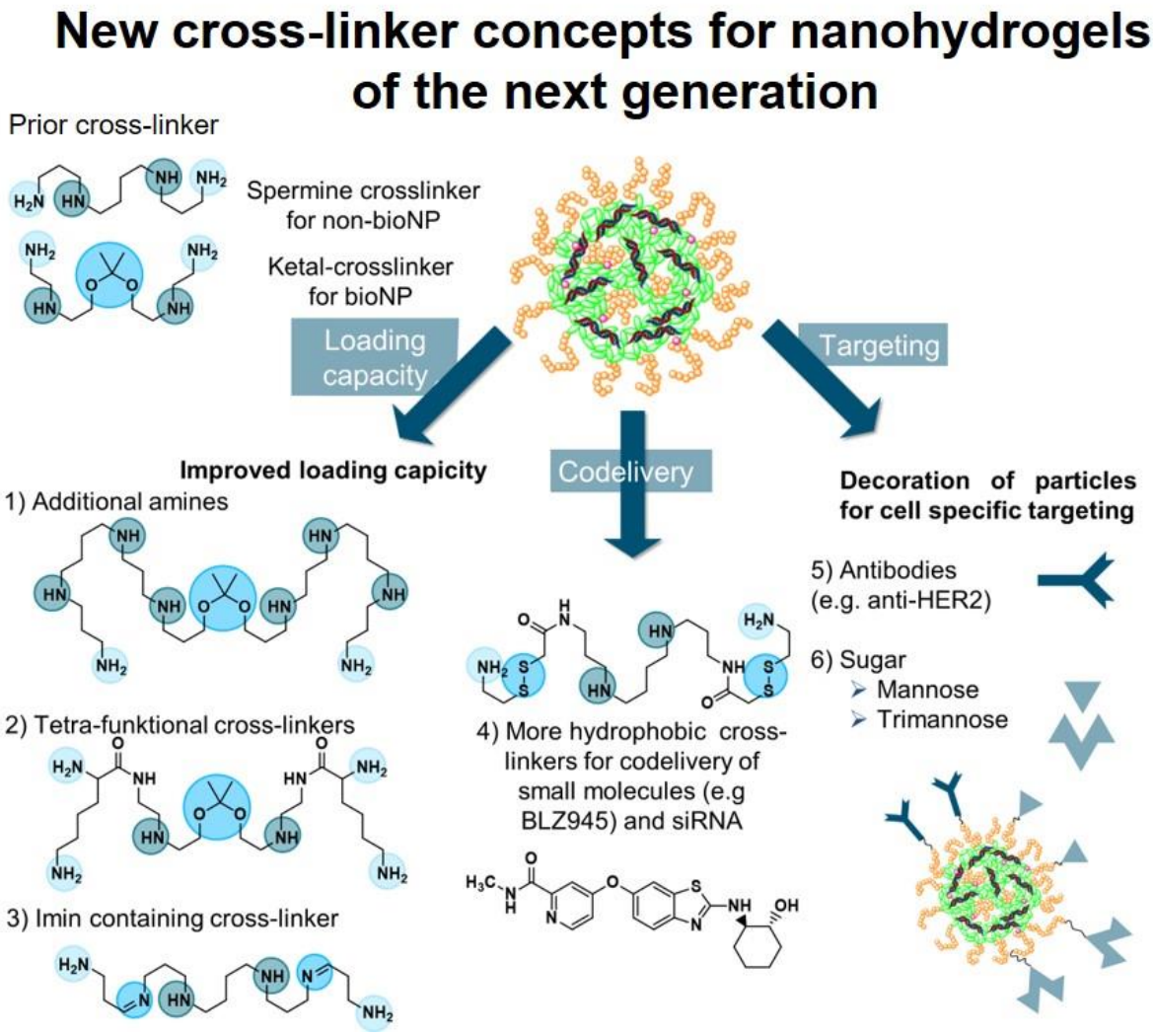

Figure 20. Novel cross-linker concepts for the upcoming generations of nanohydrogel particles. BLZ945, a pan tyrosine-kinase inhibitor, for macrophage-targeted immunotherapy (elements of this figure were gratefully received from our collaborator N Leber *et. al.*, University of Mainz, 2016).

Beside the optimization of the carrier system, siRNA itself represents a second adjusting screw to improve the therapeutic efficiency. Our commercially purchased anti-col1α1 siRNA contained a widely used modification pattern to improve its stability from nuclease degradation, whereby at both strands every second 2'-OH group of the sugar bases is alkylated by a methyl group (2'-OMe)[119]. However, further optimizations are possible.

Currently we are testing optimized 2′-deoxy-2′-fluoro (2′-F) anti-col1α1 siRNA for *in vitro* knockdown in fibroblasts. According to Manoharan *et al.* fluorinated siRNA showed superior nuclease resistance and are thermodynamically more stable compared to 2'-OMe modified siRNA[144]. In addition to stability, specificity of siRNA is compulsory for sequence specific gene silencing[61]. Insufficiently specific siRNA and inappropriate modifications or molecular lengths bear the risk of toxicity by off-target effects, e.g. via activation of toll-like receptors (TLRs) on innate immune and certain non-immune cells[145]. Off-target effects are mediated via the immune system, but also by unspecific base pairing between the siRNA seed regions (position 2-8 of either siRNA strand counting from the 5′-end) and complementary sequences

in the 3′UTR region of (off-) target transcripts[146]. Thus, chemical modification of the anti-col1α1 or other siRNA seed region can significantly mitigate such off-target effects [147].

Regarding the activation of the TLR signaling pathways by siRNA and its fragments, the replacement of the 2′-hydroxyl uridines with either 2′-fluoro, or 2′-deoxy, or 2′-O-methyl uridines seems to be a promising approach to abrogate immune recognition of siRNAs[63]. It may be assumed that the modifications of 2′-hydroxyl uridines of (sc)siRNA sequences in the present study could strengthen the (macrophage specific) CD68 reducing, anti-inflammatory effect of (sc)siRNA loaded nanohydrogels in liver.

In future studies, nanohydrogel particles will be optimized for tissue/cell specific delivery and drug loading capacity, to further improve, together with cleverly optimized siRNA sequences, their therapeutic efficacy. Needless to say, that their application will not be restricted only to liver fibrosis therapy.

7. Appendix

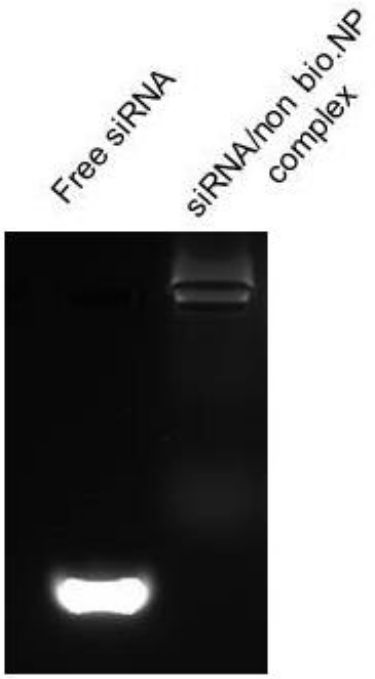

Appendix Figure S1: siRNA/(non)-NP complexes were routinely confirmed by 1% agarose gel electrophoresis (100 V, 45 min) and Gel Red staining. Since siRNA is well protected inside the carries from the intercalating Gel Red dye, siRNA complexed in nanohydrogels was less visible on the gel.

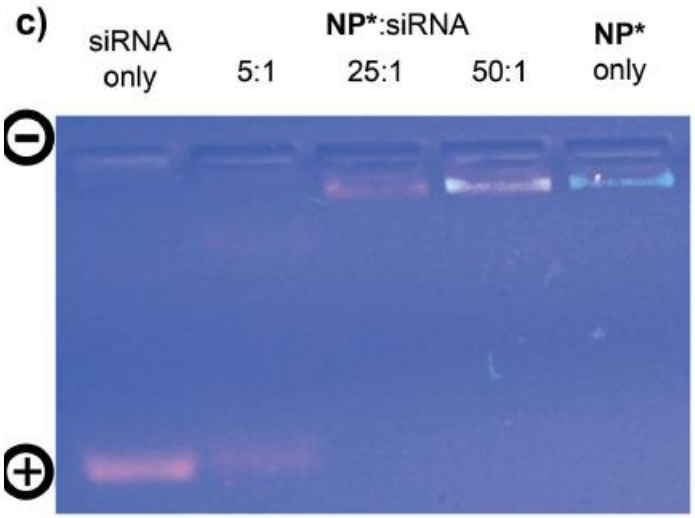

Appendix Figure S2: Complexation of siRNA (red) with cationic nanohydrogel particle NP (non-bioNP-FITC) at different weight-to-weight (w/w) ratios monitored by 1% agarose gel electrophoresis (100V, 45 min). At (w/w) ratios ≥ NP:siRNA 25:1 no free siRNA was visible, yet[1].

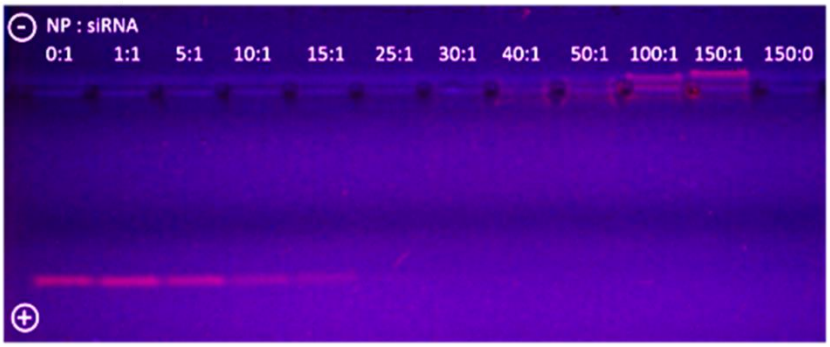

Appendix Figure S3: Agarose gel electrophoresis (1%, 100V, 45 min) of siRNA in the presence of increasing weight-to-weight (w/w) ratios of bioNP to siRNA. At (w/w) ratios ≥ NP:siRNA 30:1 no free siRNA was visible, yet.

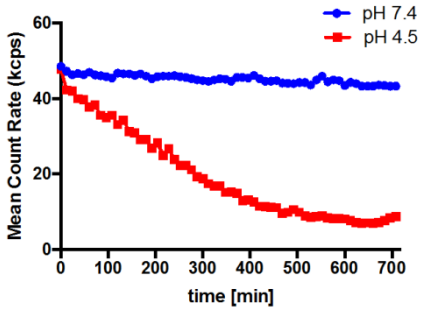

Appendix Figure S4: Corresponding DLS derived angle-dependent reciprocal hydrodynamic radii, showing a disintegration of bioNP at pH 4.5 and no damage at pH 7.5 over 12 h.

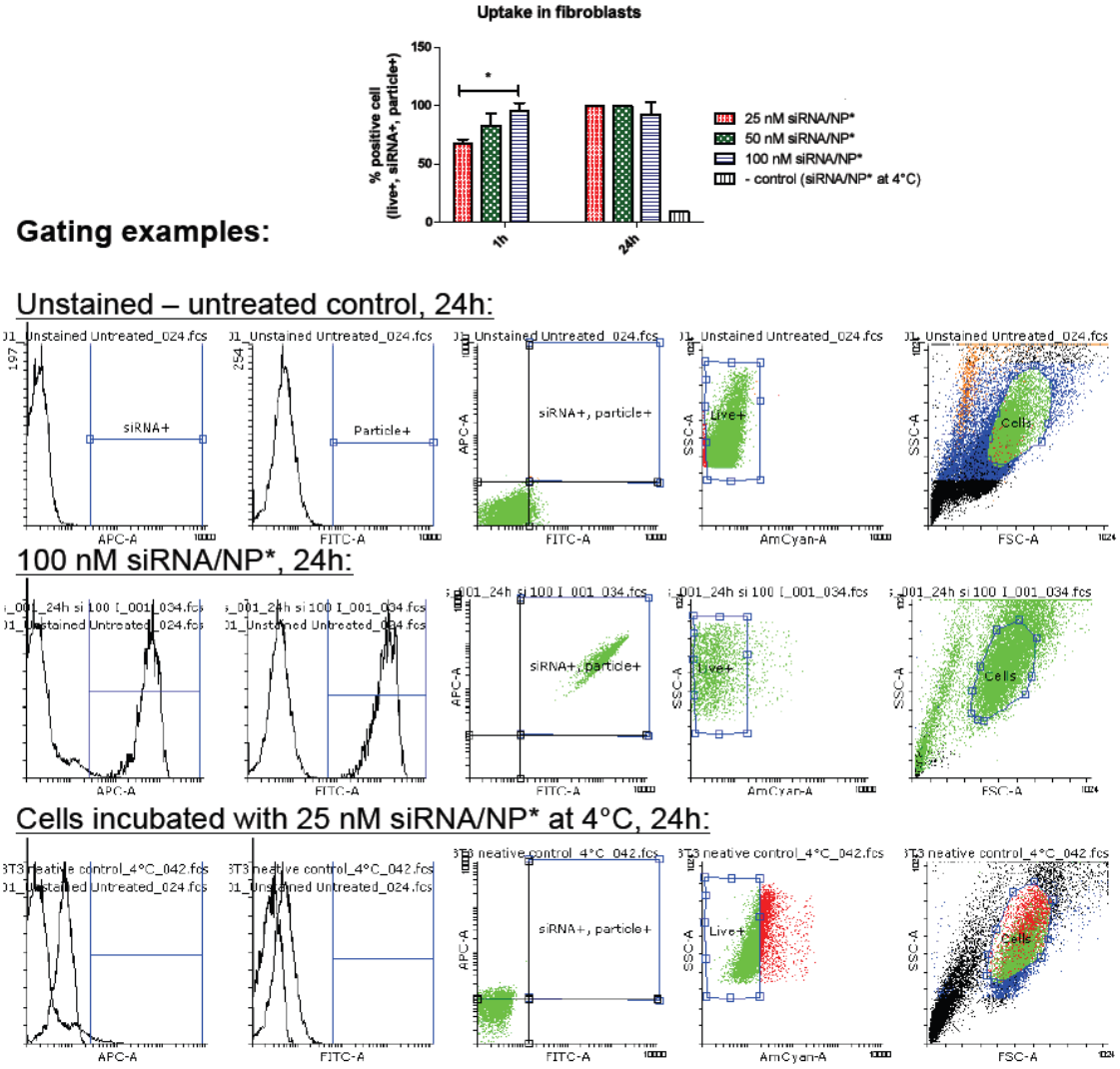

Appendix Figure S5: *In vitro* cell uptake analyzed by flow cytometry of 3T3 fibroblasts treated with Cy5 labeled siRNA complexed with NP* (FITC labeled NP) (10:1 weight-to-weight ratio (w/w) of NP-FITC:siRNA) indicated uptake of intact complexes without significant cell death – Amycan ≙ live dead dye; APC ≙ Cy5-labeled siRNA; FITC ≙ NP*.

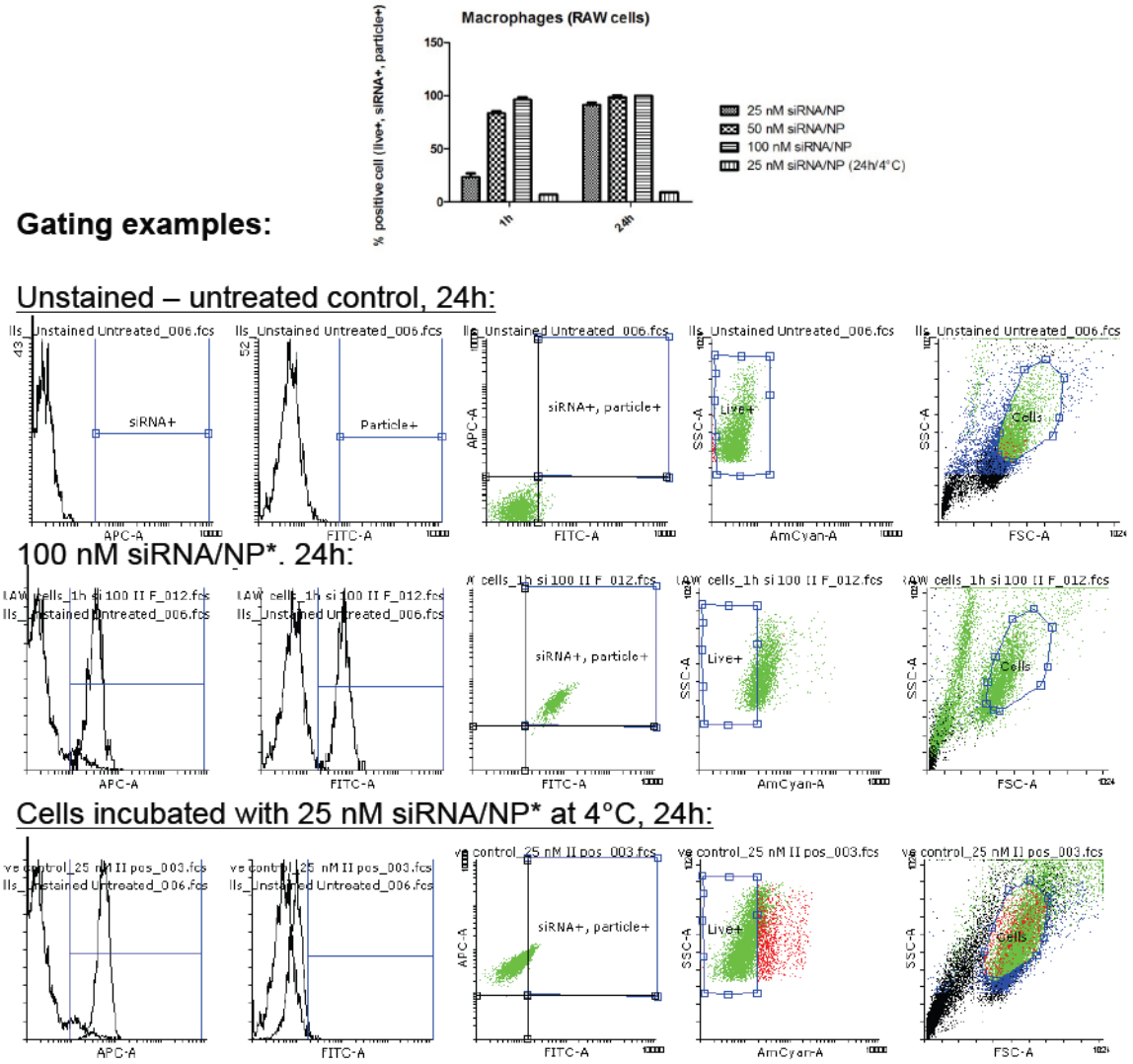

Appendix Figure S6: *In vitro* cellular uptake analyzed by flow cytometry of RAW macrophages treated with Cy5-labeled siRNA complexed with NP* (FITC labeled NP) (10:1 weight-to-weight ratio of NP-FITC:siRNA) indicated uptake of intact complexes without significant cell death – Amycan ≙ live dead dye; APC ≙ Cy5-labeled siRNA; FITC ≙ NP-FITC.

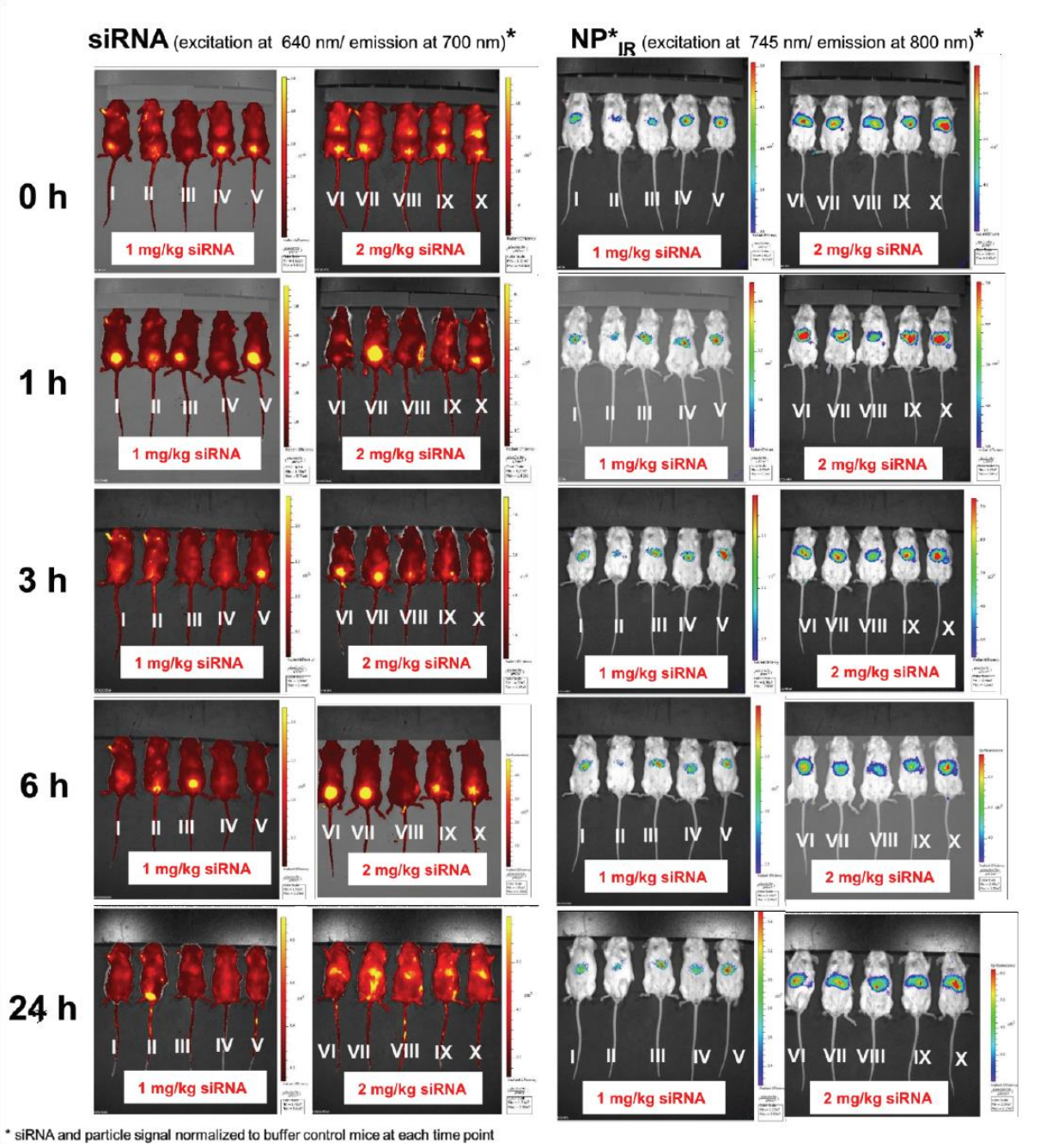

Appendix Figure S7: Fluorescence near infrared imaging of live mice after a second retroorbital injection of Cy5-siRNA loaded near infrared dye CS800 (IR) labeled nanohydrogel particles (non-bioNP-IR, weight-to-weight (w/w) ratio of NP-IR:siRNA 10:1) using an IVIS Spectrum Imaging system (Caliper LifeSciences, Hopkinton, US) demonstrated sequestration and retention of siRNA/non-bioNP mainly in the liver.

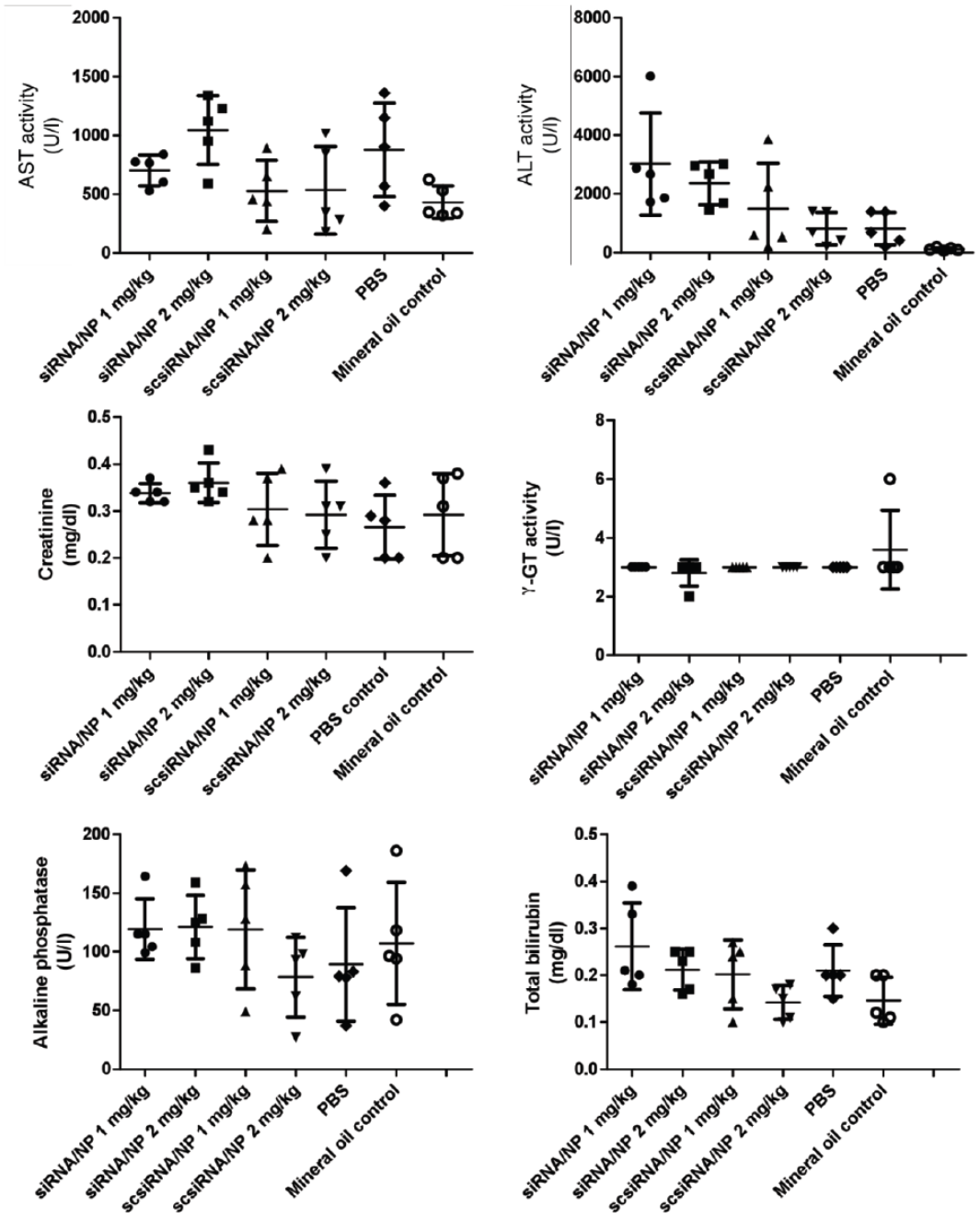

Appendix Figure S8: Acute *in vivo* toxicity after two consecutive siRNA/non-bioNP injections. No significant differences between fibrotic mice, especially when mice groups received cationic nanohydrogel particles (non-bioNP) loaded with anti-col1α1 or scrambled siRNA (means ± SD).

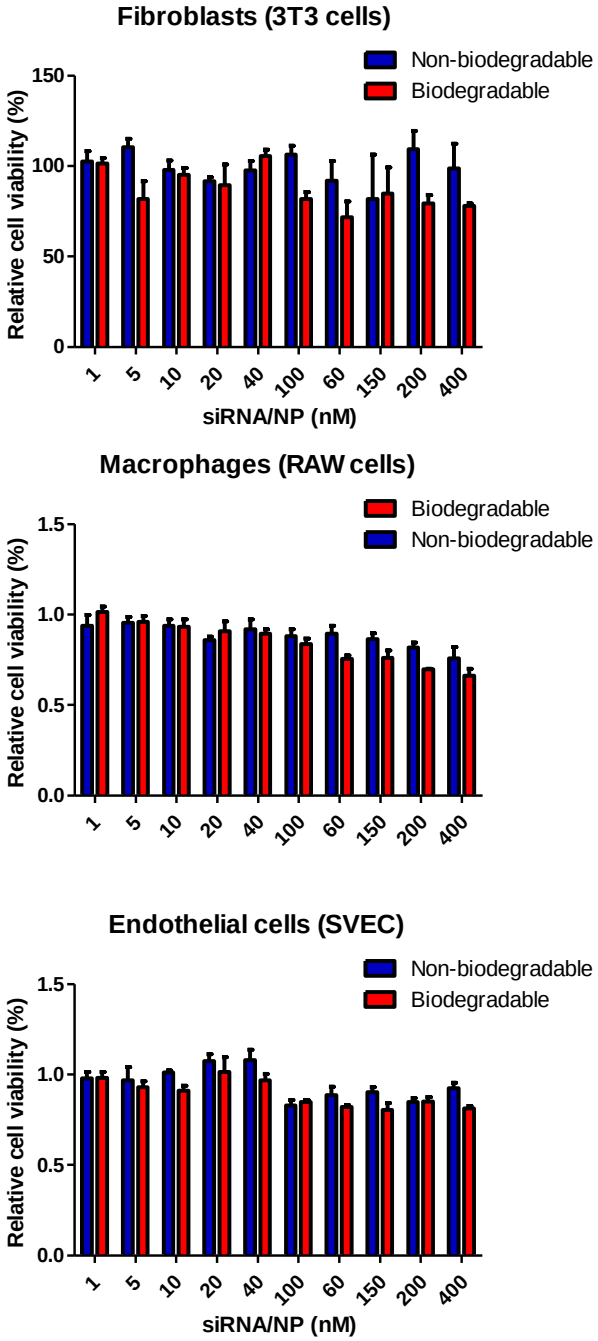

Appendix Figure S9: Cell viability of 3T3 fibroblasts, RAW macrophages and SVEC endothelial cells exposed to scsiRNA loaded non-bioNP and bioNP (weight-to-weight ratio (w/w) of non-bio NP:siRNA 10:1, (w/w) of bioNP:siRNA 30:1) at different siRNA concentrations (determined by MTT assay, incubation time 72 h, n = 3).

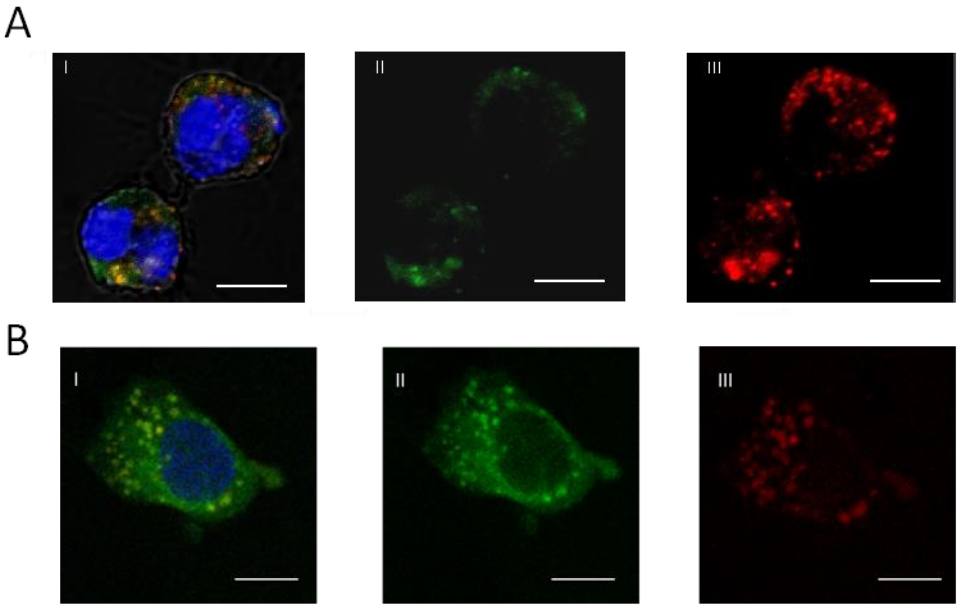

Appendix Figure S10: *In vitro* cellular uptake of non-bioNP complexed with Cy5-siRNA (weight-to-weight ratio (w/w) of non-bio NP:siRNA 10:1) monitored by confocal laser scattering microscopy (CLSM) in RAW-macrophages: A) Cy5-siRNA/non-bioNP-FITC, B) Cy5-siRNA/bioNP-FITC (2.5h incubation, 100 nM siRNA, scale bar 10 µm). I: merged picture (blue: nuclei, yellow as overlay of siRNA (red) and non-bioNP (green)), II: particle (green), III: siRNA (red)). In the cytoplasm, NP are nicely colocalized with siRNA – here in analogy to FACS dot plots, no cells either for siRNA or NP alone could be observed.

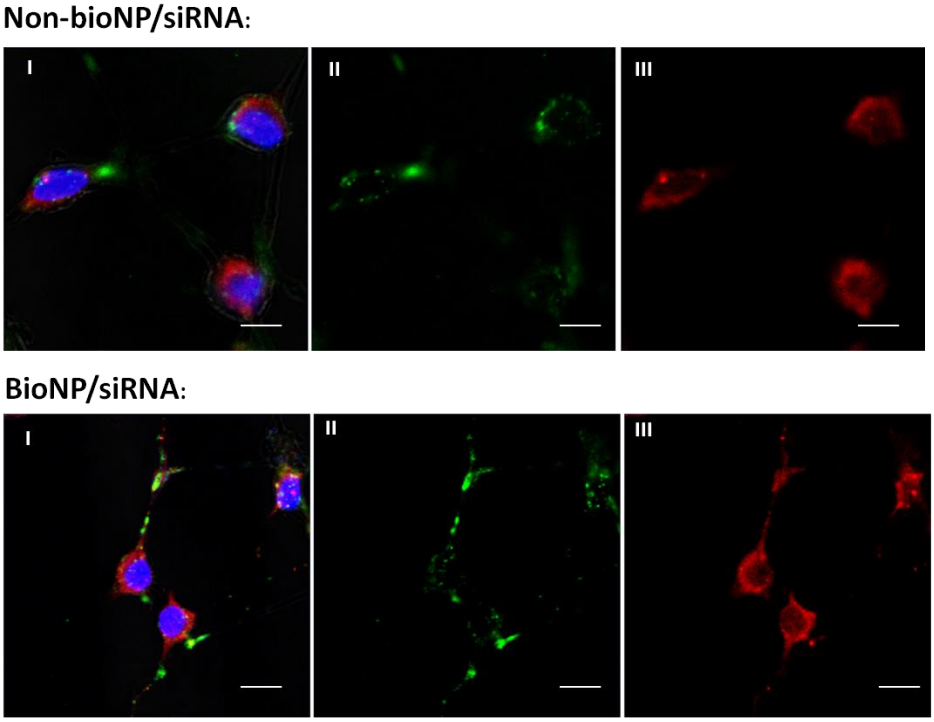

Appendix Figure S11: Cellular uptake of (non-)bioNP complexed with Cy5 labeled siRNA (non-bioNP 10:1, bioNP 30:1 weight-to-weight ratio of bio NP:siRNA) monitored by confocal laser scattering microscopy (CLSM) as morphometric control for cellular uptake in 3T3-fibroblasts (2.5h incubation, 100 nM siRNA, scale bar 10 µm). I: merged picture (blue: nuclei, yellow as overlay of siRNA (red) and (non-)bioNP (green)), II: particle (green), III: siRNA (red)).

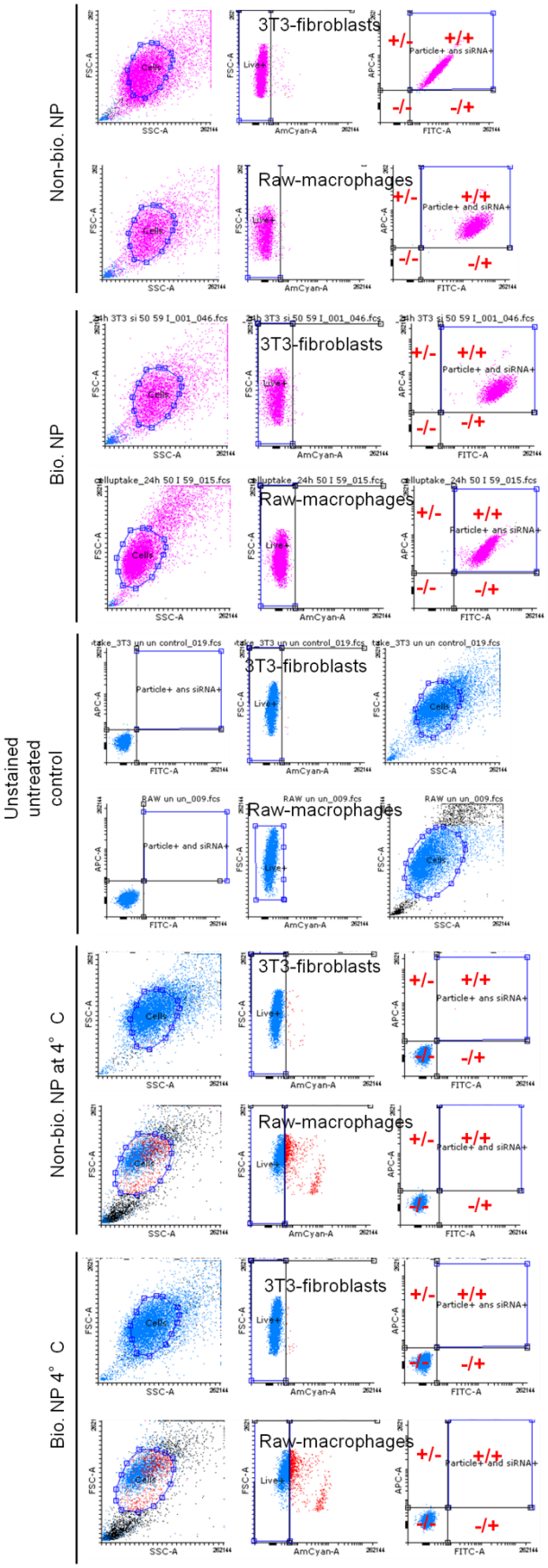

Appendix Figure S12: Exemplary FACS dot plots - *in vitro* cellular uptakes of Cy5-siRNA/(non-)bioNP-FITC after 24h incubation at 50nM siRNA and corresponding controls (unstained untreated control ~ auto-fluorescence control, 4°C control ~ unspecific uptake control) in fibroblasts and macrophages; -/- double negative cells (Cy5-siRNA and (non)-bioNP-FITC), +/+ double positive cells (Cy5-siRNA and (non-)bioNP-

FITC), -/+ or +/- single positive cells (Cy5-siRNA or (non-)bioNP-FITC). Only double positive cells (+/+) could be found, indicating uptake of intact complexes without significant cell death – Amycan ≙ live dead dye; APC ≙ Cy5-labeled siRNA; FITC ≙ non-bioNP-FITC.

Appendix


Non-biodegradable NP
siRNA (in vivo)
particle (in vivo)
0h
1h
3h
6h
12h
24h
48h
1 mg/kg
2 mg/kg
PBS
1 mg/kg
2 mg/kg
PBS

Appendix Figure S13: Fluorescence near infrared imaging of live mice after a second retroorbital injection of Cy5-siRNA loaded (non-)bioNP-IR (weight-to-weight (w/w) ratio of (non-)bioNP-IR:siRNA 10:1 and weight-to-weight (w/w) ratio of bioNP-IR 30:1) using an IVIS Spectrum Imaging system (Caliper LifeSciences, Hopkinton, US). After the first 6h free siRNA and premature degraded NP were cleared by the kidneys (ending in the bladder), whereby intact Cy5-siRNA/(non-)bioNP-IR complexes are sequestrated mainly in the liver.

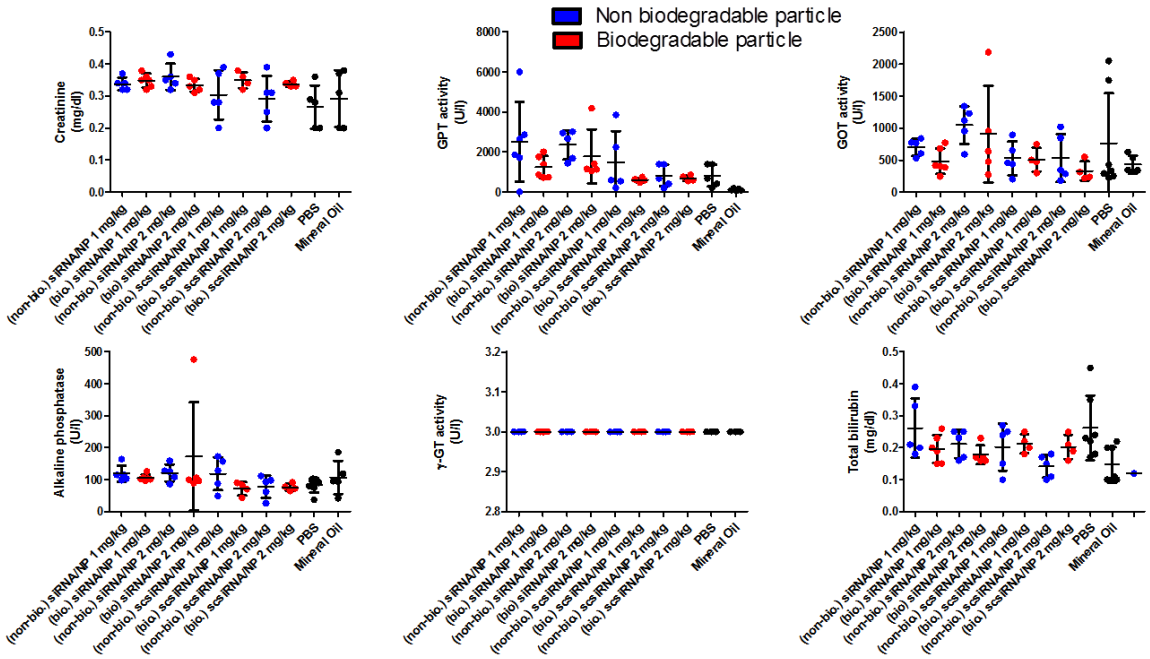

Appendix Figure S14: Serum parameters as surrogates of liver and kidney toxicity (markers for acute *in vivo* toxicity). No significant differences for serum parameter between fibrotic mice, especially when groups received non-bioNP or bioNP loaded with anti-col1α1 or scrambled siRNA (means ± SD).

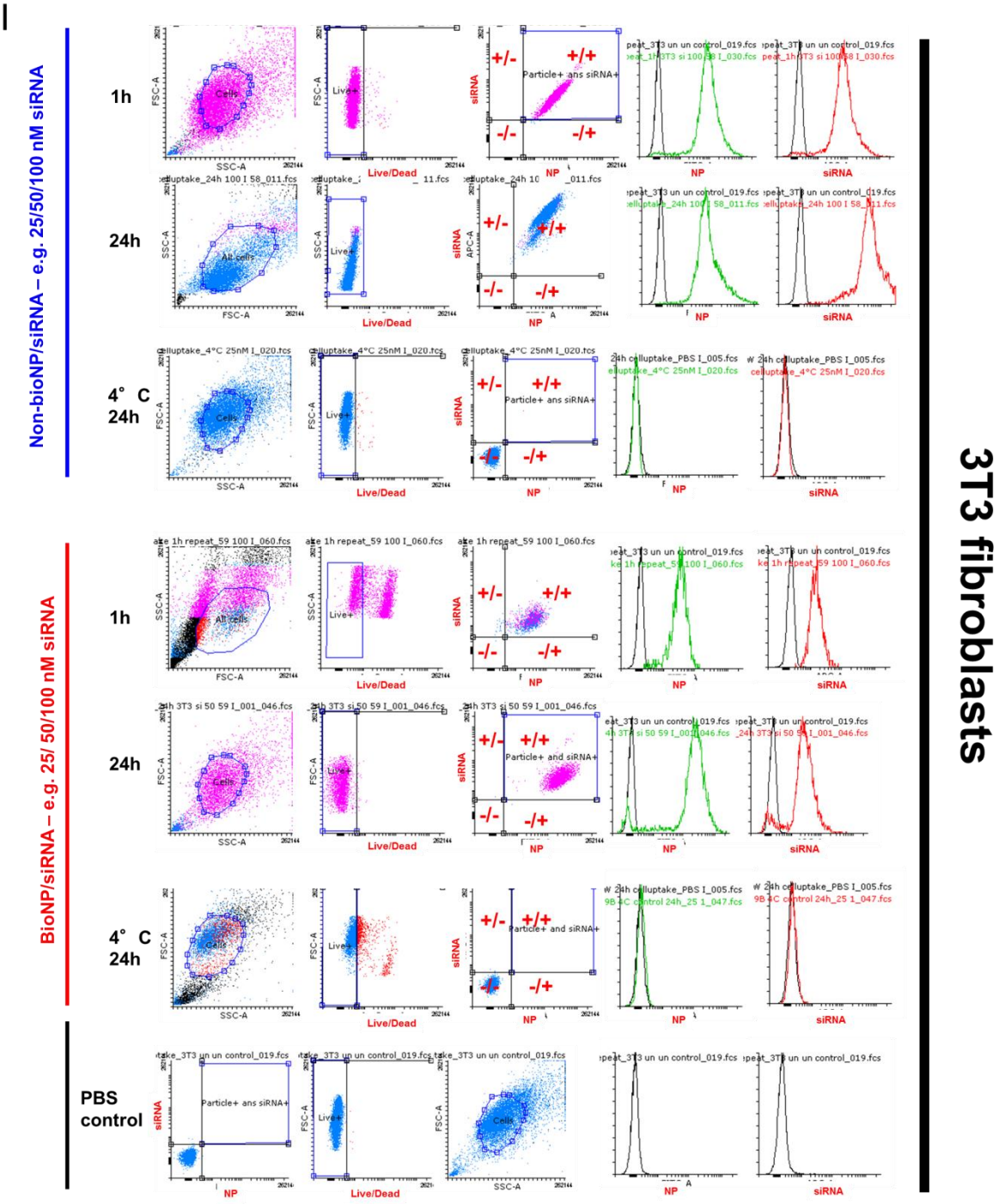
Non-bioNP/siRNA – e.g. 25/50/100 nM siRNA
BioNP/siRNA – e.g. 25/ 50/100 nM siRNA
3T3 fibroblasts
1h
24h
4° C
24h
PBS
control
Cells
All cells
Live+
Live/Dead
Particle+ ans siRNA+
Particle+ and siRNA+
+/-
+/+
-/-
-/+
NP
siRNA
FSC-A
SSC-A
APC-A

III

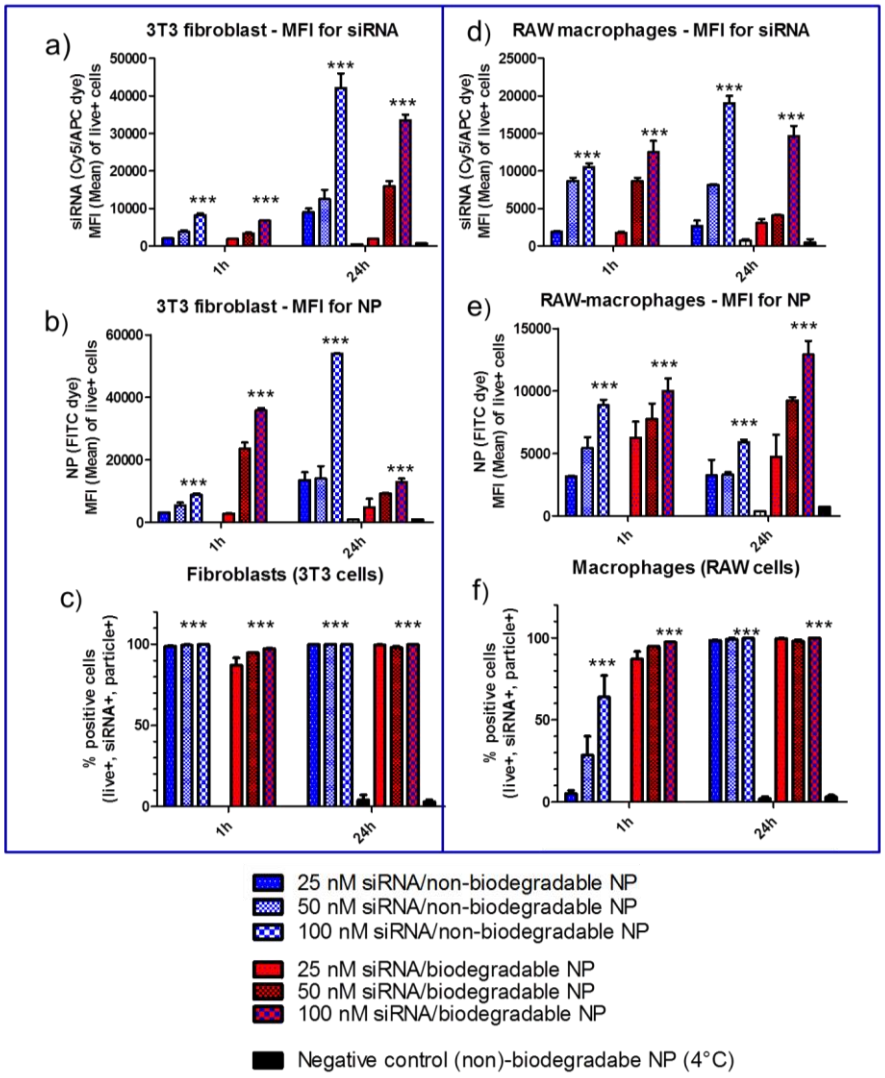

Appendix Figure S15: ***In vitro*** **cellular uptake of (non-)bioNP in 3T3 fibroblasts and RAW macrophages. Cells were incubated with Cy5-siRNA (APC like dye) loaded (non-)bioNP-FITC according to 25, 50, 100nM for 1h and 24h, stained with live/dead dye (Amcyan-channel) and analyzed by flow cytometry. I and II: Exemplary dot plots/MFI histograms of 3T3 and RAW cells incubated with siRNA/(non)-bioNP. III: MFI and double positive cells for siRNA/NP of 3T3 (a,b,c) and RAW (d,e,f) cells incubated with siRNA/(non-)bioNP. Of note, cellular uptake after 24h was minimal at 4°C (control), indicating energy-dependent uptake mechanisms (n=3). ***p < 0.0001, 100nM siRNA vs PBS/at 4°C incubated cells with 25nM (non-)bioNP, means ± SD, n=3. Statistical significance was determined by one-way ANOVA analysis.**

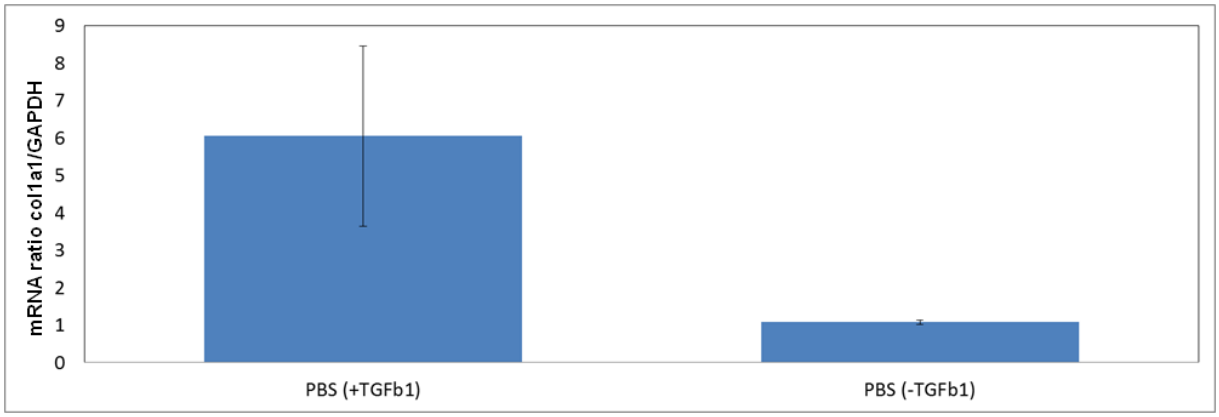

Appendix Figure S16: Quantification of col1a1 mRNA transcript in 3T3 fibroblasts after 24h induction with/without TGFβ1 (5 ng/ml) in 3T3 fibroblasts. Cells exhibited a higher and stable expression of col1a1 after induction with TGFβ1.

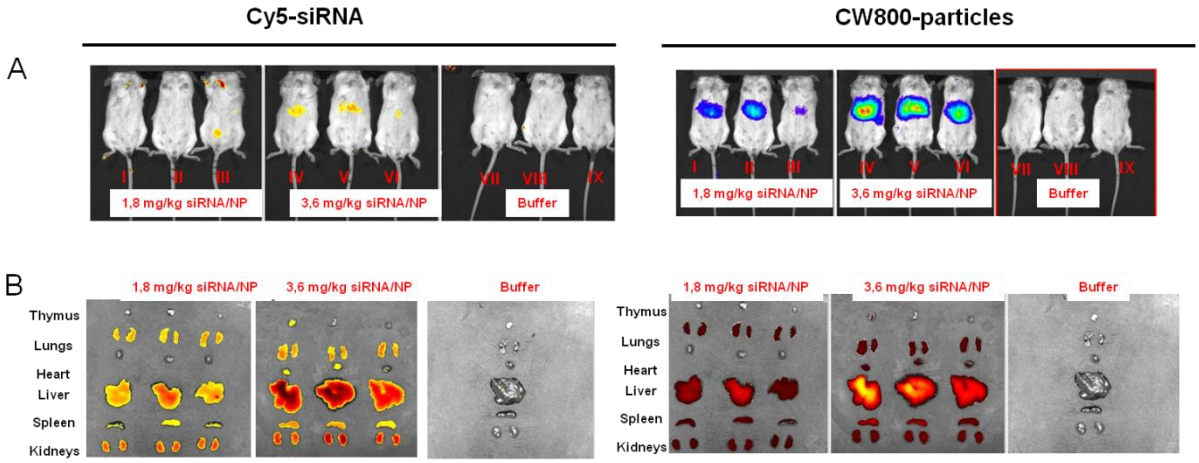

Appendix Figure S 17: Via IVIS (fluorescence near infrared imaging), *in vivo/ex vivo* biodistribution of Cy5-siRNA loaded non-bioNP-IR in healthy mice. A: 24 h after *iv* injection of siRNA/NP complexes, both siRNA and NP accumulated in liver. B: In *ex vivo* 48h after injection of siRNA/NP complexes, siRNA and NP were co-localized mainly in liver (to a minor extend siRNA and NP accumulated in lungs, spleen and kidneys)

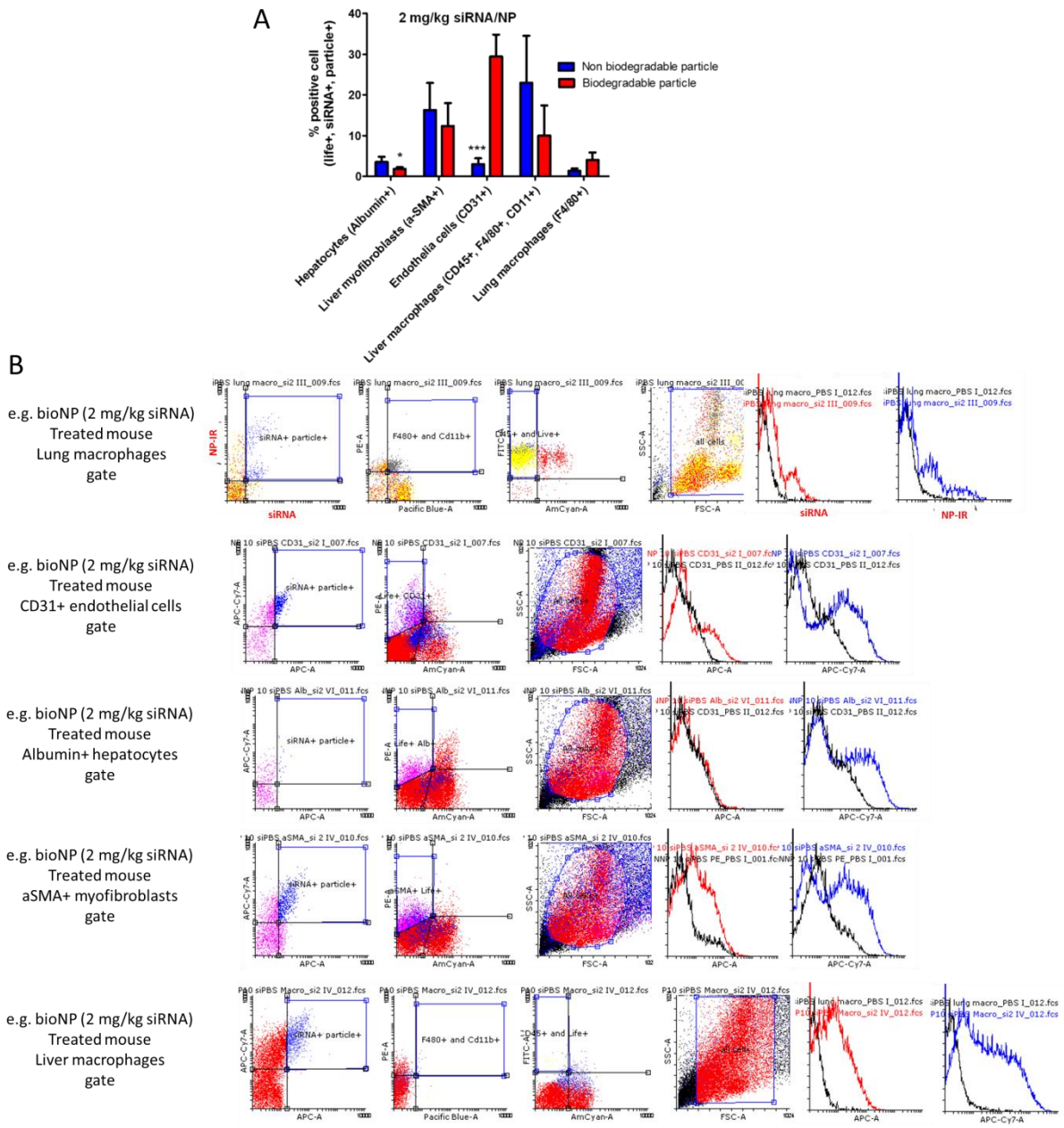

Appendix Figure S 18: *In vivo* cellular uptake of Cy5-siRNA/(non-)bioNP-IR in liver cells of liver fibrotic mice. A: Flow cytometric analysis of single cells suspensions obtained from harvested organs (lungs, livers) 48 h after injection of Cy5-siRNA loaded NP-IR. B: To (A) corresponding exemplary FACS dot plots/MFI histograms of liver/lung cells from Cy5-siRNA/(non-)bioNP-IR treated liver fibrotic mice (means ± SD, n = 3-5). (*p < 0.05, ***p < 0.0001 v. PBS/Cy5-siRNA/(non-)bio NP-IR, means ± SD, n = 3). Statistical significance was determined by one-way ANOVA analysis.

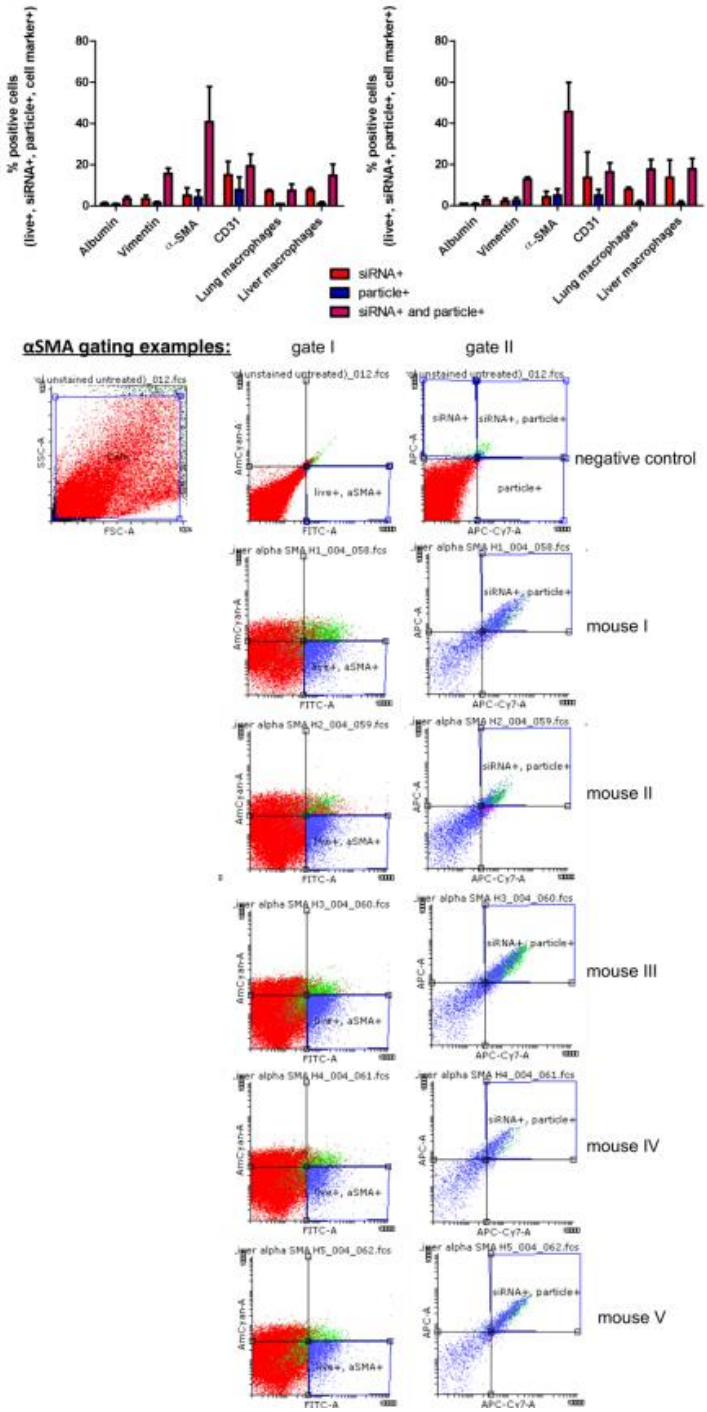

Appendix Figure S 19: ***In vivo*** **cellular uptake analyzed by flow cytometry of freshly isolated cells obtained from livers after treatment with Cy5 labeled siRNA complexed with non-bioNP-IR (10:1 weight-to-weight ratio of non-bioNP:siRNA) – Amcyan ≙ live dead dye; APC ≙ Cy5 labeled siRNA; FITC ≙ αSMA; APC-Cy7-A ≙ non-NP-IR; means ± SD; n=5/group.**

8. References

[1] L. Kaps, L. Nuhn, M. Aslam, A. Brose, F. Foerster, S. Rosigkeit, P. Renz, R. Heck, Y. O. Kim, I. Lieberwirth, D. Schuppan, R. Zentel, *Adv. Healthc. Mater.* **2015**, *4*, 2809.

[2] N. Leber, L. Kaps, M. Aslam, J. Schupp, A. Brose, D. Schäffel, K. Fischer, M. Diken, D. Strand, K. Koynov, A. Tuettenberg, L. Nuhn, R. Zentel, D. Schuppan, *J. Control. Release* **2017**, *248*, 10.

[3] Y. Popov, D. Schuppan, *Hepatology* **2009**, *50*, 1294.

[4] R. Bataller, D. Brenner, *J. Clin. Invest.* **2005**, *115*, 209.

[5] D. Schuppan, Y. O. Kim, *J. Clin. Invest.* **2013**, *123*, 1887.

[6] S. L. Friedman, *Gastroenterology* **2008**, *134*, 1655.

[7] D. Schuppan, N. H. Afdhal, *Lancet (London, England)* **2008**, *371*, 838.

[8] B. Gao, R. Bataller, *Gastroenterology* **2011**, *141*, 1572.

[9] B. N. Bohinc, A. M. Diehl, *Clin. Liver Dis.* **2012**, *16*, 549.

[10] Z. Zhang, H. Lin, M. Shi, R. Xu, J. Fu, J. Lv, L. Chen, S. Lv, Y. Li, S. Yu, H. Geng, L. Jin, G. K. K. Lau, F.-S. Wang, *J. Gastroenterol. Hepatol.* **2012**, *27*, 112.

[11] C. Barone, D. Koeberle, H. Metselaar, G. Parisi, D. Sansonno, G. Spinzi, *Ann. Oncol.* **2013**, *24*, 15.

[12] J. S. Duffield, S. J. Forbes, C. M. Constandinou, S. Clay, M. Partolina, S. Vuthoori, S. Wu, R. Lang, J. P. Iredale, *J. Clin. Invest.* **2005**, *115*, 56.

[13] S. L. Friedman, M. B. Bansal, *Hepatology* **2006**, *43*, 82.

[14] Y. Popov, D. Y. Sverdlov, A. K. Sharma, K. R. Bhaskar, S. Li, T. L. Freitag, J. Lee, W. Dieterich, G. Melino, D. Schuppan, *Gastroenterology* **2011**, *140*, 1642.

[15] P. D. Arora, C. A. G. Mcculloch, *J. Cell. Physiol.* **1994**, *159*, 161.

[16] I. N. Guha, R. P. Myers, K. Patel, J. A. Talwalkar, *Hepatology* **2011**, *54*, 1454.

[17] D. Schuppan, Y. O. Kim, **2013**, *123*, 1887.

[18] S. L. Friedman, *Nat. Clin. Pract. Gastroenterol. Hepatol.* **2004**, *1*, 98.

[19] T. Kisseleva, H. Uchinami, N. Feirt, O. Quintana-Bustamante, J. C. Segovia, R. F. Schwabe, D. A. Brenner, *J. Hepatol.* **2006**, *45*, 429.

[20] A. Kaimori, J. Potter, J. Kaimori, C. Wang, E. Mezey, A. Koteish, *J. Biol. Chem.* **2007**, *282*, 22089.

[21] A. D. Clouston, E. E. Powell, M. J. Walsh, M. M. Richardson, A. J. Demetris, J. R. Jonsson, *Hepatology* **2005**, *41*, 809.

[22] F. Tacke, H. W. Zimmermann, *J. Hepatol.* **2014**, *60*, 1090.

[23] P. Ramachandran, A. Pellicoro, M. a Vernon, L. Boulter, R. L. Aucott, A. Ali, S. N. Hartland, V. K. Snowdon, A. Cappon, T. T. Gordon-Walker, M. J. Williams, D. R.

Dunbar, J. R. Manning, N. van Rooijen, J. a Fallowfield, S. J. Forbes, J. P. Iredale, *Proc. Natl. Acad. Sci. U. S. A.* **2012**, *109*, 3186.

[24] P. Italiani, D. Boraschi, *Front. Immunol.* **2014**, *5*.

[25] K. A. Jablonski, S. A. Amici, L. M. Webb, J. D. D. Ruiz-Rosado, P. G. Popovich, S. Partida-Sanchez, M. Guerau-De-arellano, *PLoS One* **2015**, *10*, 5.

[26] H. L. Jiang, M. L. Kang, J. S. Quan, S. G. Kang, T. Akaike, H. S. Yoo, C. S. Cho, *Biomaterials* **2008**, *29*, 1931.

[27] D. Schuppan, *Semin. Liver Dis.* **1990**, *10*, 1.

[28] C. Jiménez Calvente, A. Sehgal, Y. Popov, Y. O. Kim, V. Zevallos, U. Sahin, M. Diken, D. Schuppan, *Hepatology* **2015**, *62*, 1285.

[29] D. Cejka, D. Losert, V. Wacheck, *Clin. Sci. (Lond).* **2006**, *110*, 47.

[30] G. L. Sen, H. M. Blau, *Faseb J* **2006**, *20*, 1293.

[31] C. Napoli, C. Lemieux, R. Jorgensen, *Plant Cell* **1990**, *2*, 279.

[32] N. Romano, G. Macino, *Mol. Microbiol.* **1992**, *6*, 3343.

[33] S. Guo, K. J. Kemphues, *Cell* **1995**, *81*, 611.

[34] A. Fire, S. Xu, M. K. Montgomery, S. A. Kostas, S. E. Driver, C. C. Mello, *Nature* **1998**, *391*, 806.

[35] A. J. Hamilton, *Science (80).* **1999**, *286*, 950.

[36] T. Tuschl, P. D. Zamore, R. Lehmann, D. P. Bartel, P. A. Sharp, *Genes Dev.* **1999**, *13*, 3191.

[37] S. M. Elbashir, J. Harborth, W. Lendeckel, A. Yalcin, K. Weber, T. Tuschl, *Nature* **2001**, *411*, 494.

[38] M. Ferrari, *Nat. Rev. Clin. Oncol.* **2010**, *7*, 485.

[39] "All Nobel Prizes in Physiology or Medicine," can be found under http://www.nobelprize.org/nobel_prizes/medicine/laureates/, *last access* August **2017.**

[40] A. H. Hofer, L. Sauerteig, S. M. Journal, S. K. Der, **2016**, 105.

[41] L. Aagaard, J. J. Rossi, *Adv. Drug Deliv. Rev.* **2007**, *59*, 75.

[42] H. Zhang, F. A. Kolb, L. Jaskiewicz, E. Westhof, W. Filipowicz, *Cell* **2004**, *118*, 57.

[43] G. Meister, M. Landthaler, A. Patkaniowska, Y. Dorsett, G. Teng, T. Tuschl, *Mol. Cell* **2004**, *15*, 185.

[44] J. Liu, M. A. Carmell, F. V Rivas, C. G. Marsden, J. M. Thomson, J.-J. Song, S. M. Hammond, L. Joshua-Tor, G. J. Hannon, *Science* **2004**, *305*, 1437.

[45] G. Tang, *Trends Biochem. Sci.* **2005**, *30*, 106.

[46] D. S. Schwarz, G. Hutvágner, T. Du, Z. Xu, N. Aronin, P. D. Zamore, *Cell* **2003**, *115*, 199.

[47] A. Khvorova, A. Reynolds, S. D. Jayasena, *Cell* **2003**, *115*, 209.

[48] Y. Lee, C. Ahn, J. Han, H. Choi, J. Kim, J. Yim, J. Lee, P. Provost, O. Rådmark, S. Kim, V. N. Kim, *Nature* **2003**, *425*, 415.

[49] J. Han, Y. Lee, K. H. Yeom, Y. K. Kim, H. Jin, V. N. Kim, *Genes Dev.* **2004**, *18*, 3016.

[50] S. Bagga, J. Bracht, S. Hunter, K. Massirer, J. Holtz, R. Eachus, A. E. Pasquinelli, *Cell* **2005**, *122*, 553.

[51] J. C. Burnett, J. J. Rossi, K. Tiemann, *Biotechnol. J.* **2011**, *6*, 1130.

[52] U. Bhadra, *Mol. Biol.* **2015**, *5*.

[53] B. R. Cullen, *Nat Methods* **2006**, *3*, 677.

[54] N. Senzer, M. Barve, J. Kuhn, A. Melnyk, P. Beitsch, M. Lazar, S. Lifshitz, M. Magee, J. Oh, S. W. Mill, C. Bedell, C. Higgs, P. Kumar, Y. Yu, F. Norvell, C. Phalon, N. Taquet, D. D. Rao, Z. Wang, C. M. Jay, B. O. Pappen, G. Wallraven, F. C. Brunicardi, D. M. Shanahan, P. B. Maples, J. Nemunaitis, *Mol. Ther.* **2012**, *20*, 679.

[55] D. A. Persons, C. Baum, *Mol. Ther.* **2011**, *19*, 229.

[56] C. E. Thomas, A. Ehrhardt, M. a Kay, *Nat. Rev. Genet.* **2003**, *4*, 346.

[57] K. a Whitehead, R. Langer, D. G. Anderson, *Nat. Rev. Drug Discov.* **2009**, *8*, 129.

[58] J. Zhang, M. Ding, K. Xu, L. Mao, J. Zheng, *Oncotarget* **2016**, *7*, 29824.

[59] R. J. Verheul, B. Slütter, S. M. Bal, J. A. Bouwstra, W. Jiskoot, W. E. Hennink, *J. Control. Release* **2011**, *156*, 50.

[60] L. Nuhn, M. Hirsch, B. Krieg, K. Koynov, K. Fischer, M. Schmidt, M. Helm, R. Zentel, *ACS Nano* **2012**, *6*, 2198.

[61] A. L. Jackson, P. S. Linsley, *Nat. Rev. Drug Discov.* **2010**, *9*, 57.

[62] C. R. Sibley, Y. Seow, M. J. A. Wood, *Mol. Ther.* **2010**, *18*, 466.

[63] M. Sioud, *Adv. Drug Deliv. Rev.* **2007**, *59*, 153.

[64] T. Kawasaki, T. Kawai, *Front. Immunol.* **2014**, *5*.

[65] S. Qiu, C. M. Adema, T. Lane, *Nucleic Acids Res.* **2005**, *33*, 1834.

[66] A. L. Jackson, J. Burchard, D. Leake, A. Reynolds, J. Schelter, J. Guo, J. M. Johnson, L. Lim, J. Karpilow, K. Nichols, W. Marshall, A. Khvorova, P. S. Linsley, *RNA* **2006**, *12*, 1197.

[67] S. S. Diebold, T. Kaisho, H. Hemmi, S. Akira, C. R. e Sousa, *Science* **2004**, *303*, 1529.

[68] F. Heil, H. Hemmi, H. Hochrein, F. Ampenberger, C. Kirschning, S. Akira, G. Lipford, H. Wagner, S. Bauer, *Science* **2004**, *303*, 1526.

[69] W. J. Kim, S. W. Kim, *Pharm. Res.* **2009**, *26*, 657.

[70] D. Schuppan, *Clin. Res. Hepatol. Gastroenterol.* **2015**, *39*, 51.

[71] A. R. Khomutov, N. A. Grigorenko, S. G. Skuridin, A. V. Demin, J. Vepsalainen, R. A. Casero, P. M. Woster, *Russ. J. Bioorganic Chem.* **2005**, *31*, 271.

[72] H. T. T. Duong, C. P. Marquis, M. Whittaker, T. P. Davis, C. Boyer, *Macromolecules* **2011**, *44*, 8008.

[73] C. Dingels, S. S. Müller, T. Steinbach, C. Tonhauser, H. Frey, *Biomacromolecules* **2013**, *14*, 448.

[74] J. L. Urdiales, Medina MA, F. Sánchez-Jiménez, *Eur. J. Gastroenterol. Hepatol.* **2001**, *13*, 1015.

[75] J. Van Meerloo, G. J. L. Kaspers, J. Cloos, in *Methods Mol Biol.*, **2011**, 237.

[76] L. Nuhn, S. Gietzen, K. Mohr, K. Fischer, K. Toh, K. Miyata, Y. Matsumoto, K. Kataoka, M. Schmidt, R. Zentel, *Biomacromolecules* **2014**, *15*, 1526.

[77] L. Nuhn, S. Tomcin, K. Miyata, V. Mailänder, K. Landfester, K. Kataoka, R. Zentel, *Biomacromolecules* **2014**, *15*, 4111.

[78] D. Schuppan (Director - Institute of Translational Immunology, Mainz, Germany), *oral communication* **2015**.

[79] W. Z. Mehal, D. Schuppan, *Semin. Liver Dis.* **2015**, *35*, 184.

[80] Y. Huang, W. B. de Boer, L. A. Adams, G. MacQuillan, E. Rossi, P. Rigby, S. C. Raftopoulos, M. Bulsara, G. P. Jeffrey, *Liver Int.* **2013**, *33*, 1249.

[81] Y. Huang, W. B. de Boer, L. A. Adams, G. Macquillan, E. Rossi, P. Rigby, S. C. Raftopoulos, M. Bulsara, G. P. Jeffrey, *Liver Int.* **2013**, *33*, 1249.

[82] H. A. R. Hadi, C. S. Carr, J. Al Suwaidi, *Vasc. Health Risk Manag.* **2005**, *1*, 183.

[83] J. C. Sung, B. L. Pulliam, D. A. Edwards, *Trends Biotechnol.* **2007**, *25*, 563.

[84] A. O. Garba, S. A. Mousa, *Ophthalmol. Eye Dis.* **2010**, *2*, 75.

[85] R. Kanasty, J. R. Dorkin, A. Vegas, D. Anderson, *Nat. Mater.* **2013**, *12*, 967.

[86] T. Wang, S. Shigdar, H. Al Shamaileh, M. P. Gantier, W. Yin, D. Xiang, L. Wang, S. F. Zhou, Y. Hou, P. Wang, W. Zhang, C. Pu, W. Duan, *Cancer Lett.* **2016**, 387, 77.

[87] M. H. Smith, L. A. Lyon, *Acc. Chem. Res.* **2012**, *45*, 985.

[88] J. Ramos, J. Forcada, R. Hidalgo-Alvarez, *Chem. Rev.* **2014**, *114*, 367.

[89] L. Nuhn, S. Gietzen, K. Mohr, K. Fischer, K. Toh, K. Miyata, Y. Matsumoto, K. Kataoka, M. Schmidt, R. Zentel, *Biomacromolecules* **2014**, *15*, 1526.

[90] L. Nuhn, L. Braun, I. Overhoff, A. Kelsch, D. Schaeffel, K. Koynov, R. Zentel, *Macromol. Rapid Commun.* **2014**, *35*, 2057.

[91] J. Huotari, A. Helenius, *EMBO J.* **2011**, *30*, 3481.

[92] L. Nuhn, S. Hartmann, B. Palitzsch, B. Gerlitzki, E. Schmitt, R. Zentel, H. Kunz, *Angew. Chemie* **2013**, *125*, 10846.

[93] B. Krieg, M. Hirsch, E. Scholz, L. Nuhn, I. Tabujew, H. Bauer, S. Decker, A. Khobta, M. Schmidt, W. Tremel, R. Zentel, K. Peneva, K. Koynov, J. A. Mason, M. Helm, *Pharm. Res.* **2015**, *32*, 1957.

[94] C. Wolfrum, S. Shi, K. N. Jayaprakash, M. Jayaraman, G. Wang, R. K. Pandey, K. G. Rajeev, T. Nakayama, K. Charrise, E. M. Ndungo, T. Zimmermann, V. Koteliansky, M. Manoharan, M. Stoffel, *Nat. Biotechnol.* **2007**, *25*, 1149.

[95] D. Schuppan, Y. Popov, Y. Porov, *J. Gastroenterol. Hepatol.* **2002**, *17*, 300.

[96] C. Hörtz, A. Birke, L. Kaps, S. Decker, E. Wächtersbach, K. Fischer, D. Schuppan, M. Barz, M. Schmidt, *Macromolecules* **2015**, *48*, 2074.

[97] J. K. Nair, J. L. S. Willoughby, A. Chan, K. Charisse, M. R. Alam, Q. Wang, M. Hoekstra, P. Kandasamy, A. V. Kelin, S. Milstein, N. Taneja, J. Oshea, S. Shaikh, L. Zhang, R. J. Van Der Sluis, M. E. Jung, A. Akinc, R. Hutabarat, S. Kuchimanchi, K. Fitzgerald, T. Zimmermann, T. J. C. Van Berkel, M. A. Maier, K. G. Rajeev, M. Manoharan, *J. Am. Chem. Soc.* **2014**, *136*, 16958.

[98] K. R. Karlmark, R. Weiskirchen, H. W. Zimmermann, N. Gassler, F. Ginhoux, C. Weber, M. Merad, T. Luedde, C. Trautwein, F. Tacke, *Hepatology* **2009**, *50*, 261.

[99] W. Z. Mehal, D. Schuppan, *Semin. Liver Dis.* **2015**, *35*, 184.

[100] F. Tacke, C. Trautwein, *J. Hepatol.* **2015**, *63*, 1038.

[101] J. M. Laurent, C. Vogel, T. Kwon, S. A. Craig, D. R. Boutz, H. K. Huse, K. Nozue, H. Walia, M. Whiteley, P. C. Ronald, E. M. Marcotte, *Proteomics* **2010**, *10*, 4209.

[102] Y. Zhang, A. Satterlee, L. Huang, *Mol. Ther.* **2012**, *20*, 1298.

[103] G. Grandinetti, A. E. Smith, T. M. Reineke, *Mol. Pharm.* **2012**, *9*, 523.

[104] G. Grandinetti, N. P. Ingle, T. M. Reineke, *Mol. Pharm.* **2011**, *8*, 1709.

[105] G. Unsoy, R. Khodadust, S. Yalcin, P. Mutlu, U. Gunduz, *Eur. J. Pharm. Sci.* **2014**, *62*, 243.

[106] D. Hofmann, C. Messerschmidt, M. B. Bannwarth, K. Landfester, V. Mailänder, *Chem. Commun.* **2014**, *50*, 1369.

[107] A. Verma, O. Uzun, Y. Hu, Y. Hu, H.-S. Han, N. Watson, S. Chen, D. J. Irvine, F. Stellacci, *Nat. Mater.* **2008**, *7*, 588.

[108] L. K. Mueller, L. Kaps, D. Schuppan, A. Brose, W. Chai, K. Fischer, S. Mueller, H. Frey, M. Schmidt, K. Mohr, *Mol. Pharm.* **2016**, *13*, 3636.

[109] H. S. Choi, W. Liu, P. Misra, E. Tanaka, J. P. Zimmer, B. Itty Ipe, M. G. Bawendi, J. V Frangioni, *Nat. Biotechnol.* **2007**, *25*, 1165.

[110] F. Alexis, E. Pridgen, L. K. Molnar, O. C. Farokhzad, *Mol. Pharm.* **2008**, *5*, 505.

[111] R. Gref, M. Lück, P. Quellec, M. Marchand, E. Dellacherie, S. Harnisch, T. Blunk, R. . Müller, *Colloids Surfaces B Biointerfaces* **2000**, *18*, 301.

[112] S. Tenzer, D. Docter, J. Kuharev, A. Musyanovych, V. Fetz, R. Hecht, F. Schlenk, D.

Fischer, K. Kiouptsi, C. Reinhardt, K. Landfester, H. Schild, M. Maskos, S. K. Knauer, R. H. Stauber, *Nat. Nanotechnol.* **2013**, *8*, 772.

[113] A. Brose, Cellular uptake pathways of siRNA nanohydrogel carriers: Comparison of non-biodegradable vs biodegradable nanohydrogel particles, Institute of Translational Immunology Mainz, **2016**.

[114] B. Yameen, W. Il Choi, C. Vilos, A. Swami, J. Shi, O. C. Farokhzad, *J. Control. Release* **2014**, *190*, 485.

[115] M. S. Draz, B. A. Fang, P. Zhang, Z. Hu, S. Gu, K. C. Weng, J. W. Gray, F. F. Chen, *Theranostics* **2014**, *4*, 872.

[116] H. Y. Xue, S. Liu, H. L. Wong, *Nanomedicine* **2014**, *9*, 295.

[117] K. Raemdonck, R. E. Vandenbroucke, J. Demeester, N. N. Sanders, S. C. De Smedt, *Drug Discov. Today* **2008**, *13*, 917.

[118] J. M. Williford, J. Wu, Y. Ren, M. M. Archang, K. W. Leong, H. Q. Mao, *Annu. Rev. Biomed. Eng. Vol 16* **2014**, *16*, 347.

[119] K. a Whitehead, R. Langer, D. G. Anderson, *Nat. Rev. Drug Discov.* **2009**, *8*, 129.

[120] Y.-C. Tseng, S. Mozumdar, L. Huang, *Adv. Drug Deliv. Rev.* **2009**, *61*, 721.

[121] J. Jiang, S. J. Yang, J. C. Wang, L. J. Yang, Z. Z. Xu, T. Yang, X. Y. Liu, Q. Zhang, *Eur. J. Pharm. Biopharm.* **2010**, *76*, 170.

[122] F. Braet, E. Wisse, P. Bomans, P. Frederik, W. Geerts, A. Koster, L. Soon, S. Ringer, *Microsc. Res. Tech.* **2007**, *70*, 230.

[123] F. Alexis, E. Pridgen, L. K. Molnar, O. C. Farokhzad, in *Mol. Pharm.*, **2008**, 505.

[124] D. A. Hume, *Curr. Opin. Immunol.* **2006**, *18*, 49.

[125] D. Schuppan, *Clin. Res. Hepatol. Gastroenterol.* **2015**, *39*, 51.

[126] S. S. Yu, C. M. Lau, W. J. Barham, H. M. Onishko, C. E. Nelson, H. Li, C. A. Smith, F. E. Yull, C. L. Duvall, T. D. Giorgio, *Mol. Pharm.* **2013**, *10*, 975.

[127] T. Rőszer, *Mediators Inflamm.* **2015**, *2015*, 816460.

[128] D. F. Williams, *Biomaterials* **2008**, *29*, 2941.

[129] R. E. Serda, J. Gu, R. C. Bhavane, X. Liu, C. Chiappini, P. Decuzzi, M. Ferrari, *Biomaterials* **2009**, *30*, 2440.

[130] J. Davda, V. Labhasetwar, *Int. J. Pharm.* **2002**, *233*, 51.

[131] D. B. Cines, E. S. Pollak, C. a Buck, J. Loscalzo, G. a Zimmerman, R. P. McEver, J. S. Pober, T. M. Wick, B. a Konkle, B. S. Schwartz, E. S. Barnathan, K. R. McCrae, B. a Hug, a M. Schmidt, D. M. Stern, *Blood* **1998**, *91*, 3527.

[132] D. Peer, J. M. Karp, S. Hong, O. C. Farokhzad, R. Margalit, R. Langer, *Nat. Nanotechnol.* **2007**, *2*, 751.

[133] A. Albanese, P. S. Tang, W. C. W. Chan, *Annu. Rev. Biomed. Eng.* **2012**, *14*, 1.

[134] L. Xiong, T. Yang, Y. Yang, C. Xu, F. Li, *Biomaterials* **2010**, *31*, 7078.

[135] J. W. Park, D. B. Kirpotin, K. Hong, R. Shalaby, Y. Shao, U. B. Nielsen, J. D. Marks, D. Papahadjopoulos, C. C. Benz, in *J. Control. Release*, **2001**, 95.

[136] R. Bansal, J. Prakash, E. Post, L. Beljaars, D. Schuppan, K. Poelstra, *Hepatology* **2011**, *54*, 586.

[137] S. C. Alley, N. M. Okeley, P. D. Senter, *Curr. Opin. Chem. Biol.* **2010**, *14*, 529.

[138] K. Cho, X. Wang, S. Nie, Z. G. Chen, D. M. Shin, *Clin. Cancer Res.* **2008**, *14*, 1310.

[139] O. V. Markov, N. L. Mironova, E. V. Shmendel, R. N. Serikov, N. G. Morozova, M. A. Maslov, V. V. Vlassov, M. A. Zenkova, *J. Control. Release* **2015**, *213*, 45.

[140] P. Ramachandran, A. Pellicoro, M. a Vernon, L. Boulter, R. L. Aucott, A. Ali, S. N. Hartland, V. K. Snowdon, A. Cappon, T. T. Gordon-Walker, M. J. Williams, D. R. Dunbar, J. R. Manning, N. van Rooijen, J. a Fallowfield, S. J. Forbes, J. P. Iredale, *Proc. Natl. Acad. Sci. U. S. A.* **2012**, *109*, 3186.

[141] M. A. Gibbons, A. C. MacKinnon, P. Ramachandran, K. Dhaliwal, R. Duffin, A. T. Phythian-Adams, N. Van Rooijen, C. Haslett, S. E. Howie, A. J. Simpson, N. Hirani, J. Gauldie, J. P. Iredale, T. Sethi, S. J. Forbes, *Am. J. Respir. Crit. Care Med.* **2011**, *184*, 569.

[142] A. Tuettenberg, K. Steinbrink, D. Schuppan, *Nanomedicine* **2016**, *11*, 2735.

[143] S. M. Pyonteck, L. Akkari, A. J. Schuhmacher, R. L. Bowman, L. Sevenich, D. F. Quail, O. C. Olson, M. L. Quick, J. T. Huse, V. Teijeiro, M. Setty, C. S. Leslie, Y. Oei, A. Pedraza, J. Zhang, C. W. Brennan, J. C. Sutton, E. C. Holland, D. Daniel, J. A. Joyce, *Nat. Med.* **2013**, *19*, 1264.

[144] M. Manoharan, A. Akinc, R. K. Pandey, J. Qin, P. Hadwiger, M. John, K. Mills, K. Charisse, M. A. Maier, L. Nechev, E. M. Greene, P. S. Pallan, E. Rozners, K. G. Rajeev, M. Egli, *Angew. Chem. Int. Ed.* **2011**, *50*, 2284.

[145] Y. Fedorov, E. M. Anderson, A. Birmingham, A. Reynolds, J. Karpilow, K. Robinson, D. Leake, W. S. Marshall, A. Khvorova, *RNA* **2006**, *12*, 1188.

[146] K. T. Love, K. P. Mahon, C. G. Levins, K. a Whitehead, W. Querbes, J. R. Dorkin, J. Qin, W. Cantley, L. L. Qin, T. Racie, M. Frank-Kamenetsky, K. N. Yip, R. Alvarez, D. W. Y. Sah, A. de Fougerolles, K. Fitzgerald, V. Koteliansky, A. Akinc, R. Langer, D. G. Anderson, *Proc. Natl. Acad. Sci. U. S. A.* **2010**, *107*, 1864.

[147] Y. Pei, T. Tuschl, *Nat. Methods* **2006**, *3*, 670.

9. Curriculum vitae

Personal data

- Name: Leonard Kaps
- Date of birth: [redacted]
- Nationality: [redacted]
- Civil status: [redacted]
- [redacted]Resident: [redacted],

Education

Schooling:

[redacted]

University:

[redacted]

[redacted]

Internships

[redacted]

Publications

- Friedrich Foerster, Sebastian Boegel, Rosario Heck, Geethanjali Pickert, Nina Rüssel, Sebastian Rosigkeit, Matthias Bros, Stephanie Strobl, **Leonard Kaps**, Misbah Aslam, Mustafa Diken, John Castle, Ugur Sahin, Andrea Tüttenberg, Ernesto Bockamp, and Detlef Schuppan, **"**Enhanced protection of C57BL/6 vs Balb/c mice to melanoma liver metastasis is mediated by NK cells**",** Cancer Research (2017) *submitted*

- **Leonard Kaps**, Nadine Leber, Misbah Aslam, Jonathan Schupp, Alexander Brose, David Schäffel, Karl Fischer, Mustafa Diken, Dennis Strand, Kaloian Koynov, Andrea Tuettenberg, Lutz Nuhn, Rudolf Zentel, Detlef Schuppan, "SiRNA-mediated In Vivo Gene Knockdown by Acid-Degradable Cationic Nanohydrogel Particles", *J. controlled release*, (2016)
- Laura K. Müller, **Leonard Kaps**, Detlef Schuppan, Alexander Brose, Wenqiang Chai, Karl Fischer, Sophie Müller, Holger Frey, Manfred Schmidt, Kristin Mohr, „Physicochemical and Preclinical Evaluation of Spermine-Derived Surfactant Liposomes for in Vitro and in Vivo siRNA-Delivery to Liver Macrophages", *Mol. Pharmaceutics*, Vol. 13 (2016), 3636–3647
- Lutz Nuhn, **Leonard Kaps**, Mustafa Diken, Detlef Schuppan, Rudolf Zentel, "Reductive Decationizable Block Copolymers for Stimuli - Responsive mRNA Delivery", *Macromol. Rapid Commun.*, Vol. 37(2016), 924-33
- Foerster F, Bamberger D, Schupp J, Weilbächer M, **Kaps L**, Strobl S, Radi L, Diken M, Strand D, Tuettenberg A, Wich P, Schuppan D, „Dextran-based therapeutic nanoparticles for hepatic drug delivery", *Nanomedicine (Lond)*, 11(2016), 2663-77.
- Hörtz C, Birke A, Barz M, **Kaps L**, Brose A, Schuppan D, Decker S, Fischer K, Schmidt M, "Cylindrical Brush Polymers with Polysarcosine Side Chains: A Novel Biocompatible Carrier for Biomedical Applications", *Macromolecules*, Vol.48 (2015), 2074-2086.
- **Leonard Kaps**, Lutz Nuhn, Misbah Aslam, Alexander Brose, Friedrich Foerster, Sebastian Rosigkeit, Patricia Renz, Rosario Heck, Yong Ook Kim, Ingo Lieberwirth, Detlef Schuppan, Rudolf Zentel, "*In Vivo* Gene-Silencing in Fibrotic Liver by siRNA-Loaded Cationic Nanohydrogel Particles", *Advanced healthcare materials*, 4(2015), 2809-15
- Julienne K. Muenzner, Bernhard Biersack, Hussein Kalie, Ion C. Andronache, **Leonard Kaps**, Detlef Schuppan, Florenz Sasse, Rainer Schobert, „Gold(I) biscarbene complexes with Vessel-disrupting combretastatin A-4 show altered cellular and molecular target profiles with increased antimetastatic potential", *ChemMedChem*, Vol. 9 (2014),1195-204.
- **Leonard Kaps**, Bernhard Biersack, Helge Müller-Bunz, Katharina Mahal, Julienne Münzner, Matthias Tacke, Thomas Mueller, Rainer Schobert, „Gold(I)-NHC complexes of antitumoral diarylimidazoles, structures, cellular uptake routes and anticancer activities", *Journal of Inorganic Biochemistry*, Vol. 106 (2012), 52-58
- R. Mayap Talom, G. Fuks, **L. Kaps**, J. Oberdisse, C. Cerclier, C. Gaillard, C. Mingotaud, F. Gauffre, "DNA-Polymer Micelles as Nanocontainers with Recognition Ability", *Chemistry- A European journal*, Vol. 17 (2011), 13495-13501.
- Siddappa Patil, Anthony Deally, Frauke Hackenberg, **Leonard Kaps**, Helge Müller-Bunz, Rainer Schobert, Matthias Tacke, "Novel Benzyl- or p-Cyanobenzyl-Substituted N-Heterocyclic Carbene-Silver(I) Bromide and Gold(I) Chloride Complexes: Synthesis and Preliminary Cytotoxicity Studies", *Helvetica Chimica Acta*, Vol. 94 (2011), 1551-1562.

Presentations

- Speaker - BSS - Hepatic regenerative: Gene editing and gene therapy for liver disease, EASL, 52th EASL, The International Liver Congress, Amsterdam (NE), 19 - 23 Apr. 2017, “siRNA therapies for liver regeneration and repair Fellow lecture: In vivo gene silencing in the liver: Comparison of siRNA-loaded non-biodegradable vs. biodegradable cationic nanohydrogel particles for antifibrotic therapy” **Leonard Kaps**, Nadine Leber, Lutz Nuhn, Misbah Aslam, Alexander Brose, Friedrich Foerster, Sebastian Rosigkeit, Rosario Heck, Rudolf Zentel, Detlef Schuppan
- Speaker - parallel session 33: Clinical and Translational Fibrosis Research, AASLD, The liver meeting, Boston (USA), 13 - 17 Apr. 2016, “In vivo gene silencing in the liver: Comparison of siRNA-loaded non-biodegradable vs. biodegradable nanohydrogel particles for antifibrotic therapy” **Leonard Kaps**, Nadine Leber, Lutz Nuhn, Misbah Aslam, Alexander Brose, Friedrich Foerster, Sebastian Rosigkeit, Rosario Heck, Rudolf Zentel, Detlef Schuppan
- Short presentation, VISZERALMEDIZIN 2016, Hamburg 21 – 23 Sept., "In vivo cell specific gene silencing in the liver using novel siRNA-loaded biodegradable nanohydrogel particles", **Leonard Kaps**, Nadine Leber, Lutz Nuhn, Misbah Aslam, Alexander Brose, Friedrich Foerster, Sebastian Rosigkeit, Rosario Heck, Rudolf Zentel, Detlef Schuppan,
- Oral poster presentation, 51th EASL, The International Liver Congress, Barcelona (ES), 13 - 17 Apr. 2016, “In vivo gene silencing in the liver: Comparison of siRNA-loaded non-biodegradable vs. biodegradable nanohydrogel particles for antifibrotic therapy” **Leonard Kaps**, Nadine Leber, Lutz Nuhn, Misbah Aslam, Alexander Brose, Friedrich Foerster, Sebastian Rosigkeit, Rosario Heck, Rudolf Zentel, Detlef Schuppan
- Sonderforschungsbereich 1066 – Minisymposium, Mainz 17 Dec. 2015, “*In vivo* gene silencing in the liver: Comparison of siRNA-loaded non-biodegradable vs biodegradable nanohydrogel particles for antifibrotic therapy”
- Collaborating group meeting, Bordeaux, 11 Oct. 2009, presentation of the project “Nano-objects based on copolymers containing a small single strand DNA”
- Nanotool-Day conference, Toulouse, 20 Nov. 2009, presentation of the project “Self assembly of DNA and polymers hybrids”

Poster presentation

- VISZERALMEDIZIN, Hamburg 21 – 23 Sept., "In vivo cell specific gene silencing in the liver using novel siRNA-loaded biodegradable nanohydrogel particles", **Leonard Kaps**, Nadine Leber, Lutz Nuhn, Misbah Aslam, Alexander Brose, Friedrich Foerster, Sebastian Rosigkeit, Rosario Heck, Rudolf Zentel, Detlef Schuppan
- 51th EASL, The International Liver Congress, Barcelona, 13 - 17 Apr. 2016, “In vivo gene silencing in the liver: Comparison of siRNA-loaded non-biodegradable vs. biodegradable nanohydrogel particles for antifibrotic therapy” **Leonard Kaps**, Nadine Leber, Lutz Nuhn, Misbah Aslam, Alexander Brose, Friedrich Foerster, Sebastian Rosigkeit, Rosario Heck, Rudolf Zentel, Detlef Schuppan

- AASLD, The Liver Meeting, San Francisco, 17-20 Nov. 2015, "*In vivo* gene silencing in the liver using novel siRNA-loaded nanohydrogel particles for liver fibrosis therapy" **Leonard Kaps**, Lutz Nuhn, Misbah Aslam, Alexander Brose, Friedrich Foerster, Sebastian Rosigkeit, Patricia Renz, Rosario Heck, Yong Ook Kim, Ingo Lieberwirth, Detlef Schuppan, Rudolf Zentel
- 50th EASL, The International Liver Congress, Wien, 21-24 Apr. 2015, "*In vivo* gene silencing in the liver using novel siRNA-loaded nanohydrogel particles for liver fibrosis therapy" **Leonard Kaps**, Lutz Nuhn, Misbah Aslam, Alexander Brose, Friedrich Foerster, Sebastian Rosigkeit, Patricia Renz, Rosario Heck, Yong Ook Kim, Ingo Lieberwirth, Detlef Schuppan, Rudolf Zentel
- 39th Colloque, National du GFP, Le Mans, 24-26 Nov. 2009, "Self assembly of DNA and polymers hybrids" Renée Mayap Talom, **Leonard Kaps**, Gad Fuks, Jallal Dehmoune, Fabienne Gauffre, Christophe Mingotaud, Nancy Lauth-De Viguerie, J.-D. Marty, Patricia Vicendo, Jacques Leng, Julian Oberdisse (IMRCP - Toulouse)

Recently published abstracts

- **Leonard Kaps**, Nadine Leber, Lutz Nuhn, Misbah Aslam, Alexander Brose, Friedrich Foerster, Sebastian Rosigkeit, Rosario Heck, Rudolf Zentel, Detlef Schuppan, AASLD, The liver meeting, Boston (USA), 13 - 17 Apr. 2016, "In vivo gene silencing in the liver: Comparison of siRNA-loaded non-biodegradable vs. biodegradable nanohydrogel particles for antifibrotic therapy"
- **Leonard Kaps**, Nadine Leber, Lutz Nuhn, Misbah Aslam, Alexander Brose, Friedrich Foerster, Sebastian Rosigkeit, Rosario Heck, Rudolf Zentel, Detlef Schuppan, VISZERALMEDIZIN 2016, Hamburg 21 – 23 Sept., "In vivo cell specific gene silencing in the liver using novel siRNA-loaded biodegradable nanohydrogel particles"
- **Leonard Kaps**, Lutz Nuhn, Misbah Aslam, Alexander Brose, Friedrich Foerster, Sebastian Rosigkeit, Mustafa Diken, Rosario Heck, Andrea Tüttenberg, Rudolf Zentel, Detlef Schuppan, *"In vivo* myofibroblast specific gene silencing in the liver using novel siRNA-loaded biodegradable nanohydrogel particles", EASL 2016 (Barcelona).
- **Kaps L**, Nuhn L, Foerster F, Brose A, Heck S, Diken S, Zentel R, Schuppan D. "In vivo gene silencing in the liver using novel siRNA-loaded nanohydrogel particles", EASL (Wien) and AASLD 2015 (San Francisco).

Awards

[redacted]

CV

Command of languages

[redacted]

Hobbies

- [redacted]